UNIVERSITÀ DEGLI STUDI DI SALERNO

UNIVERSITÀ DEGLI STUDI DI SALERNO
Dipartimento di Farmacia

PhD Program in

Drug Discovery and Development

XXX Cycle — Academic Year 2017/2018

PhD Thesis in

Role of CD73 - A_{2A}/A_{2B} receptors axis in cancer

Candidate

Claudia Sorrentino

Supervisor

Prof. *Silvana Morello*

PhD Program Coordinator: Prof. *Gianluca Sbardella*

A mamma, papà e Gennaro.

Abstract

The adenosinergic pathway plays a critical role in cancer development and progression, as well as in drug resistance to chemotherapy and/or targeted-therapy.

The goal of this PhD thesis was to investigate and fully characterize the role of CD73/adenosine A_{2A}-A_{2B} receptors axis in cancer, highlighting the therapeutic potential of inhibitors of the adenosinergic pathway.

We firstly characterized the mechanism/s by which A_{2B}R promotes immunosuppression and angiogenesis in tumor-bearing hosts, focusing on the role of myeloid-derived suppressor cells (MDSCs) and cancer-associated fibroblasts (CAFs). The results revealed that treatment of melanoma-bearing mice with Bay60-6583, a selective A_{2B}R agonist, is associated with 1. increased tumor VEGF-A expression and vessel density, and 2. increased accumulation of tumor-infiltrating CD11b+Gr1+cells (MDSCs). MDSCs strongly contribute to the immunosuppressive and angiogenic effects of Bay60-6583. Melanoma-bearing mice treated with a selective A_{2B}R antagonist PSB1115 showed reduced tumor growth compared to controls and this effect was associated with reduced tumor angiogenesis, low levels of MDSCs and increased number of tumor-infiltrating CD8+ T cells. Furthermore, blockade of A_{2B}R increased the anti-tumor effects of VEGF-A inhibitors. Next, we verified that A_{2B}R activation also drives fibroblasts activation within melanoma tissues, by increasing the number of FAP positive cells within tumor lesions. FAP is a common marker of activated fibroblasts also named cancer-associated fibroblasts. These cells produce and secrete various tumor-promoting factors, including fibroblast growth factor (FGF)-2 and CXCL12 or stromal-derived factor 1 α (SDF1α), that were increased both in melanoma tissue and fibroblasts isolated from melanoma tissue or from skin upon Bay60-6583 treatment. Bay60-6583-induced FGF-2 from fibroblasts contributed to melanoma cells proliferation. The CXCL12/CXCR4 pathway, instead, was involved in the pro-angiogenic effects of A_{2B}R agonist, but not in its immunosuppressive effects. These effects were significantly blocked by the A_{2B}R antagonists PSB1115. Taken together, these data elucidate the pivotal role of

$A_{2B}R$ in establishing a positive cross-talk between tumor-infiltrating immune cells, fibroblasts and endothelial cells that sustain tumor growth, reinforcing the therapeutic potential of $A_{2B}R$ blockers for cancer therapy.

We next investigated the immunosuppressive mechanism mediated by $A_{2A}R$ that occurs through the Notch signalling pathway in CD8+ T cells. $A_{2A}R$ stimulation with CGS-21680 downregulated Notch1 expression in CD3/CD28-stimulated CD8+ T cells at the protein level but not at transcriptional level. The inhibitory effects of CGS-21680 on effector functions of CD8+ T cells were enhanced in presence of the Notch1 inhibitor, PF-03084014. Similar results were obtained also in CD8+ T cells treated with forskolin, an activator of adenylate cyclase, which mimics the effects of CGS-21680. The $A_{2A}R$ agonist did not influence the expression of Notch1 in CD8+ T cells after TCR activation, suggesting that stimulation of $A_{2A}R$ affects the expression of TCR-induced Notch expression. These results were confirmed by using transgenic CD8+ T cells from N1IC mice (N1IC CD8+ T cells) that were less sensitive to the inhibitory effects of CGS-21680. CD8+ T cells deficient of $A_{2A}Rs$ were instead sensitive to the inhibitory effects of the Notch inhibitor PF-03084014. Overall, our results indicate that the inhibitory effects of adenosine via A_{2A} receptor occurs, at least in part, by reducing the Notch1 expression and activity, by blocking the TCR-mediated signalling transduction in CD8+ T cells.

Finally, we evaluated the associations of soluble CD73 (sCD73) enzyme activity with clinical outcomes of patients with metastatic melanoma receiving the anti-PD1 agent nivolumab. In a retrospective study we found that melanoma patients stage IV with high basal serum level of sCD73 enzyme activity, before starting nivolumab treatment, had a lower response rate to nivolumab, shorter survival and higher rates of progression of disease. Patients obtaining partial response to nivolumab or stable disease had low levels of sCD73 activity in the serum, thus suggesting a predictive role of response to nivolumab therapy for sCD73. This evidence could be very helpful to select patients to an appropriate therapy and then, neutralizing CD73 with clinically validated CD73 monoclonal antibodies could represent a highly potent and innovative therapy in combination regimen.

In conclusion, we provide new insights into the mechanisms by which adenosinergic molecules modulate immune- and stromal-cells responses in the tumor environment, that is important for developing combination strategies for cancer therapy.

Index

Index

Chapter 1

1. Introduction

1.1 Role of adenosine in cancer: an overview

Adenosine is a purine nucleoside involved in the regulation of several homeostatic mechanisms (1). In physiological conditions, adenosine is mainly produced at the intracellular level by S-adenosyl-homocysteine through the S-adenosyl-homocysteine hydrolase (SAH); while, in pathological conditions, its synthesis occurs at the extracellular level starting from ATP by two ectoenzymes, the ecto-nucleoside triphosphate diphosphohydrolase-1 (CD39) and the ecto-5'-nucleotidase (CD73) expressed on both hematopoietic and non- hematopoietic cells (Figure 1.1) (2, 3).

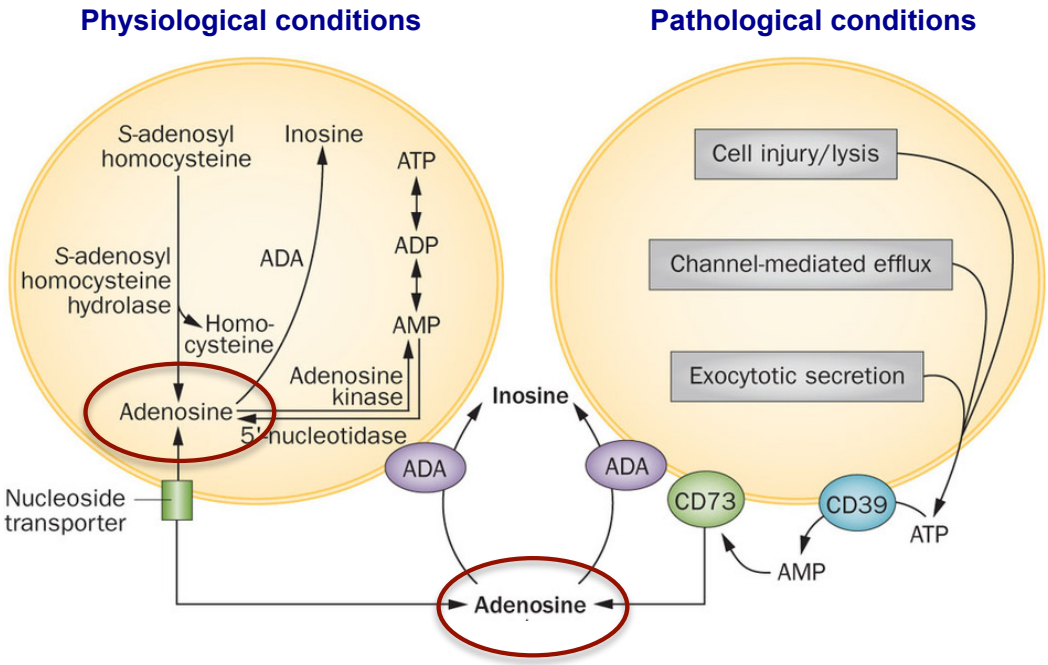

Figure 1.1: Adenosine synthesis in physiological conditions by S-adenosyl-homocysteine hydrolase-SAH and in pathological conditions mainly by two ectoenzymes, ecto-5'- nucleotidase (CD73) and ectonucleoside triphosphate diphosphohydrolase-1 (CD39). [Modified by Krysko et al., 2012_ (4)].

Once released in the extracellular space, adenosine elicits its functions by binding

to one of the four membrane adenosine receptors (A_1, A_{2A}, A_{2B}, A_3) which contain seven transmembrane domains coupled to G proteins (5). Thus, adenosine can inhibit (via A_1 and A_3) or stimulate (via A_{2A} and A_{2B}) the adenylyl cyclase resulting in a decrease or increase in cyclic AMP (cAMP) accumulation, respectively (Figure 1.2) (6).

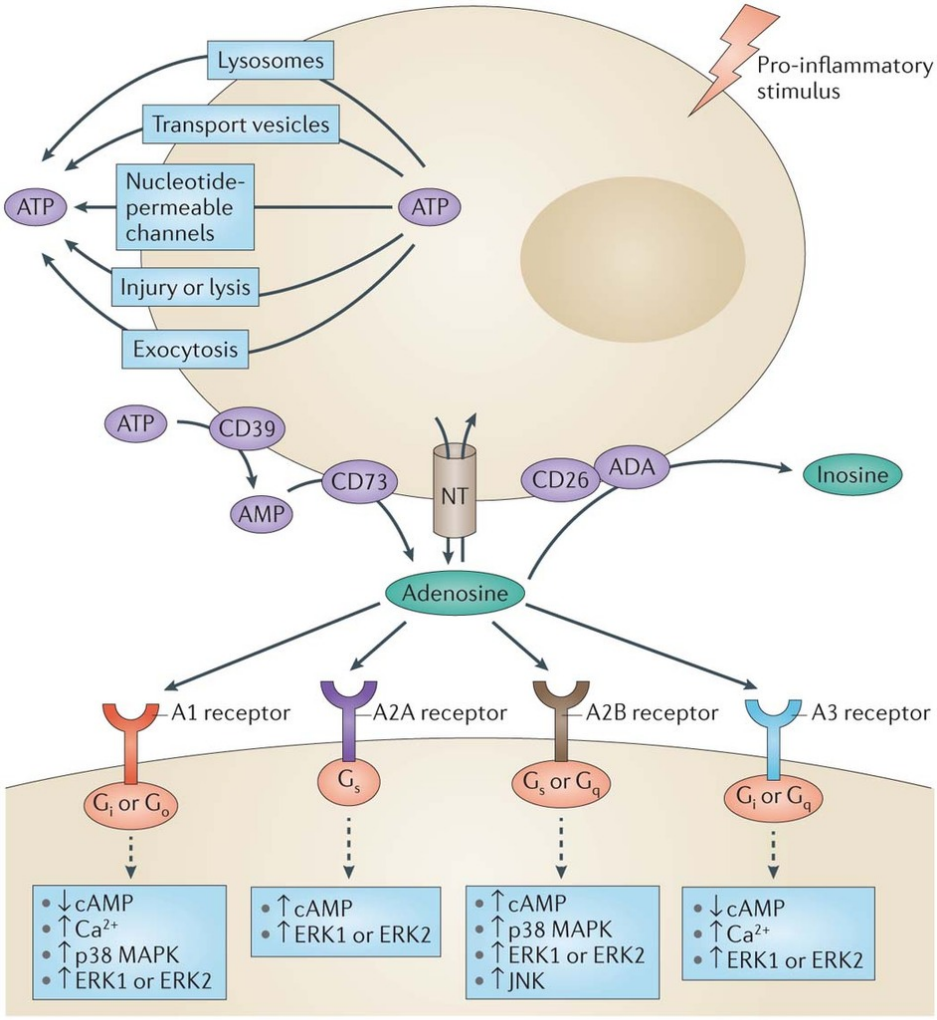

Figure 1.2: A schematic illustrating the adenosine biosynthesis and the catabolism and its interaction with the four membrane adenosine receptors (A_1, A_{2A}, A_{2B}, A_3) (1).

In response to tissue injury, ATP is strongly released from stressed, damaged

and/or tumor cells and it is rapidly converted in ADP and AMP through two reversible steps via CD39; then AMP is irreversible degraded into adenosine by CD73 (3) (Figure 1.2). Under homeostatic conditions extracellular adenosine level is low, while during pathophysiological events (including stress, infection, inflammation and cancer) extracellular adenosine levels can be increased from 10-200 nmol/L up to 10-100 μmol/L (7). In contrast to ATP, adenosine is a potent immunosuppressive and anti-inflammatory mediator. These latter effects are mainly mediated by cAMP-elevating adenosine A_{2A} and/or A_{2B} receptors. In the context of cancer, adenosine within tumor microenvironment potently suppresses anti-tumor T-cell responses promoting tumor growth (8). Indeed, the adenosinergic pathway represents one of the major immunosuppressive mechanism within the tumor microenvironment, that could also potentially limit the therapeutic success of existing and new immunotherapeutic agents.

Importantly, the expression of adenosine-generating enzymes and adenosine receptor subtypes can be regulated within tumor microenvironment by many factors and their expression often correlates with poor prognosis in patients with cancer. For example, inflammatory mediators, hypoxia and genetic drivers can up-regulate adenosine signalling pathway (8) (Figure 1.3). In particular, hypoxia within tumor microenvironment is one of the main factors responsible of the increased production of adenosine in many solid tumors. Indeed, CD39 and CD73 expression increases under hypoxic conditions, while the expression of the adenosine kinase, which inhibits the metabolism of adenosine, is down-regulated (9). At the same time, the expression of $A_{2A}R$ and $A_{2B}R$ is also up-regulated (10). Consequently, adenosine along with other HIF-induced immunosuppressive factors and cells, contributes to modulate the functions of tumor cells, tumor-infiltrating immune cells and/or other stroma cells (Figure 1.3).

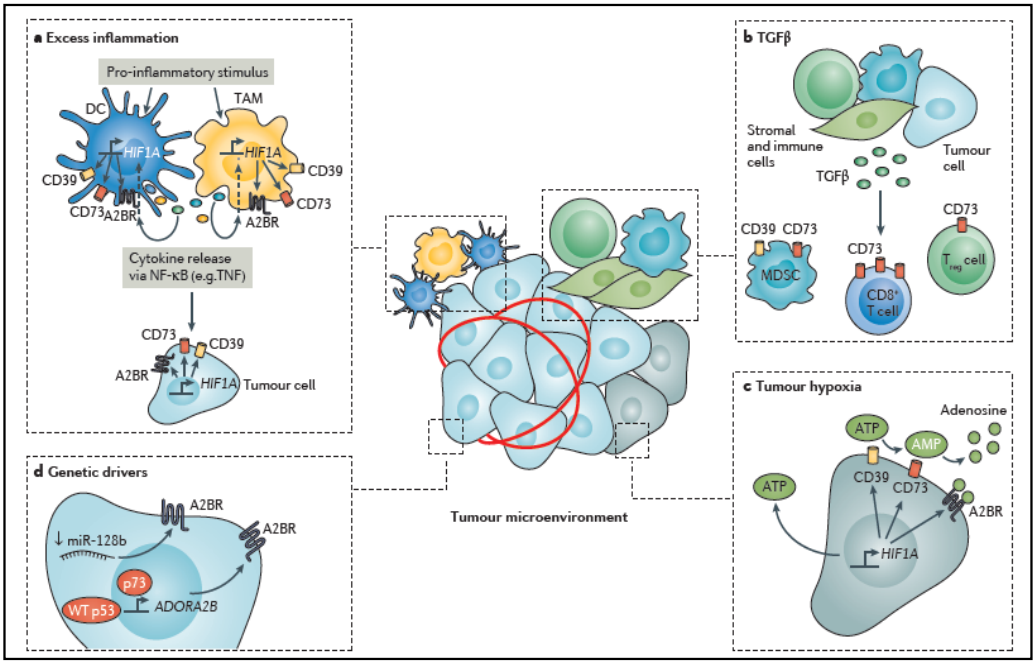

Figure 1.3: Main factors that influence the expression of adenosine receptors within tumor microenvironment (8).

A large number of pre-clinical studies indicate that selective adenosine receptor antagonists or inhibitors of adenosine-generating enzymes induce effective anti-tumor immune responses, and some of them represent new attractive therapeutic agents for cancer therapy, recently included in clinical trials in patients with malignancies (8).

In the following paragraph the main objectives of this PhD thesis are summarized and here I will give you few basic concepts to guide you in reading this thesis.

1.2 Aim of the PhD project and specific objectives

Targeting adenosine signalling pathway with specific inhibitors could effectively suppress tumor progression and metastases through multiple mechanisms (1). CD73-generating adenosine and their receptors A_{2A} and A_{2B} affect the behaviour of multiple cell populations within tumor microenvironment. In addition, recent evidence indicate that adenosine signalling pathway can be regulated in response to immunotherapy or targeted-therapy, including anti-PD1 agents, T-cell therapy or BRAF/MEK inhibitors in cancer patients (11, 12). Therefore, understanding the mechanisms by which adenosinergic molecules modulate immune- and stromal-cells responses in the tumor environment is important for developing combination therapies. Furthermore, evaluating the adenosinergic-targeted molecules before treatment with currently used immunotherapies, such as anti-PD1 agents, and how they relate to response is of interest in clinical practice.

For this purpose, the specific objectives of this project were:

1) To evaluate the role of A_{2B} receptor in tumor and surrounding stroma in a mouse model of melanoma

Background and rationale. Over the years, $A_{2B}R$ has been the less characterized receptor among adenosine receptor subtypes, due to its low expression in physiological conditions and low adenosine affinity. However, emerging evidence suggest that $A_{2B}R$ may play a pivotal role in adenosine-mediated tumor progression (13, 14) because of high adenosine levels and/or increased $A_{2B}R$ expression on many cell types. Indeed, $A_{2B}R$ is the main adenosine receptor subtype expressed on myeloid cells and it may play a role in promoting tumor proliferation, metastases, immunosuppression and angiogenesis (13, 14) (Figure 1.1.1).

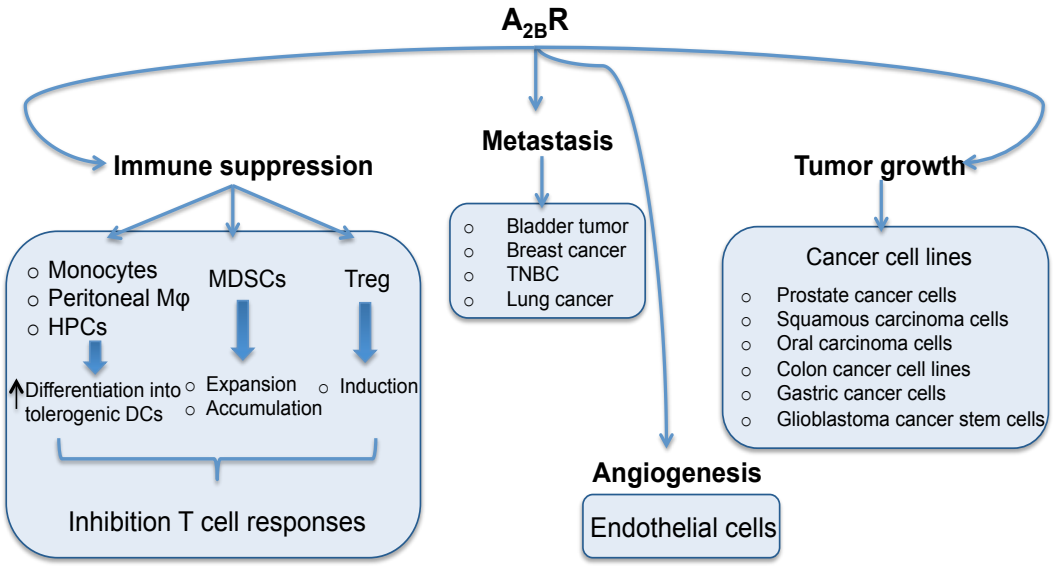

Figure 1.1.1: $A_{2B}R$ pathway is involved in several functions on different cell types within tumor microenvironment (14).

Targeting the $A_{2B}R$ has proved to be therapeutically effective in some murine tumor models (14), but the mechanisms of these effects are still incompletely understood.

Here, we evaluate the effects of pharmacological $A_{2B}R$ modulators in a mouse melanoma model, evaluating:

1.1 the role of myeloid-derived suppressor cells (MDSCs) in the pro-angiogenic effects of $A_{2B}R$ and whether blockade of $A_{2B}R$ with selective antagonists could enhance the efficacy of anti-VEGF treatment;

1.2 the role of $A_{2B}R$ in modulating the activity of cancer-associated fibroblasts (CAFs).

2) To study the Notch1-$A_{2A}R$ cross-talk in murine activated CD8+ T cells.

Background and rationale. $A_{2A}R$ is the main adenosine receptor subtype expressed on lymphoid cells (15). Stimulation of $A_{2A}R$ on CD8+ T cells potently suppresses the TCR-mediated proliferation and activation in a cAMP-dependent manner (Figure 1.1.2) (16). $A_{2A}R$ activation is also able to inhibit the functions of innate and adaptive immune cells, other than CD8+ T cells (17); consequently, $A_{2A}R$ blockade has been advocated to facilitate tumor immunotherapy.

T cells are essential effectors of tumor immunity (18). One of the crucial signalling pathways involved in T-cell development, lineage selection and activation is Notch. Recent studies highlight the pivotal role of Notch signalling in the differentiation and function of several T cell subsets (19). It is well documented that Notch is activated after T-cell receptor (TCR) engagement (20) and that Notch signalling is required for T-cell activation and for the cytotoxic activity of CD8+ T cells. Notch1 is also required for the differentiation of CD8+ T effector cells (21) and constitutive expression of active Notch1 renders CD8+ T cells resistant to the immune suppressive activity of MDSCs (22).

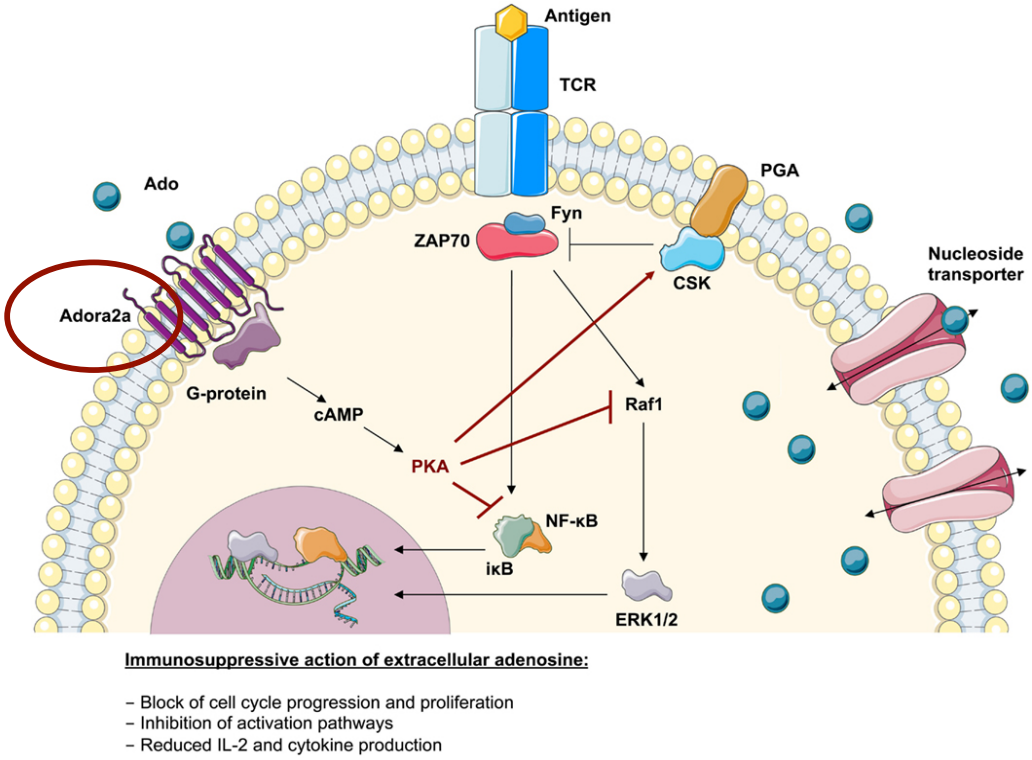

Figure 1.1.2: $A_{2A}R$ pathway in T cells; interaction with the early events upon T cell receptor (TCR) activation (23).

Thanks to the collaboration with Dr. Lucio Miele at the Stanley S. Scott Cancer Center (Louisiana State University Health Science Center_LSUHSC) I could work in his Laboratory in order to further investigate the mechanism/s through which $A_{2A}R$ suppresses the functions of activated CD8+ T cells, we evaluated the Notch1 signalling pathway upon $A_{2A}R$ stimulation.

3) To measure soluble CD73 levels in the peripheral blood of patients with advanced melanoma receiving nivolumab as potential biomarker of response to immunotherapy

Background and rationale. Pre-clinical data suggest that high expression of CD73 in cancer is associated to a reduced effectiveness of therapies with anti-PD1 (24). CD73 is highly expressed in different types of tumors in patients and often its expression correlates with poor prognosis and/or resistance to conventional therapies (24). Nowadays, specific inhibitors of CD73 entered clinical trials in patients with malignancies, alone or in combination with anti-PD1 agents (8). Here, we proposed to measure the CD73 activity in the peripheral blood of patients with metastatic melanoma before receiving the anti-PD1 agent, nivolumab, in order to evaluate the potential predictive value of response to immunotherapy of CD73, and possible provide additional information to better select subsets of patients who will benefit from immunotherapies in combination with anti-CD73 agents.

Chapter 2

CHAPTER 2

2.1 Role of $A_{2B}R$ in tumor and surrounding stroma

2.1.1 $A_{2B}R$ expression and transduction

$A_{2B}R$ is largely expressed in our organism. As explained in Chapter 1, $A_{2B}R$ binds adenosine with a lower affinity than $A_{2A}R$ ($A_{2B}R$-EC_{50} is 24 µmol/L). Therefore, its signalling capacity depends on the adenosine concentration as well as on its density on the cell surface. The expression of $A_{2B}R$ on cells is influenced by metabolic, inflammatory and hormonal factors including adenosine itself. $A_{2B}R$ expression is transcriptionally regulated through the oxygen-regulated transcription factor hypoxia inducible factor (HIF-1 α) (25). As illustrated in Figure 2.1.1, $A_{2B}R$ couples to both G_s and G_q proteins but the most studied intracellular signalling pathway is the G_s-mediated signalling, that increased cAMP levels leading to activation of to the cAMP-dependent protein kinase PKA. Moreover, $A_{2B}R$ activates the mitogen activated protein (MAP) kinase signalling (26).

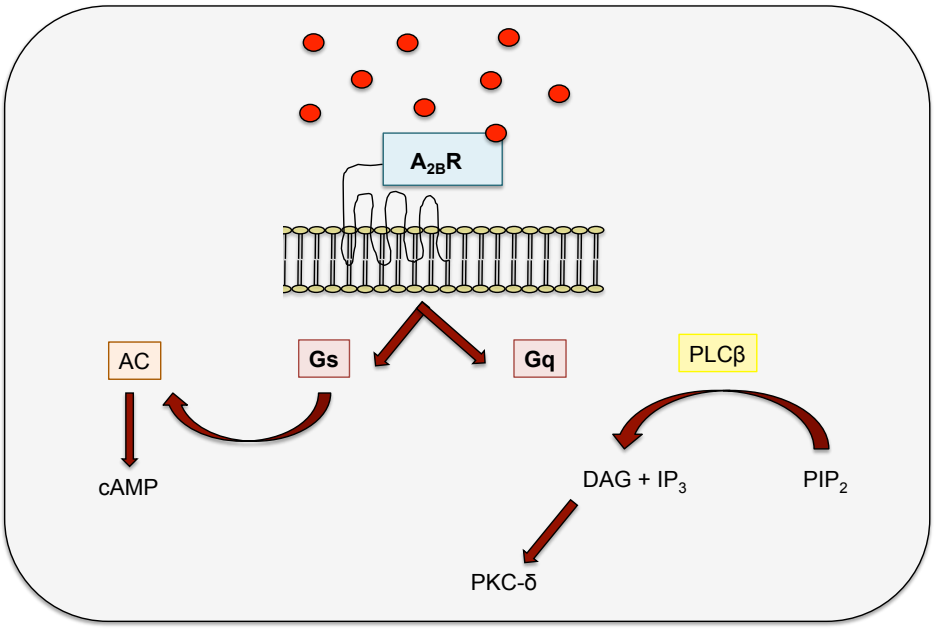

Figure 2.1.1_ $A_{2B}R$ signalling transduction.

2.2.2 $A_{2B}R$ in cancer

$A_{2B}R$ is important in some pathophysiological conditions, including vascular injury (27), chronic lung disease (28), vascular leak (29), and ischemic disease (30). Recent evidence show that $A_{2B}R$ plays an important role in mediating also the pro-tumor effects of adenosine. Ryzhov and collaborators (13) in 2008 provided the first genetic evidence for a pivotal role of $A_{2B}R$ in tumor progression, showing that tumor growth in $A_{2B}R$ deficient mice was reduced compared to that observed in wild type mice. A number of studies indicate that $A_{2B}R$ can directly affect the proliferation/migration of tumor cells and the function of tumor-infiltrating immune cells and other stroma cells that populate the tumor niche, including endothelial cells (Reviewed in Ref 14). $A_{2B}R$ may influence the features of some immune cell populations, including Treg cells and dendritic cells (31, 32) and some experimental evidence in tumor mouse models suggest that the selective blockade of $A_{2B}R$ may ameliorate T cell-mediated immune surveillance by impairing the accumulation of suppressive cells and the levels of inflammatory factors in the tumor microenvironment (13, 33-35). Despite these evidence, further studies are needed to better investigate thoroughly the mechanisms by which blockers of this receptor limit tumor growth. Understanding the relative role of A_{2B} receptor in tumor, depending on the cell types, on its distribution and expression, will help to potentially apply $A_{2B}R$-targeted agents for cancer treatment.

2.1.3 $A_{2B}R$ and MDSCs

$A_{2B}R$ has been detected on several immune cell populations such as mast cells (36), neutrophils (29), dendritic cells (32), macrophages (37), lymphocytes (38) and on immune suppressive cells such as MDSCs (39). MDSCs are a heterogeneous population of immature myeloid cells expressing CD11b and Gr1 and their accumulation can be considered as a hallmark of chronic inflammation leading to T cells suppression through different mechanisms. This cell population is made up of myeloid progenitor cells and immature myeloid cells (IMCs). Normally IMCs, generated in the bone marrow, differentiate into mature

granulocytes, macrophages or dendritic cells but in pathological condition (infection, sepsis, trauma, cancer) IMCs undergo a block in their differentiation and an upregulation of their immune suppressive factors such as arginase1, inducible nitric oxide synthase (iNOS), nitric oxide (NO) and reactive oxygen species (ROS) production (40) (Figure 2.1.2).

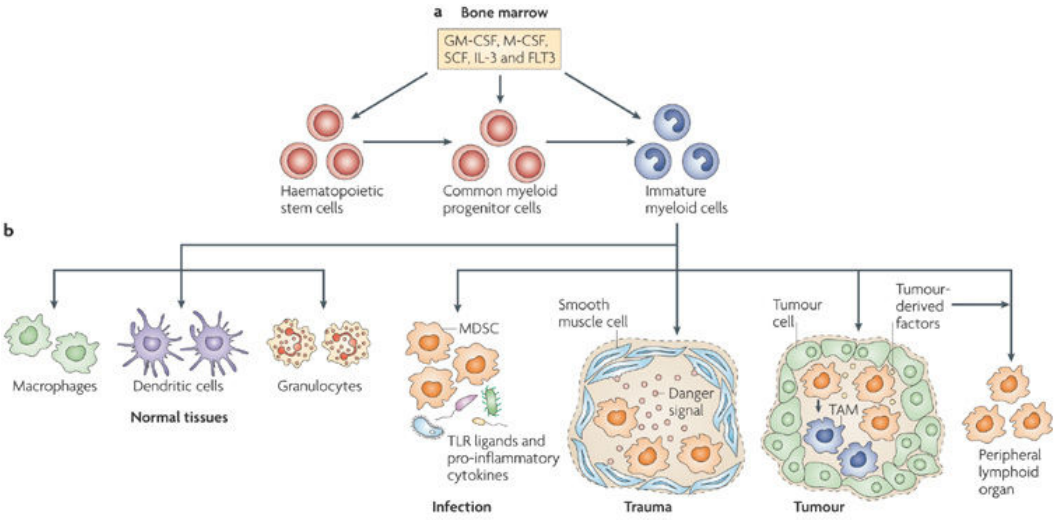

Figure 2.1.2_ a) Generation of MDSCs from their bone marrow's progenitors **b)** in both normal and pathological conditions (40).

MDSCs-mediated immunosuppressive activity needs a direct contact between cells suggesting that these cells act through both membrane receptors and the release of short-lived soluble factors (41). MDSCs play a critical role in leading immunosuppression acting as potent suppressors of T cell-mediated responses within tumor milieu, promoting tumor growth (42). Recent evidence suggest that the signal transducer and activator of transcription 3 (STAT3) could be the main transcription factor concerning MDSCs expansion (40, 41). The transcription factor STAT3 translocates into the nucleus where it directly binds to DNA sequences upon phosphorylation at tyrosine 705. In fact, STAT3 phosphorylation is significantly increased in IMCs from tumor-bearing mice compared to control mice (43). In addition, MDSCs produce pro-angiogenic factors such as VEGF-A, in a STAT3-dependent manner, stimulating tumor angiogenesis (44). VEGF-A is the most potent pro-angiogenic factor that induces proliferation, sprouting and tube formation of endothelial cells. Moreover, these pro-angiogenic factors can

themselves promote MDSCs accumulation in the tumor microenvironment creating a vicious circle (44). Ryzhov and colleagues demonstrated that the activation of $A_{2B}R$ promotes MDSCs expansion *in vitro* contributing to induce immunosuppression by producing adenosine (45). Moreover, $A_{2B}R$ deficient mice showed reduced amounts of CD11b+ Gr1+ cells suggesting that $A_{2B}R$ suppresses immune system activity (13). These and more other evidence, previously demonstrated in our laboratory, show that the selective $A_{2B}R$ blockade might improve T cell-mediated immune surveillance by impairing MDSCs accumulation within tumor microenvironment (34). Accordingly, our aim was to evaluate the role of MDSCs in the pro-angiogenic effects of $A_{2B}R$ and whether blockade of $A_{2B}R$ could enhance the efficacy of anti-VEGF treatment.

2.1.4 $A_{2B}R$ and tumor-associated fibroblasts

Tumor microenvironment is made up not only of tumor and immune suppressive cells but also of stroma cells that contribute to the release of inflammatory mediators including cytokines, chemokines and growth factors, which contribute to enhance tumor growth. As showed in Figure 2.1.3, stromal cells that characterize tumor milieu comprise endothelial cells, fibroblasts, inflammatory cells and extra-cellular matrix which communicate with neoplastic cells through the release of multiple soluble factors.

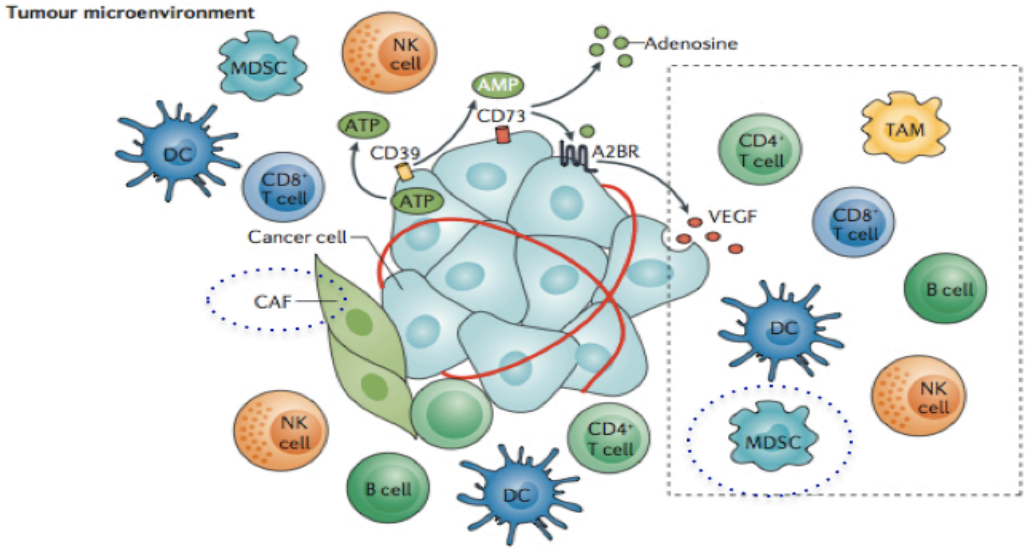

Figure 2.1.3_ Adenosine synthesis and its functions on several cell populations [Modified fromVijayan et al., Nature, 2017 (8)].

One of the major component of tumor stroma are cancer associated fibroblasts (CAFs) that, together with other stromal cells, can both modulate tumor initiation and progression and induce drug resistance to chemotherapy and/or targeted-therapy, in a soluble factor- and cell adhesion-manner (reviewed in references 46, 47). Therefore, understanding thoroughly the mechanisms that regulate the interplay between stromal cells and neoplastic cells is of great interest.

Fibroblasts are critical component of tumor stroma (10, 25, 48-51) and they are involved in tumor initiation and progression through the production of paracrine factors such as SDF-1 or FGF-2 (stromal derived factor-1 and fibroblast growth factor-2, respectively, which are both considered as markers of fibroblasts activation) (52). Activated fibroblasts are associated with tumor growth and angiogenesis (53). In fact, VEGF-A is released by cancer cells but also inflammatory cells (like MDSCs as described above) and fibroblasts contribute to VEGF-A release (44, 52).

Previous data show that fibroblasts express adenosine receptors (10, 25, 48-51). Accordingly, our aim was to study the role of $A_{2B}R$ in the modulation of stromal fibroblasts activity.

2.2 Materials and Methods

2.2.1 Cells, mice and treatments

A murine melanoma cell line, B16-F10 from American Type Culture Collection (LGC Standards srl., Milan, Italy), was used to create a murine melanoma model for our studies. B16-F10 cells were cultured according to company's instructions using DMEM (Dulbecco's Modified Eagle Medium) supplemented with 10% FBS (Fetal Bovine Serum), 100 U/ml penicillin and 0.1 mg/ml streptomycin. A suspension of 2.5×10^5 cells in PBS (Phosphate-Buffered Saline) was injected s.c. (subcutaneously) into the right flank of C57Bl6j mice (6–8 week-old females) that were obtained from Charles River (Charles River, Lecco, Italy). All the experiments performed using mice were approved by Italian Health Ministry (protocol n° 12827) and conducted according to institutional animal care guidelines, Italian Law 26/2014 based on the European Community Law for Animal Care 2010/63/UE.

On day 7, after melanoma cells injection, mice were randomly grouped and treated as follows:

- Bay60-6583 (0.2 mg/kg) (34, 54, 55) a selective $A_{2B}R$ agonist or PSB1115 (1 mg/kg) (34, 56, 57) a selective $A_{2B}R$ antagonist (both from Tocris, UK) were injected p.t. (peritumorally) every day to evaluate the effects of $A_{2B}R$ stimulation or $A_{2B}R$ blockade within tumor microenvironment, respectively. As control for Bay60-6583 was used phosphate-buffered solution (PBS) containing DMSO (0.1%).
- 120 mg/kg gemcitabine (Sigma Aldrich, Milan, Italy) was administered i.p. (intraperitumorally) every three days until endpoint, to deplete MDSCs in mice (34, 58-60).
- 50 μg of anti-VEGF A antibody (BioLegend, Campoverde, Milan, Italy) was administered i.p. every day for VEGF neutralization experiments, using isotype IgG as control.
- S3I-201 (5 mg/kg) (Sigma Aldrich) was administered i.p. every two days until endpoint, to block STAT3 signalling (61-63).
- AMD3100 2.5 mg/kg p.t. as selective antagonist of CXCR4 (Sigma-Aldrich).

Tumor volume was monitored every two days during the treatment period using an electronical caliper and calculated as $4/3\pi \times$ (long diameter / 2) × (short diameter / 2) (46). After one week of treatment mice were sacrificed and tumor tissues were harvested from each mouse for further analyses.

2.2.2 Flow cytometry analysis

Melanoma tissues were harvested from mice and digested with collagenase 1U/ml (Sigma Aldrich, Italy), passed through 70 μm cell strainers and red blood cells (RBC) were lysed. The single cell suspension obtained from each sample was pre-incubated with anti-mouse CD16/CD32 (eBioscience, San Diego, CA, USA) to block non-specific Fc-mediated interactions. Antibodies against CD11c-FITC, CD11b-PeCy5.5, Gr1-PE or Gr1- allophycocyanin, CD3-PeCy5.5; CD8-allophycocyanin or CD8-PE; CD4-allophycocyanin; NK1.1-PE (eBioscience and BioLegend) were used. Data were acquired with a FACSCalibur flow cytometer (BD Biosciences).

2.2.3 Isolation of CD11b+ cells

Melanoma tissues were collected aseptically and digested with collagenase 1U/ml. Cells were passed through 70 μm strainers, followed by RBC lysis. CD11b+ cells were isolated by positive magnetic kit (CD11b EasySep Isolation kit; Stem Cell Tech) according to manufacturer's instruction. Purity of CD11b+ cells was checked by flow cytometry and it was around 90%.

2.2.4 Fibroblasts isolation and treatments

To investigate the role of $A_{2B}R$ in modulating the activity of stromal fibroblasts, we isolated fibroblasts from either melanoma or skin tissues. The culture medium used for these studies was RPMI 1640 supplemented with 1μg/L, 10% FBS, 100 U/ml penicillin, 0.1 mg/ml streptomycin (Lonza, Milan, Italy).

- To isolate cancer-associated fibroblasts, we collected the entire melanoma capsule aseptically and, after several washes with sterile PBS (Euroclone, Milan, Italy), we placed the capsule in a Petri dish with polylysine-coated surfaces.

- To isolate fibroblasts from the skin (64) we shaved C57Bl6j mice and aseptically harvested skin samples which were dissociated both mechanically by cutting the tissue into 1 mm pieces using a scalpel blade and enzymatically by using 1 U/ml collagenase A (Sigma-Aldrich, Milan, Italy). In both cases, the entire melanoma capsule and the digested skin fragments, were placed in a Petri dish with polylysine-coated surfaces using the supplemented RPMI medium described above and left for 5-7 days in a tissue culture incubator allowing fibroblasts to migrate from the tissue into the Petri dish.

Isolated fibroblasts were treated with 1, 10 or 100 nM Bay60-6583 ($A_{2B}R$ agonist) for further analyses and 10 nM Bay60-6583 was chosen to perform *in vitro* experiments as it achieved optimal effects in preliminary studies. Moreover, $A_{2B}R$ antagonist, PSB1115 100 nM was used in some experiments.

To mimic tumor microenvironment, skin isolated fibroblasts were exposed to 100 μM $CoCl_2$ used as hypoxia inducer (55) at different time points (0-24 hours). Fibroblasts exposed to hypoxia were also treated with 10 nM Bay60-6583 for 24 h for further analyses. Some experiments were also performed in presence of the $A_{2A}R$ agonist (1 μM) as described above.

2.2.5 Western blot analysis

Tumor tissues harvested from mice were homogenized in RIPA buffer (RIA Precipitation Buffer in which were freshly added 1mM Protease and Phosphatase Inhibitor Cocktail, 1 mM PMSF and 1 mM sodium orthovanadate), centrifuged and protein concentrations in supernatants were measured by Bio-Rad protein assay. Forty micrograms of total proteins were analysed by 10% denaturing polyacrylamide gels and then transferred electrophoretically to nitrocellulose membranes (Immobilon-NC, Millipore). Anti–VEGF (A-20) (Santa Cruz Biotechnology, DBA, Milan, Italy) and anti-tubulin (or anti-actin) (Sigma-Aldrich) primary antibodies were used (Santa Cruz Biotechnology). VEGF-A expression was also measured in isolated CD11b+ cells.

Isolated fibroblasts from tumor and/or skin were collected and suspended in RIPA buffer (Radio-Immuno Precipitation Assay Buffer in which were freshly added 1mM Protease and Phosphatase Inhibitor Cocktail, 1 mM PMSF and 1 mM

sodium orthovanadate), centrifuged and protein concentrations in supernatants were measured by Bio-Rad protein assay. Forty micrograms of proteins were analysed by 10% denaturing polyacrylamide gels and transferred electrophoretically to PVDF membranes (Immobilon-NC, Millipore, Italy). Membranes were stained overnight at 4°C in humidified chamber with the primary antibodies that follows:

- anti-$A_{2B}R$ (H-40) (clone N-19) (Santa Cruz Biotechnology);
- anti-HIF1α (A300-286A) (Bethyl Laboratories, Tema Ricerca, Italy);
- anti-CD73 (5NT5E, C-terminal) (Sigma-Aldrich, Milan, Italy).

After 1 h at room temperature with the secondary antibodies, immunoreactive protein bands were detected by enhanced chemiluminescence reagents (Amersham Pharmacia Biotech, Buckinghamshire, UK) and analysed by Las4000 (GE Healthcare Life Sciences).

2.2.6 Immunofluorescence analysis by confocal microscopy

Immunofluorescence analyses were performed on both melanoma frozen sections and isolated fibroblasts from tumor and/or skin. Tumor tissues were fixed with 0.5% neutral buffered paraformaldehyde at 4°C for 2 hours and then incubated with 15% sucrose at 4°C overnight. Fixed samples were later frozen in Optimum Cutting Temperature (OCT) medium (Pella, Milan, Italy) and 10–20 μm thick sections were cut. To reduce nonspecific binding sites, slides were blocked in PBS with 20% normal goat serum (GIBCO BRL) or 5% Bovine Serum Albumin (BSA) containing 0.5% TritonX-100 for 30 minutes at room temperature. As far as isolated fibroblasts plated on poly-lysine-coated slides, after two washes in PBS they were fixed in 4% PFA, and nonspecific binding sites were blocked using 20% goat serum or 5% bovine serum albumin (BSA) for 30 minutes at room temperature, as appropriate. In both cases, slides were stained overnight at 4°C in humidified chamber with the primary antibodies and 2 h at room temperature with the secondary antibodies. The following antibodies were used:

- VEGF (A-20) (1:100; Santa Cruz Biotechnology), detected with Alexa Fluor® 488 Goat Anti-Rabbit IgG (H+L) (1:1000) secondary antibodies;

- FITC anti-mouse CD31 (MEC 13.3) (1.100, BioLegend);
- Gr1 (Ly-6G, clone RB6–8C5) (1:100; eBioscience), (1:200; Abcam, Cambridge, UK), detected with Alexa Fluor® 555 Goat Anti-Rat IgG (H+L) (1:1000) (Life Technologies, Italy) secondary antibodies;
- $A_{2B}R$ (N-19) (1:50; Santa Cruz Biotechnology), detected with DyeLightTM 549-conjugated AffinePure Donkey anti-goat IgG (H+L) or DyeLightTM 488-conjugated AffinePure Donkey anti-goat IgG (H+L) (Jackson Immunoresearch Laboratories Inc.) secondary antibodies;
- FAPα (H-56) or FGF-2 (147) (1:100; Santa Cruz Biotechnology) were detected with Alexa Fluor® 488 or 555 Goat Anti-Rabbit IgG (H+L) (1:5000) secondary antibodies (Life Technologies, Italy);
- CXCL12 (1:100; Santa Cruz Biotechnology) (clone P-159X) was detected with the secondary antibody Alexa Fluor® 488 Goat Anti-Mouse IgG (H+L) (1:5000);
- Vimentin (E-5) (1:500; Santa Cruz Biotechnology) or fibronectin (A17) (1:200; Abcam) were detected with the secondary antibody Alexa Fluor® 555 Goat Anti-Mouse IgG (H+L) (1:5000);
- CXCR4 (clone L276F12) (1:100; BioLegend) was detected with Alexa Fluor® 555 Goat Anti-Rat IgG (H+L) (1:5000).

Slides were incubated overnight with primary antibodies in a humidified chamber at 4°C and with the secondary antibody for 2 hours at room temperature. DAPI was used to counterstain nuclei. In all staining experiments, isotype-matched IgG and omission of the primary Ab was used as controls. Slides were observed using a Zeiss LSM 710 Laser Scanning Microscope (Carl Zeiss MicroImaging GmbH). Samples were vertically scanned from the bottom of the coverslip with a 63x or 40x (1.40 NA) Plan-Apochromat oil-immersion objective. Images were generated with Zeiss ZEN Confocal Software (Carl Zeiss MicroImaging GmbH).

2.2.7 Proliferation assay

96 well plates were used to culture melanoma-derived fibroblasts, B16-F10 cells or co-cultures of melanoma-derived fibroblasts and B16-F10 cells (1:1 ratio). Cells were treated with 10 nM Bay60-6583, 100 nM PSB1115 and/or both and cell proliferation assay was performed at 24-48-72 hours.

In some co-culture experiments was used an anti-FGF2 antibody at 100 ng/ml (recombinant FGF-β, Lonza, Italy, tested at the concentrations of 30-100 ng/ml) alone or in presence of 10 nM Bay60-6583.

2.2.8 Elisa assay

A mouse CXCL12/SDF-1 alpha ELISA kit (R&D Systems, Abingdon, UK) was used, according to manufacturer's instruction, to determine the levels of CXCL12 in the supernatant of isolated fibroblasts treated with 1, 10 or 100 nM Bay60-6583 for 24 h with or without 100 nM PSB1115.

2.2.9 Statistical analysis

Data are from at least two-three independent experiments and results are expressed as mean ± SEM. Concerning immunofluorescence analysis, sections derived from tumors were obtained from at least 5-6 different mice per condition. Two sections were stained for each tumor and positive cells were counted in four-to-five randomly selected fields per tumor section. The results of immunofluorescence in fibroblasts are expressed as mean (±S.E.M.) of 4 separate fibroblast preparations, each isolated from C57Bl6 mice. The optical density of the protein bands detected by Western blotting was performed with ImageQuantTL (Ge Healthcare). Data were analysed with GraphPad Prism 6 (GraphPad Software). Two-tailed Student's t test (2-group comparisons) or ANOVA (> 2-group comparisons) were performed as appropriate. P values < 0.05 were considered significant.

2.3 Results

2.3.1 $A_{2B}R$ stimulation promotes tumor growth

To evaluate the effects of $A_{2B}R$ stimulation in tumor-bearing mice we treated mice with a selective $A_{2B}R$ agonist Bay60-6583 seven days later B16-F10 melanoma cells implantation. Mice treated with Bay60-6583 (0.2 mg/kg, p.t.) showed a significant increase in tumor volume compared with control mice (Figure 2.3.1), suggesting that $A_{2B}R$ has a pro-tumor role, in line with previous findings (39).

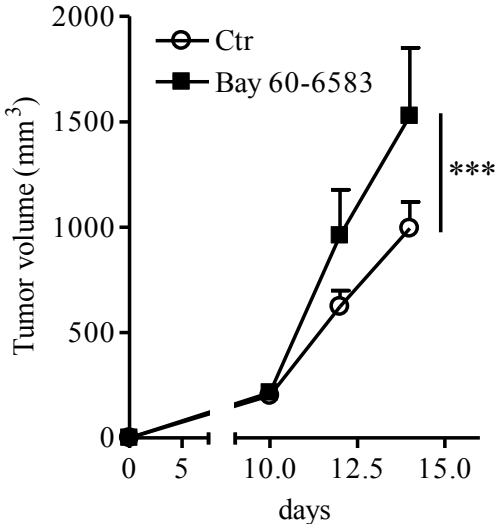

Figure 2.3.1 Tumor growth monitored during the treatment with $A_{2B}R$ agonist. Data are from two independent experiments and represent mean ± SEM (n=9 per group). ***p<0.001.

Notably, proliferation of B16-F10 melanoma cells was not affected by Bay60-6583 treatment *in vitro* (data not shown) (39).

2.3.2 $A_{2B}R$ stimulation enhances VEGF-A release in the tumor tissue

Next we observed that VEGF-A expression was significantly increased in tumor tissues of mice treated with Bay60-6583 compared to controls (Figure 2.3.2 A). This effect was associated with an increased vessel density in Bay60-6583-treated mice compared to the vehicle (control mice), as assessed by staining melanoma tissue sections with the endothelial marker CD31 and VEGF-A (Figure 2.3.2 B).

Moreover, while B16-F10 melanoma cells used in this model did not express VEGF-A, endothelial cells in the tumor tissue did express $A_{2B}R$ (Figure 2.3.2 C). Therefore, although we did not have a direct evidence on the role of $A_{2B}R$ on these cells in the tumor microenvironment, it is likely that stimulation of $A_{2B}R$ on endothelial cells could enhance the release of VEGF-A within tumor tissue (65, 66). All these pro-tumoral effects mediated by Bay60-6583 treatments were partially inhibited by using an anti-VEGF A antibody (150 µg/mouse, i.p. every two days). Indeed, when VEGF-A was blocked with a specific antibody in melanoma-bearing mice, the pro-tumor activity of Bay60-6583 was significantly attenuated and the tumor growth was decreased (Figure 2.3.2 D).

A)

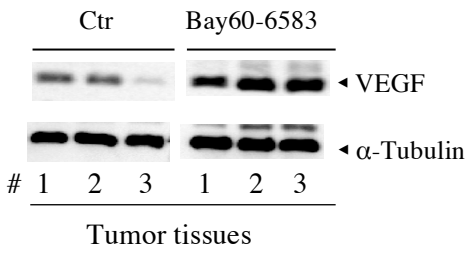

B)

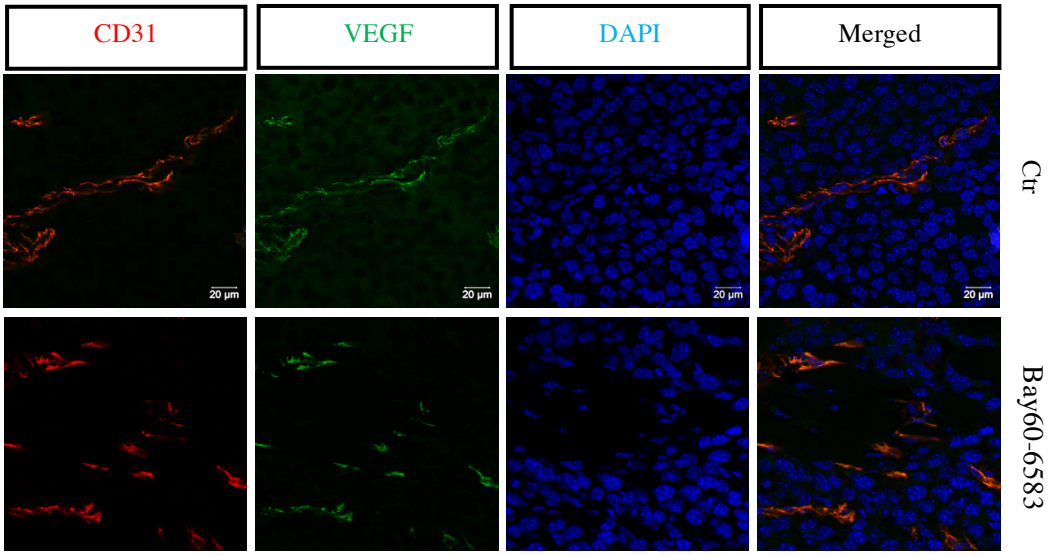

C)

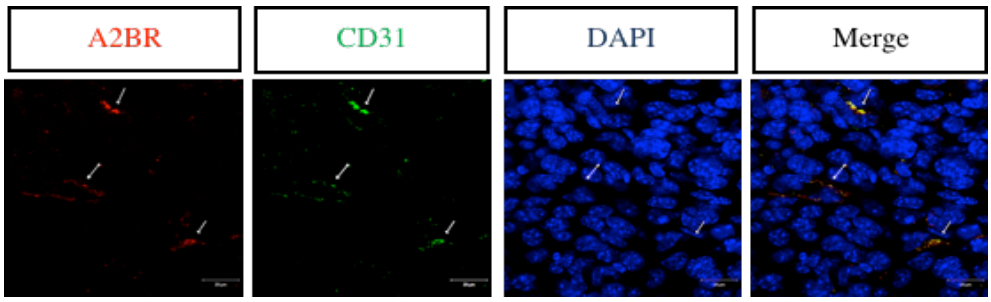

D)

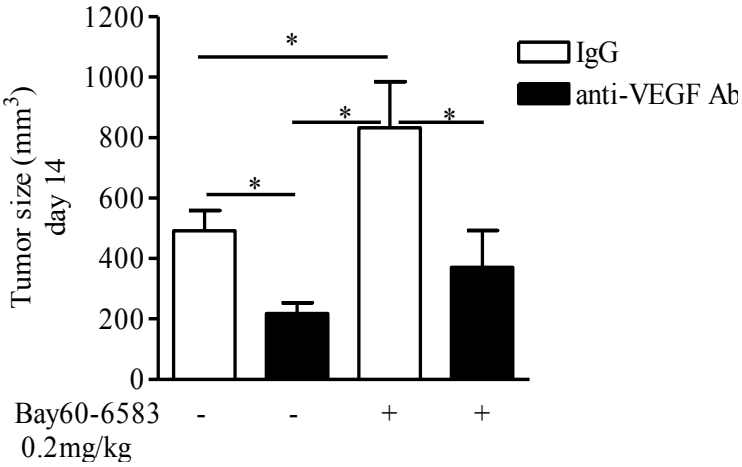

Figure 2.3.2 A) VEGF-A expression in melanoma lysates harvested from mice treated with Bay60-6583 or vehicle (ctr). **B)** Immunofluorescence staining of CD31 and VEGF-A in melanoma sections of mice treated with Bay60-6583 or vehicle (ctr) and **C)** representative image of $A_{2B}R$ expression on CD31 positive cells in melanoma sections. Magnification 63x, scale bars represent 20µm. **D)** Tumor volume measured at day 14 after tumor cell injection of mice treated with Bay60-6583 or vehicle receiving anti-VEGF antibody or IgG. Data represented are from three different experiments and represent mean ±SEM (n=6-10 per group). *p<0.05, **p<0.01, ***p<0.001.

Taken together, these results indicate that $A_{2B}R$ activation induces tumor angiogenesis that promotes tumor growth.

2.3.3 MDSCs contribute to the angiogenesis mediated by $A_{2B}R$ stimulation

We have previously demonstrated that stimulation of $A_{2B}R$ induces immunosuppression within tumor microenvironment, which favours tumor growth (34). Indeed, Bay60-6583-treated mice showed an increased accumulation of tumor-infiltrating MDSCs (identified as CD11b+Gr1+ cells) (Figure 2.3.3 A). This effect was associated to a significant reduction in the percentage of tumor-infiltrating CD8+ T cells, NKT and NK1.1+ cells compared to control mice (34) (Figure 2.3.3 B). These results confirm that the activation of tumor $A_{2B}R$ modulates the presence of tumor-infiltrating immune cells and leads to immunosuppression and tumor growth.

MDSCs are potent suppressor of T cells functions (40, 41) and they produce pro-angiogenic factors, including VEGF-A (67-69). By means of immunofluorescence analysis, we showed that MDSCs in melanoma sections expressed VEGF-A (Figure 2.3.3 C) and also $A_{2B}R$ (Figure 2.3.3 D). Based on these results we hypothesized that MDSCs could contribute not only to the immunosuppression but also to angiogenic activities of Bay60-6583. Therefore, we first verified if the stimulation of $A_{2B}R$ could directly modulate the release of VEGF-A from MDSCs. Isolated splenic CD11b+ cells did express VEGF-A but there was no difference in VEGF-A expression levels in CD11b+ cells treated with Bay60-6583 compared with control (data not shown) nor in CD11b+ cells isolated from Bay60-6583-treated mice compared with control mice (Figure 2.3.3 E). Nonetheless, tumor-infiltrating CD11b+Gr1+ cells were increased in Bay60-6583-treated mice compared to control mice (34) (Figure 2.3.3 F). Therefore, to clarify the involvement of MDSCs in $A_{2B}R$-mediated tumor angiogenesis, we treated mice with gemcitabine to deplete MDSCs in melanoma-bearing mice treated with Bay60-6583 or vehicle. Gemcitabine was administered in a single low dose, which did not significantly alter the percentage of CD3+, CD4+, CD8+ T cells and NK1.1+ cells in spleen or the viability of B16-F10 cells, but reduced significantly the percentage of MDSCs either in the tumor tissue (Figure 2.3.3 F) and in the spleen as we have previously demonstrated (34). Bay60-6583-treated mice receiving gemcitabine showed a significant reduction of VEGF-A expression in tumor tissue compared with control group (Figure 2.3.3 G).

A)

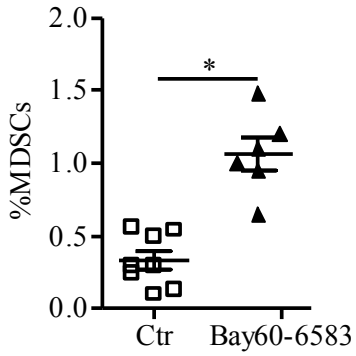
2.0
1.5
1.0
0.5
0.0
%MDSCs
*
Ctr
Bay60-6583

B)

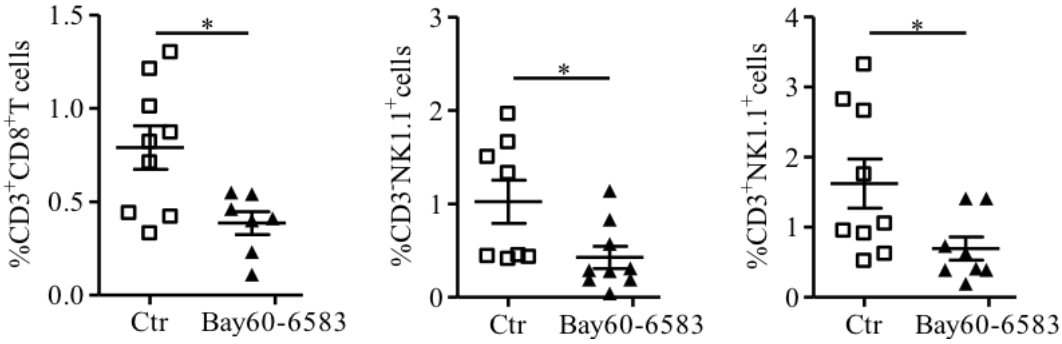
%CD3+CD8+T cells
%CD3-NK1.1+cells
%CD3+NK1.1+cells
*
Ctr
Bay60-6583

C)

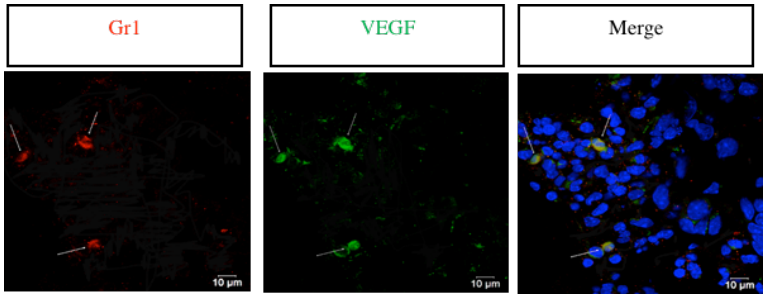
Gr1
VEGF
Merge
10 µm

D)

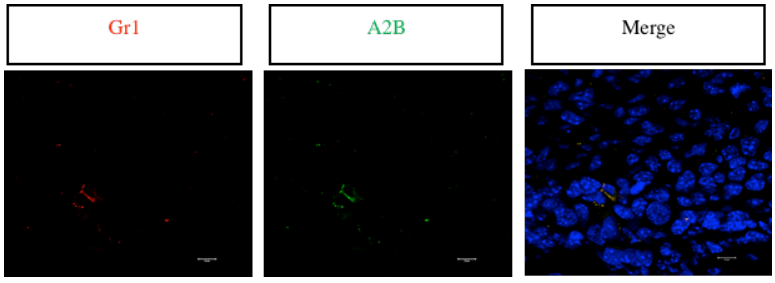
Gr1
A2B
Merge

E)

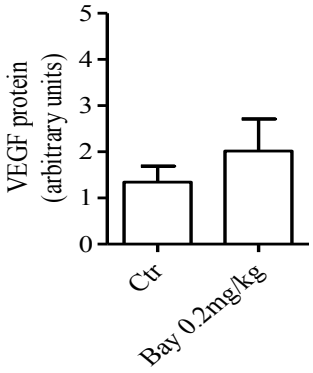

F)

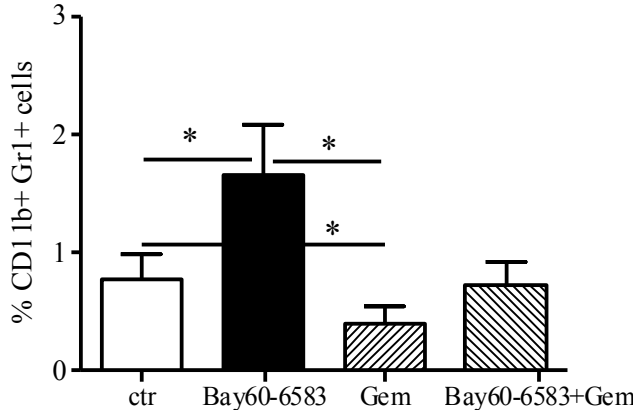

G)

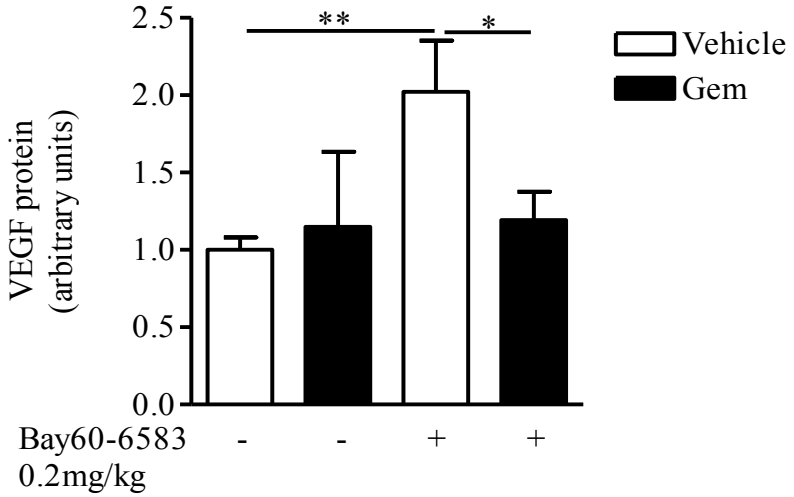

Figure 2.3.3 A) Percentage of MDSCs in tumor tissues of mice treated with Bay60-6583 or vehicle (ctr). **B)** Percentage of tumor-infiltrating CD3+CD8+T cells, CD3-NK1.1+cells and CD3+NK1.1+cells respectively of mice treated with

Bay60-6583 or vehicle (ctr). **C)** Immunofluorescence staining of Gr1 and VEGF-A and **D)** Gr1 and $A_{2B}R$ in melanoma sections. Magnification 63x, scale bars represent 20μm. **E)** VEGF-A expression analysed by Western blotting in CD11b+ cells isolated from melanoma sections harvested from mice treated with Bay60-6583 or vehicle (ctr). **F)** Percentage of CD11b+Gr1+ cells in tumor tissues from mice treated with Bay60-6583, Gemcitabine, in combination or vehicle (ctr) and **G)** VEGF-A expression in melanoma sections obtained from mice treated as described above. Data represented are from three independent experiments and represent mean ±SEM (n=10 per group). *p<0.05, **p<0.01, ***p<0.001.

These results indicate that the increased number of MDSCs induced by Bay60-6583 contributes to produce VEGF-A within tumor microenvironment.

2.3.4 Involvement of STAT3 in melanoma progression in Bay60-6583-treated mice

Within tumor microenvironment, many signals can trigger VEGF-A expression and secretion, including STAT-3 (70, 71). Mechanistically, in Bay60-6583-treated mice, we observed an enhanced activation of STAT-3 since expression levels of phospho-(p)STAT3 increased compared to control mice (Figure 2.3.4 A). In melanoma-bearing mice, treated with the highly selective STAT3 inhibitor, S3I-201, which preferentially inhibits STAT3 phosphorylation and STAT3 DNA-binding activity (72-74), the expression of p-STAT3 significantly reduced (Figure 2.3.4 B) as well as VEGF-A expression in melanoma tissue of Bay60-6583-treated mice and control mice (Figure 2.3.4 C). These effects were associated with a strong inhibition of tumor growth in both groups (Figure 2.3.4 D).

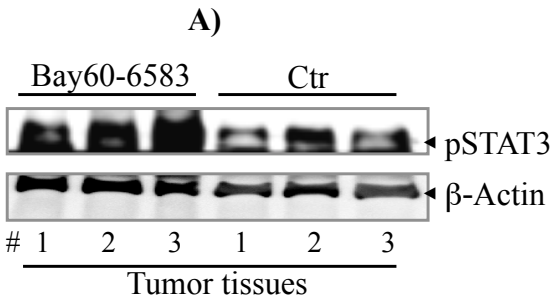

B)

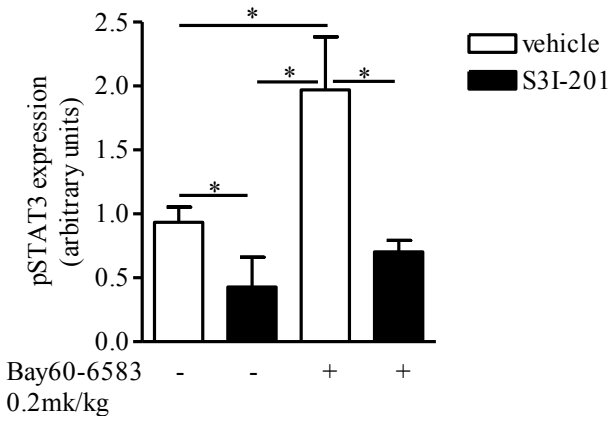
pSTAT3 expression
(arbitrary units)
2.5
2.0
1.5
1.0
0.5
0.0
*
*
*
*
vehicle
S3I-201
Bay60-6583 - - + +
0.2mk/kg

C)

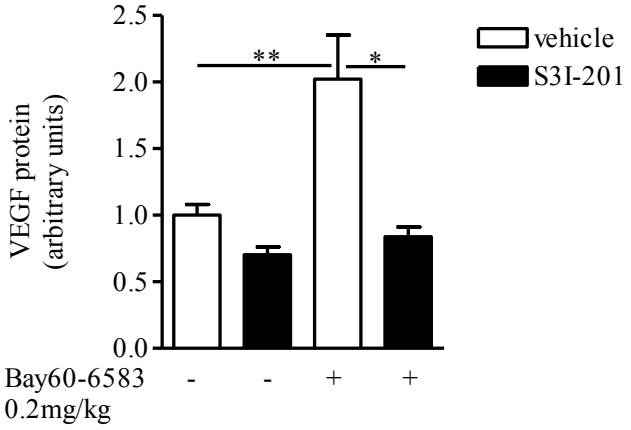
VEGF protein
(arbitrary units)
2.5
2.0
1.5
1.0
0.5
0.0
**
*
vehicle
S3I-201
Bay60-6583 - - + +
0.2mg/kg

D)

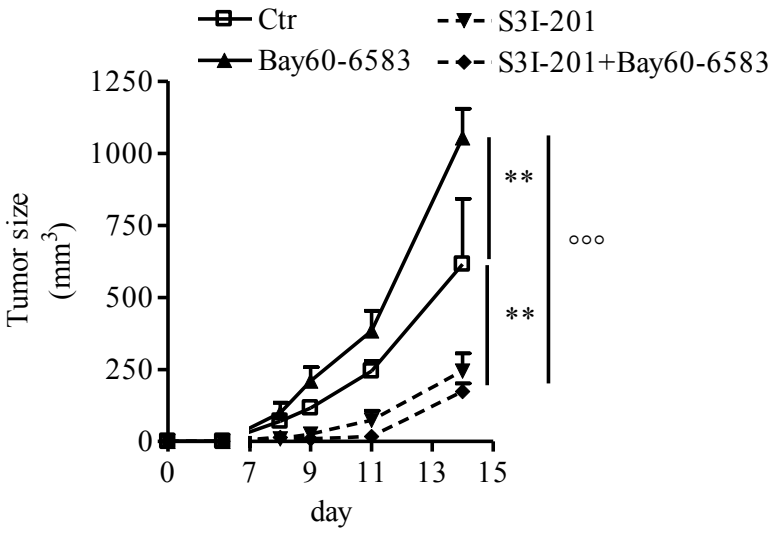
Ctr
S3I-201
Bay60-6583
S3I-201+Bay60-6583
Tumor size
(mm3)
1250
1000
750
500
250
0
0
7
9
11
13
15
day
**
**
°°°

Figure 2.3.4 A) and B) phospho-STAT3 (pSTAT3) expression analysis in tumor tissues from mice treated with Bay60-6583 or vehicle (ctr), receiving or not the STAT3 inhibitor S3I-201. **C)** VEGF-A expression in tumor tissues of mice treated with Bay60-6583 or vehicle (ctr), receiving the STAT3 inhibitor S3I-201 or vehicle. **D)** Tumor volume measured in mice treated as described above. Data are from three different experiments and represent mean ±SEM (n=6-10 per group). *p<0.05, **p<0.01, ***/ °°°p<0.001.

2.3.5 Pharmacological blockade of $A_{2B}R$ reduces angiogenesis by preventing MDSCs accumulation

Found out that $A_{2B}R$ stimulation promotes tumor growth and angiogenesis in melanoma-bearing hosts, we verified whether pharmacological inhibition of $A_{2B}R$ could have a therapeutic potential in reducing tumor angiogenesis. Melanoma-bearing mice were treated with the selective $A_{2B}R$ antagonist PSB1115 (1 mg/kg, p.t.) every day for one week. Tumor growth was significantly reduced in PSB1115-treated mice (Figure 2.3.5 A). This effect was associated with reduced VEGF-A expression (Figure 2.3.5 B), and microvessel density (Figure 2.3.5 C). As we have previously demonstrated (39), $A_{2B}R$ blockade reduces tumor accumulation of MDSCs, preventing T-cells suppression in mice with melanoma (34). These results, together with those described above, support the critical role of MDSCs in contributing to the tumor-promoting activity of $A_{2B}R$, including angiogenesis.

Inasmuch as MDSCs accumulation is a resistance factor to anti-VEGF therapies (75, 76), we hypothesized that PSB1115, by reducing the accumulation of tumor-infiltrating MDSCs, might potentiate the effects of anti-VEGF treatment when used in combination with it. PSB1115 alone reduced tumor growth (Figure 2.3.5 A). Treatment of mice with anti-VEGF antibody delayed tumor growth compared to controls (Figure 2.3.5 D) and the combination of anti-VEGF treatment with PSB1115 inhibited tumor growth much better than anti-VEGF or PSB1115 alone (Figure 2.3.5 D). Moreover we verified that mice treated with both drugs showed reduced number of tumor-infiltrating MDSCs (Figure 2.3.5 E) and increased number of CD8+ T cells and NKT cells (Figure 2.3.5 F).

A)

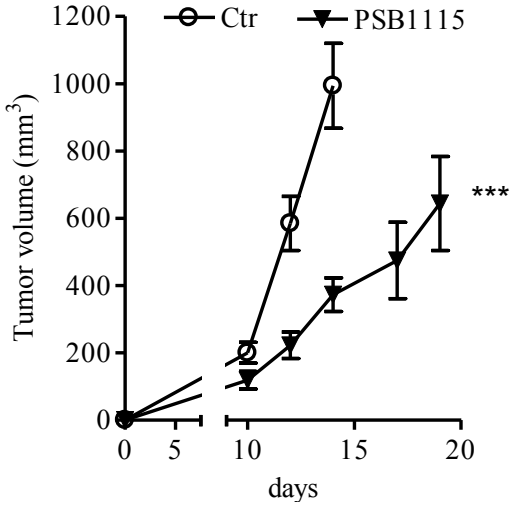
Ctr
PSB1115
Tumor volume (mm3)
1200
1000
800
600
400
200
0
0
5
10
15
20
days
***

B)

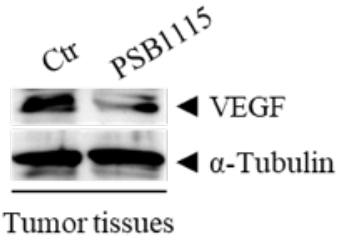
Ctr
PSB1115
VEGF
α-Tubulin
Tumor tissues

C)

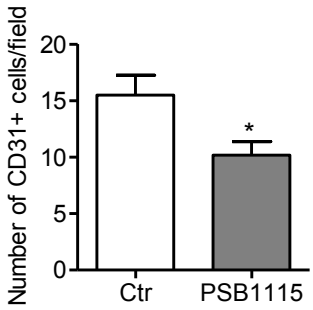
Number of CD31+ cells/field
20
15
10
5
0
*
Ctr
PSB1115

D)

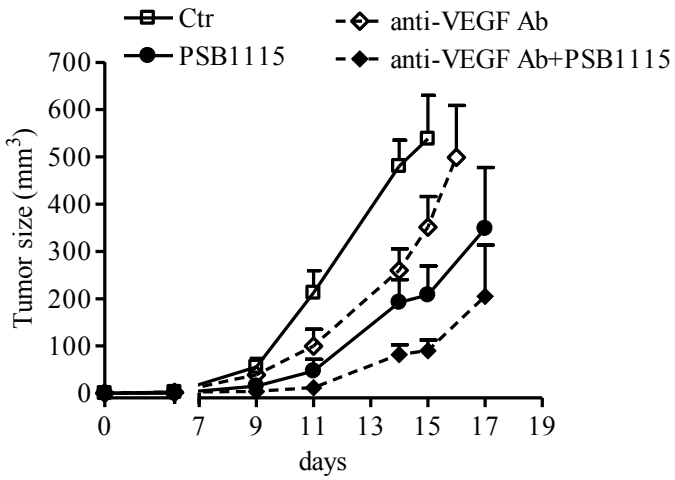
Ctr
PSB1115
anti-VEGF Ab
anti-VEGF Ab+PSB1115
Tumor size (mm3)
700
600
500
400
300
200
100
0
0
7
9
11
13
15
17
19
days

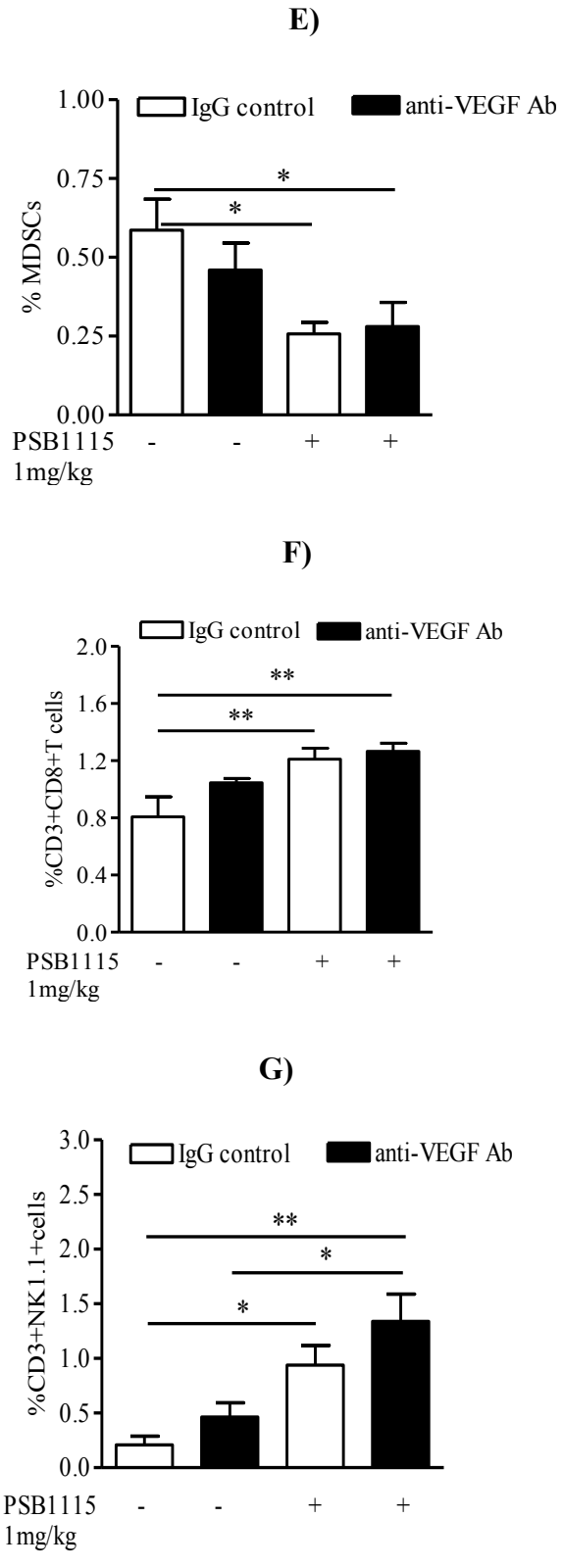

Figure 2.3.5 A) Tumor volume of mice treated with PSB1115 or vehicle (ctr). **B)** VEGF-A expression in melanoma lysates harvested from mice treated with PSB1115 or vehicle (ctr). **C)** Number of CD31 positive cells analysed by

immunofluorescence staining in melanoma sections of mice treated with PSB1115 or vehicle (ctr). **D)** Measurement of tumor growth after PSB1115 or vehicle in combination with anti-VEGF antibody treatment. **E) F) and G)** Percentage of MDSCs and CD3+CD8+ cells or CD3+NK1.1+ cells, respectively. Data are from three different experiments and represent mean ±SEM (n=9-12 per group). *p<0.05, **p<0.01, ***p<0.001.

To sum up, our data show that treatment of mice with $A_{2B}R$ antagonist was able to reduce tumor growth through the inhibition of both angiogenesis and immunosuppression. These effects are, at least in part, dependent on the activity of PSB1115 in reducing tumor-infiltrating MDSCs. The latter could also justify the enhanced effectiveness of VEGF-A inhibitor treatment.

2.3.6 $A_{2B}R$ stimulation induces CXCL12 expression in FAP positive cells within melanoma tissues

In an attempt to fully characterize the role of $A_{2B}R$ in the surrounding stroma, we then focused our attention also on the activity of stromal fibroblasts within tumor microenvironment upon $A_{2B}R$ stimulation or inhibition.

Fibroblasts in tumor tissue express $A_{2B}R$ (Figure 2.3.6 A), in line with previous findings (50, 77). To verify whether $A_{2B}R$ stimulation could drive fibroblasts activation within melanoma tissues we examined in melanoma sections the expression of fibroblast activation protein (FAP). FAP is a common marker of activated fibroblasts also named cancer-associated fibroblasts (78, 79). The number of FAP positive cells in melanoma sections harvested from mice treated with Bay60-6583 resulted significantly increased compared with those observed in control mice (Figure 2.3.6 B). Tumor-associated fibroblasts are important players within tumor stroma, able to produce and secrete various tumor-promoting factors, including fibroblast growth factor (FGF)-2 and CXCL12 or stromal-derived factor 1 α (SDF1α) (52, 80). We observed that both FGF-2 and CXCL12 expression were higher in tissues harvested from mice treated with Bay60-6583 than controls (Figure 2.3.6 C). FAP positive cells are one of the major source of these mediators under our experimental conditions (Figure 2.3.6 D), in line with previous studies (52).

A)

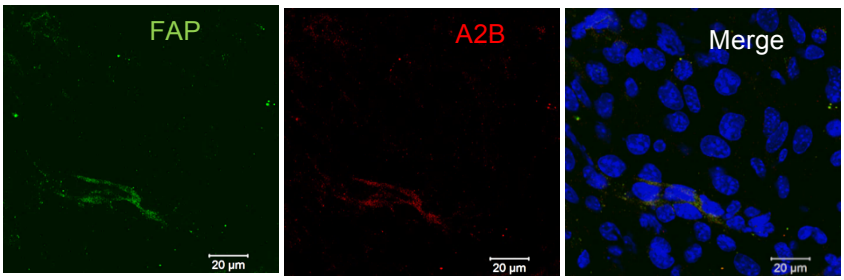
FAP
A2B
Merge
20 µm
20 µm
20 µm

B)

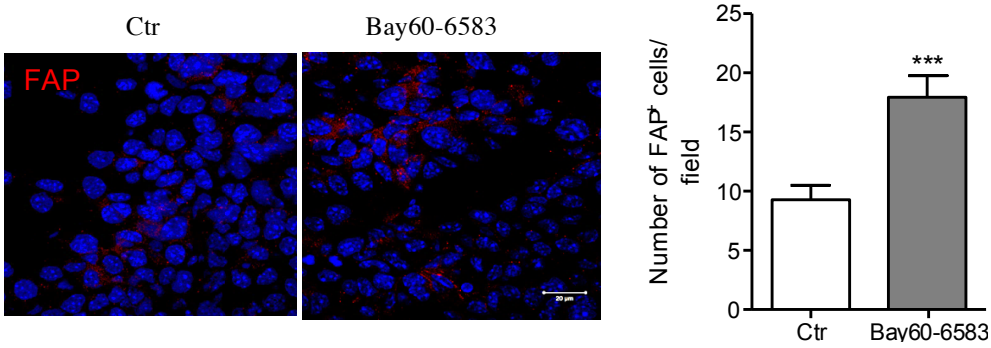
Ctr
Bay60-6583
FAP
Number of FAP+ cells/ field
25
20
15
10
5
0
***
Ctr
Bay60-6583

C)

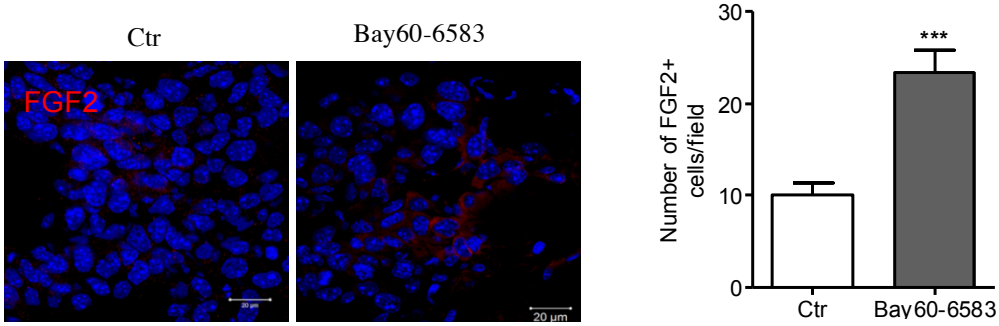
Ctr
Bay60-6583
FGF2
20 µm
Number of FGF2+ cells/field
30
20
10
0
***
Ctr
Bay60-6583

D)

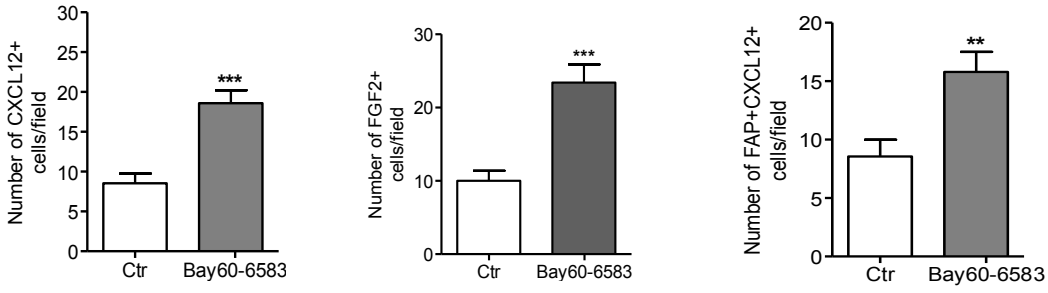
Number of CXCL12+ cells/field
30
25
20
15
10
5
0
***
Ctr
Bay60-6583
Number of FGF2+ cells/field
30
20
10
0
***
Ctr
Bay60-6583
Number of FAP+CXCL12+ cells/field
20
15
10
5
0
**
Ctr
Bay60-6583

Figure 2.3.6 Immunofluorescence analysis of **A)** $A_{2B}R$ expression on FAP+ cells **B)** FAP+ cells and **C)** FGF-2+ cells in melanoma sections harvested from mice treated with Bay60-6583 or vehicle (ctr). **D)** Number of CXCL12+ cells, FGF2+ cells and FAP+ CXCL12+ cells in tumor tissues harvested from mice treated with Bay60-6583 or vehicle (ctr). Data represented are from three different experiments and represent mean ±SEM (n=6-10 per group). *p<0.05, **p<0.01, ***p<0.001.

2.3.7 $A_{2B}R$ stimulation induces FGF-2 and CXCL12 expression in isolated melanoma-associated fibroblasts

We then isolated fibroblasts from melanoma tissue. Isolated cells treated with 10 nM Bay60-6583 for 24 hours showed increased expression of both FGF2 and CXCL12 compared to vehicle-treated cells (Figure 2.3.7_1 A). These effects were reverted by treating melanoma-associated fibroblasts with the $A_{2B}R$ antagonist PSB1115 at 100 nM (Figure 2.3.7_1 B), demonstrating that the increased FGF-2 and CXCL12 expression in melanoma-associated fibroblasts treated with Bay60-6583 occur in an $A_{2B}R$-dependent manner.

A)

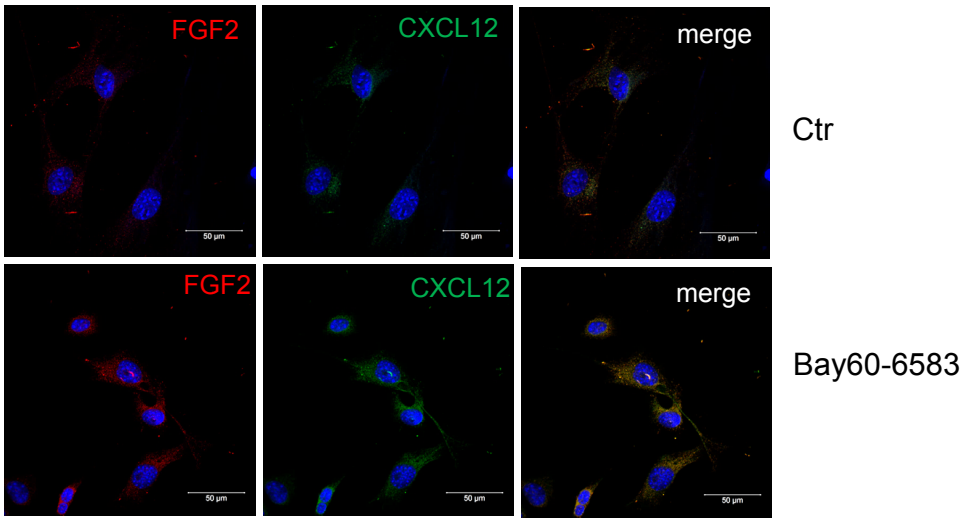

B)

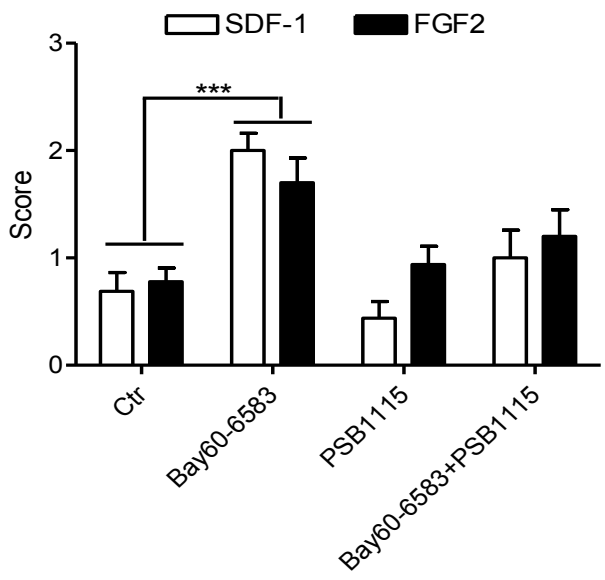

Figure 2.3.7_1 A) Representative immunofluorescence image of melanoma-isolated fibroblasts from mice treated with Bay60-6583 or vehicle (ctr), stained with FGF-2 and CXCL12 antibodies. **B)** Analysis of CXCL12 and FGF2 expression in melanoma-isolated fibroblasts stimulated or not with Bay60-6583 10nM or PSB1115 100nM for 24 hours.

Similar results were also obtained in fibroblasts isolated from skin of C57Bl6 mice exposed for 24 hours to a hypoxia-inducing treatment ($CoCl_2$ 100 μM) as a tumor stressor (81) and then treated with Bay60-6583 for other 24 hours (Figure 2.3.7_2 A). In these experimental conditions, the expression of HIF-1α was induced in hypoxic cells compared with control cells (Figure 2.3.7-2 D). Although, the expression of $A_{2B}R$ could be induced in a HIF-1α-dependent manner (50), we surprisingly observed that the $A_{2B}R$ expression was not induced in hypoxic fibroblasts (Figure 2.3.7_2 B), while CD73, the enzyme responsible for the production of extracellular adenosine, was induced (Figure 2.3.7_2 C).
Since $A_{2B}R$ share with the $A_{2A}R$ many similarities, to verify whether $A_{2B}R$ was the only adenosine receptor involved in promoting fibroblasts activation in our melanoma model, we treated isolated fibroblasts with the selective $A_{2A}R$ agonist CGS21680 (1 μM) showing that $A_{2A}R$ stimulation did not have any effect on the expression of CXCL12 and FGF2 (Figure 2.3.7_2 D).

A)

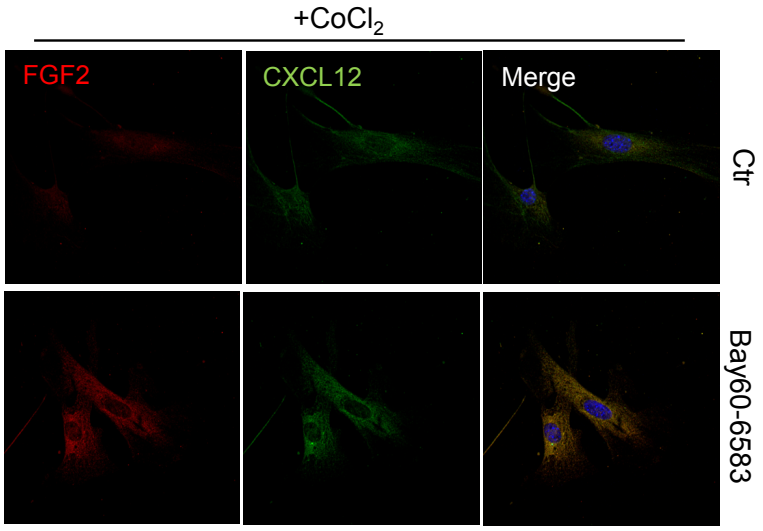
+CoCl2
FGF2
CXCL12
Merge
Ctr
Bay60-6583

B)

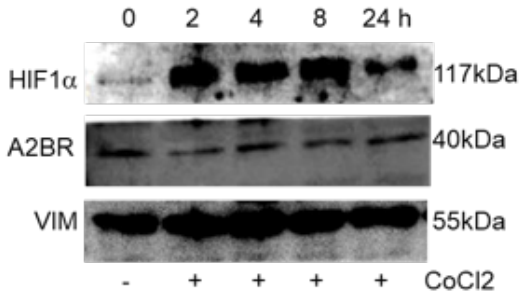
0 2 4 8 24 h
HIF1α
117kDa
A2BR
40kDa
VIM
55kDa
- + + + + CoCl2

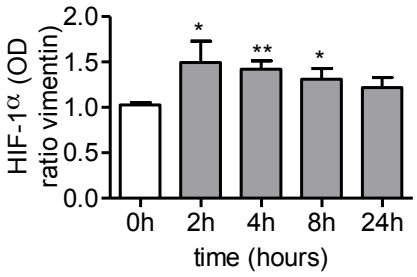
HIF-1α (OD ratio vimentin)
2.0
1.5
1.0
0.5
0.0
*
**
*
0h 2h 4h 8h 24h
time (hours)

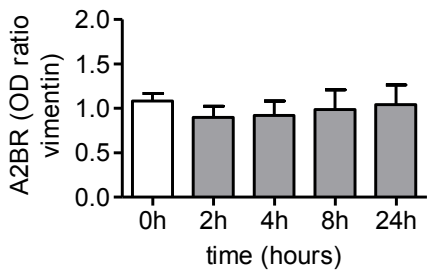
A2BR (OD ratio vimentin)
2.0
1.5
1.0
0.5
0.0
0h 2h 4h 8h 24h
time (hours)

C)

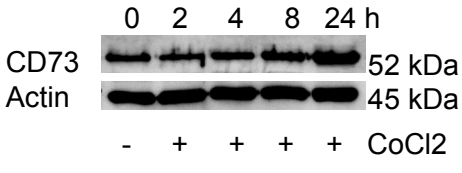
0 2 4 8 24 h
CD73
52 kDa
Actin
45 kDa
- + + + + CoCl2

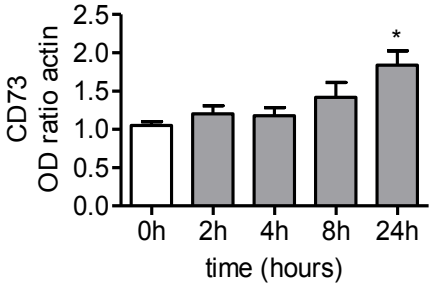
CD73 OD ratio actin
2.5
2.0
1.5
1.0
0.5
0.0
*
0h 2h 4h 8h 24h
time (hours)

D)

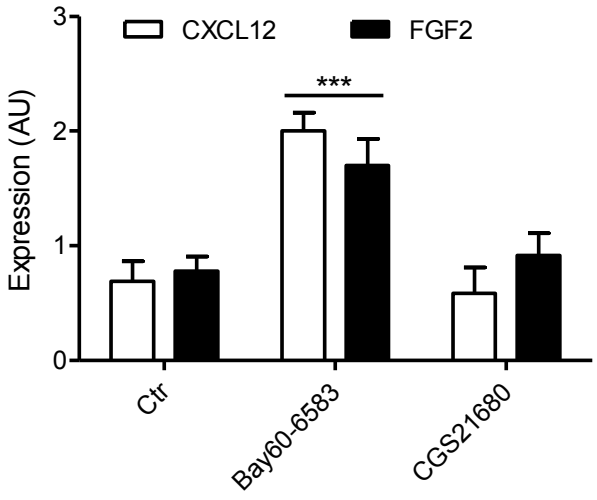

Figure 2.3.7_2 A) Immunofluorescence image of skin-derived fibroblasts exposed to hypoxia (100μM CoCl2) for 24 hours and then stimulated with Bay60-6583 10nM for another 24 hours or control cells. Western blotting analysis of **B)** HIF1α and $A_{2B}R$ expression and **C)** CD73 expression in skin-derived fibroblasts under hypoxic conditions. **D)** Expression of CXCL12 and FGF2 upon $A_{2B}R$ (Bay60-6583) and $A_{2A}R$ (CGS21680) stimulation in isolated fibroblasts. Data represented are from three different experiments and represent mean ±SEM (n=10 per group). *p<0.05, **p<0.01, ***p<0.001.

Accordingly, our findings suggest a sole role of $A_{2B}R$ in fibroblast activation within tumor microenvironment, which helps to promote tumor growth.

2.3.8 FGF-2 released from fibroblasts upon $A_{2B}R$ stimulation induces melanoma cells proliferation

The proliferation of B16-F10 melanoma cells co-cultured with fibroblasts *in vitro* increased after administration of Bay60-6583 and it was blocked when the $A_{2B}R$ antagonist PSB1115 was added to the co-culture (Figure 2.3.9 A). Since stimulation of $A_{2B}R$ in fibroblasts induces FGF-2 expression we hypothesized that the increased proliferation of B16-F10 cells co-cultured with fibroblasts was due to fibroblast-derived FGF-2 upon Bay60-6583 administration. To test this hypothesis, we administered to cells an anti-FGF2 antibody (30-100 ng/ml) that was able to abrogate the effect of Bay60-6583 (Figure 2.3.9 A). Importantly, the

proliferation of neither isolated fibroblasts (Figure 2.3.9 B) nor B16.F10 melanoma cells alone (data not showed) was affected by Bay60-6583 treatment.

A) **B)**

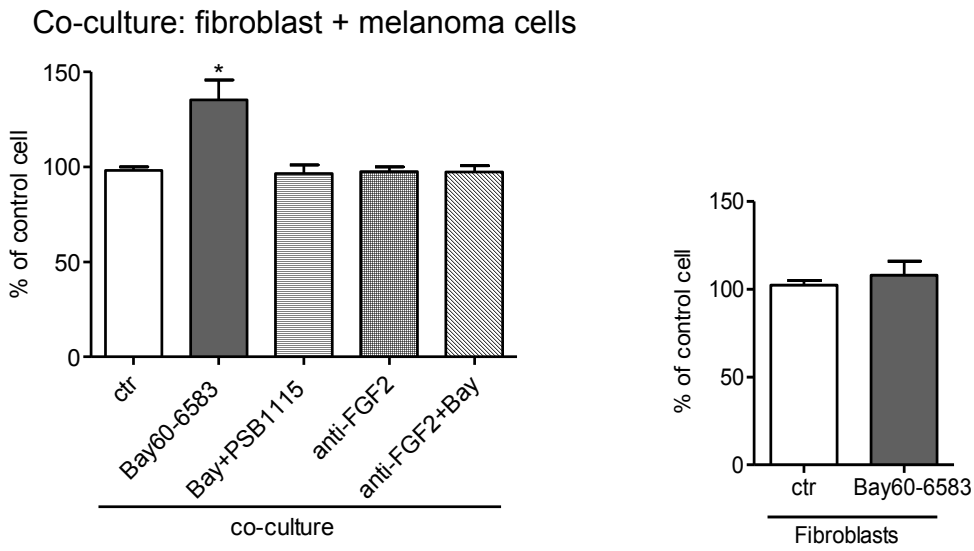

Figure 2.3.9 A) Proliferation of B16-F10 melanoma cells co-cultured with tumor-associated fibroblasts (ratio 1:1) in presence of vehicle (ctr), Bay60-6583, anti-FGF2 antibody or both in combination for 24 hours. **B)** Proliferation of melanoma-associated fibroblasts. Data represented are from two different experiments and represent mean ±SEM. *p<0.05, **p<0.01, ***p<0.001.

Altogether, these findings suggest that FGF-2, released from fibroblasts upon $A_{2B}R$ stimulation, induces melanoma cells proliferation, as reported by other authors (82-85).

2.3.9 $A_{2B}R$-induced CXCL12 expression in stromal cells contributes to its pro-angiogenic effect

Afterwards, we decided to investigate and study the involvement of CXCL12/CXCR4 pathway in our experimental conditions. CXCL12 and its receptor CXCR4 are important for immunosuppressive cells recruitment such as MDSCs and Tregs within tumor microenvironment (34) and for tumor angiogenesis (39). To study the possible involvement of the CXCL12/CXCR4

pathway in $A_{2B}R$-mediated effects within tumor environment, melanoma-bearing mice were treated with AMD3100, a selective CXCR4 receptor antagonist (86, 87), which was able to partially block the pro-tumor activity of Bay60-6583 *in vivo* (Figure 2.3.10 A). AMD3100 treatment did not suppress either the accumulation of MDSCs or the percentage of tumor-infiltrating CD8+, CD4+ T cells or FoxP3+ T cells (Figure 2.3.10 B, C, D and E, respectively). Conversely, CXCR4 blockade was able to reduce the microvessel density induced by Bay60-6583 (Figure 2.3.10 F).

A)

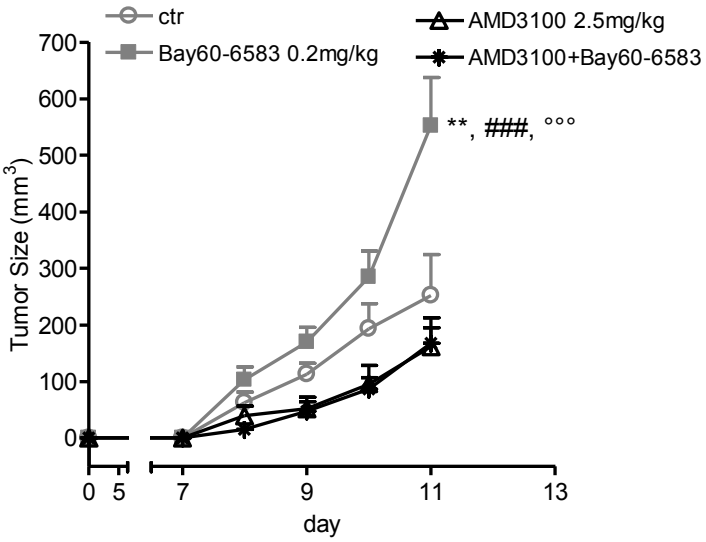

B)

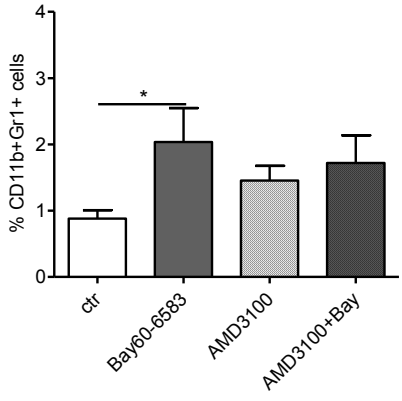

C)

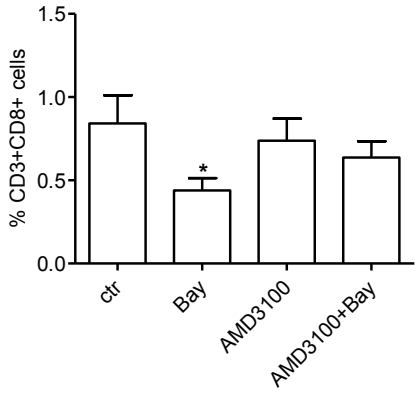

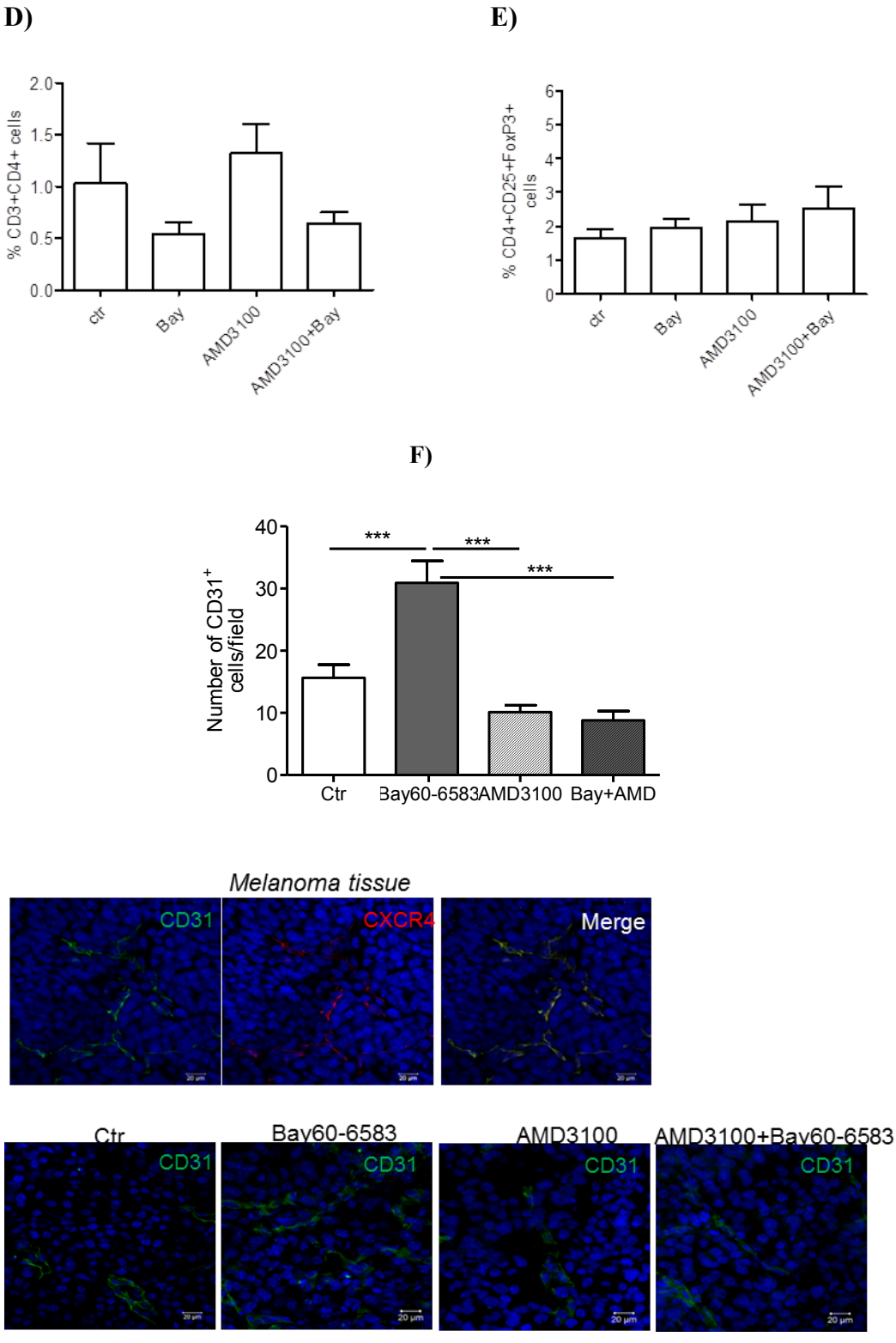

Figure 2.3.10: A) Tumor growth measured in control mice (ctr) or mice treated with Bay60-6583, AMD3100, AMD3100+Bay60-6583. Data represented are from two different experiments and represent mean ±SEM. **p<0.01 versus Ctr,

###, p<0.001 versus AMD3100 and °°°, p<0.001 versus AMD3100 + Bay60-6583 (ANOVA). **B)**, **C), D) and E)** Cytofluorimetric analysis of CD11b+Gr1+ cells, CD3+CD4+ T cells, CD3+CD8+ T cells and CD4+FoxP3+CD25+ cells, respectively, in melanoma tissues of mice treated as described. **F)** Number of CD31+ cells (*upper*) and immunofluorescence image showing CD31 and CXCR4 expression (*lower*) in melanoma tissue sections of mice treated as described above. Data represented are from two different experiments and represent mean ±SEM. *p<0.05, **p<0.01, ***p<0.001.

Taken together, these data suggest that A_{2B}R-induced CXCL12 expression in stromal cells contributes to its pro-angiogenic effect rather than immune-suppressive effects, establishing a positive cross-talk between fibroblasts and endothelial cells that sustains tumor growth.

2.3.10 A_{2B}R inhibition reduces FAP and FGF-2 expression within melanoma tissues

Our results indicate that A_{2B}R may have an important role in enhancing the activation of stromal cells, that release tumor-promoting mediators. To prove the translational potential of these findings we verified whether the administration of A_{2B}R antagonist PSB1115 in mice was able to affect the activity of melanoma-associated fibroblasts *in vivo*. Melanoma sections from PSB1115-treated mice showed a reduced number of FAP+ cells (Figure 2.3.11 A) and these data were also confirmed by flow cytometric analysis (Figure 2.3.11 B).

Since the number of FAP cells could be related to the tumor volume, and in PSB1115-treated mice the tumor volume results significantly lower than those observed in control mice, we performed these analyses in tumors of similar sizes harvested from either PSB1115-treated mice and control mice. The number of FAP+ cells did not correlate with the size of tumor (Figure 2.3.11 C) suggesting that the reduced number of these cells in PSB1115-treated mice is dependent on the treatment rather than reduced tumor size. Moreover, we also verified that melanoma sections of mice treated with PSB1115 also showed reduced expression of FGF-2 and CXCL12 (Figure 2.3.11 D).

A)

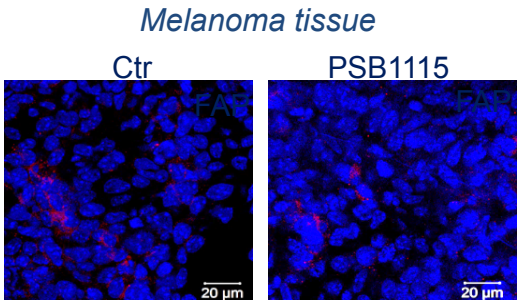
Melanoma tissue
Ctr
PSB1115
FAP
20 µm
FAP
20 µm

B)

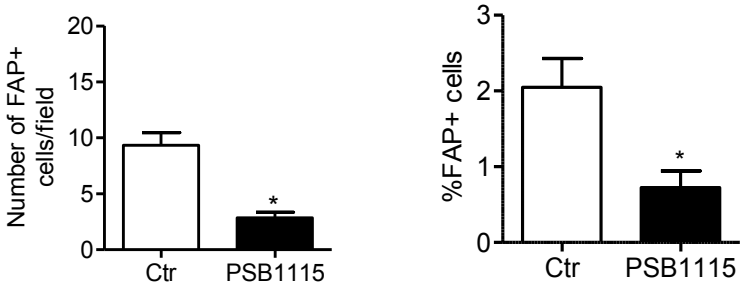
Number of FAP+ cells/field
20
15
10
5
0
*
Ctr
PSB1115
%FAP+ cells
3
2
1
0
*
Ctr
PSB1115

C)

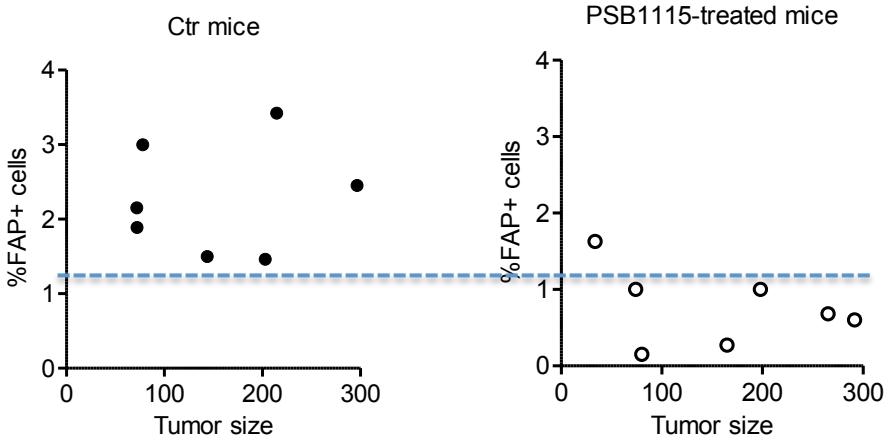
Ctr mice
%FAP+ cells
4
3
2
1
0
0
100
200
300
Tumor size
PSB1115-treated mice
%FAP+ cells
4
3
2
1
0
0
100
200
300
Tumor size

D)

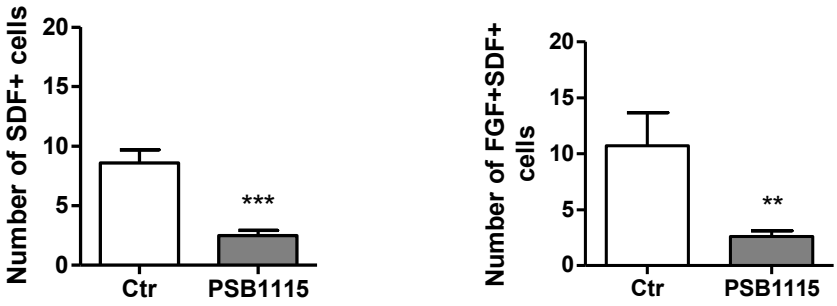
Number of SDF+ cells
20
15
10
5
0
***
Ctr
PSB1115
Number of FGF+SDF+ cells
20
15
10
5
0
**
Ctr
PSB1115

Figure 2.3.11 A) Representative immunofluorescence image (left panel) and number of FAP+cells (right panel) in melanoma tissues from PSB1115 treated mice and control mice (ctr). **B)** FAP positive cells in PSB1115 treated mice compared to control mice analysed by flow cytometry. **C)** Number of FAP+ cells in control mice and mice treated with PSB1115 in correlation with the tumor size. **D)** Number of SDF+ (or CXCL12+) cells (*left panel*) and FGF2+ SDF+ cells (*right panel*) in PSB1115-treated mice compared with control mice. Data represented are from two different experiments and represent mean ±SEM. *p<0.05, **p<0.01, ***p<0.001.

2.4 Discussion

Tumor microenvironment is made up of several different types of cells, including malignant cells, endothelial cells, cancer-associated fibroblasts and tumor-infiltrating immune cells that cooperate to the development of cancer. Adenosine plays a pivotal role in tumor immunity, angiogenesis and metastasis, promoting the development of anti-cancer strategies to inhibit tumor adenosine production and functions (for example by using CD73 inhibitors or selective $A_{2A}R$ blockers alone or in combination with chemotherapeutic agents and immune-checkpoints inhibitors). Emerging evidence suggest that $A_{2B}R$ can mediate the pro-tumor effects of adenosine in the tumor microenvironment and targeting $A_{2B}R$ has proved to be effective in some murine tumor models but the mechanisms underlying these effects are still incomplete.

Here we investigated the effects of pharmacological modulators of $A_{2B}R$ in tumor tissue and surrounding stroma. We firstly demonstrated that $A_{2B}R$ stimulation promotes tumor growth *in vivo* by inducing both tumor immunosuppression and angiogenesis. These effects were associated with an increased presence of MDSCs within tumor lesion, that can critically impair T cell proliferation and activity, as well as tumor angiogenesis.

Anti-VEGF therapy can be effective in controlling tumor growth especially in human cancer patients (88-91) but the efficacy of these therapies can be limited by several mechanisms, including accumulation of MDSCs in tumor lesions (92). Melanoma-bearing mice treated with Bay60-6583, a selective ligand of $A_{2B}R$, showed accumulation of CD11b+Gr1+ cells, reduced number of T cells and enhanced VEGF-A expression and vessel density within tumor tissue. Several cell types may contribute to A_{2B}-induced VEGF-A secretion including endothelial cells, which express $A_{2B}R$. Stimulation of both melanoma cells and isolated CD11b+ cells with Bay60-6583 did not induce VEGF-A secretion. However, the selective depletion of Gr1+CD11b+ cells *in vivo* reduced VEGF-A expression in tumor tissues, leading to a significant delay in the tumor progression. Therefore, MDSCs accumulation within tumor lesions induced by $A_{2B}R$ stimulation is responsible not only for MDSC-mediated immune suppression in the tumor

microenvironment but also for enhanced tumor angiogenesis. Furthermore, one of the main transcriptional activators of VEGF-A expression in tumor lesions is STAT3, whose activation upregulates the expression of inflammatory and pro-angiogenic genes, including VEGF-A leading a strong tumor progression and angiogenesis (93). We observed that the activation of STAT3 enhanced in melanoma tissue of mice treated with Bay60-6583. Accordingly, inhibition of STAT3 abrogated the pro-tumor activity of Bay60-6583 and reduced tumor VEGF-A expression. Nevertheless, we still do not know if in our model, A_{2B} stimulation can directly act through STAT3 considering that STAT3 can be also activated by other pro-angiogenic factors. Previously our group demonstrated that adenosine could increase the IL10 release (34) that could lead to STAT3 activation in M2-like macrophages in an $A_{2B}R$ dependent manner (94). This hypothesis reserve more future investigations.

Importantly, pharmacological blockade of $A_{2B}R$ with PSB1115 significantly reduced tumor growth. This effect is associated with reduced expression of VEGF-A and vessel density within melanoma sections and reduced the presence of MDSCs in the tumor, which critically contribute both to inhibit T cell response and release VEGF-A. Of note, the effectiveness of anti-VEGF treatment enhanced in mice treated with PSB1115. Therefore, targeting $A_{2B}R$ with a selective antagonist can limit tumor growth by reducing tumor angiogenesis and MDSC-mediated immunosuppression.

Tumor-associated fibroblasts are critical component of tumor stroma and they produce and secrete various tumor-promoting factors including CXCL12/SDF1α. We next demonstrated that $A_{2B}R$ stimulation resulted in enhanced number of FAP and FGF-2 positive cells in melanoma lesions and accordingly PSB1115-treated mice showed a reduced number of FAP and FGF-2 positive cells compared to controls. Stimulation of $A_{2B}R$ was also correlated to an increased CXCL12 expression in FAP+ cells both in melanoma tissues and in isolated tumor-associated fibroblasts. Similar results were obtained in isolated mouse skin fibroblasts exposed to CoCl2 to mimic hypoxic conditions, a common feature of tumor microenvironment. These effects were $A_{2B}R$-dependent as demonstrated by the co-administration of $A_{2B}R$ antagonist PSB1115 and by data from cells treated

with the $A_{2A}R$ agonist CGS-21680, which did not affect either FGF-2 or CXCL12 expression. We evaluated the expression of $A_{2B}R$ in the cell lysates and, in contrast to our expectation, we were unable to find any regulation of $A_{2B}R$ expression. Conversely, CD73 expression was up-regulated in hypoxic fibroblasts confirming that these cells can contribute to the production of extracellular adenosine. We also observed that FGF-2 stimulation directly promoted the proliferation of B16-F10 melanoma cells co-cultured with tumor-isolated fibroblasts. Altogether, these findings suggest that this growth factor, FGF-2, released from fibroblasts upon $A_{2B}R$ stimulation may participate to the pro-tumor effects of the $A_{2B}R$ by inducing melanoma cells proliferation. The next step was to investigate and study the involvement of CXCL12/CXCR4 pathway in our melanoma mouse model. In our melanoma mouse model, B16-F10 melanoma cells did not express CXCL12 or CXCR4. From the literature we know that the inhibition of CXCR4 with AMD3100 improves T-cell responses in pancreatic cancer or prevents immune suppression in UV-induced skin cancer (95-97). In our melanoma mouse model, AMD3100 did not suppress the accumulation of tumor MDSCs and did not change the number of FoxP3 regulatory T-cells or CD8+T cells infiltrated into the melanoma lesions of Bay60-6583-treated mice compared to control mice. Instead, CXCR4 blockade was able to reduce the microvessel density induced by Bay60-6583.

To sum up, in this Chapter, we described a novel role for $A_{2B}R$ which consists in promoting tumor growth by 1. contributing to the adenosine–mediated immunosuppressive effects, by regulating the accumulation of MDSCs within tumor tissue (MDSCs are potent suppressors of T effector cells) that critically contribute also to the pro-angiogenic effects of $A_{2B}R$ within tumor microenvironment and 2. modulating the activity of stromal fibroblasts that, in turn, produce tumor-promoting soluble factors such as FGF-2 and CXCL12.

These results provide new insights into the mechanisms through which pharmacological manipulation of $A_{2B}R$ regulates intercellular crosstalk in the tumor microenvironment and support the therapeutic potential of A_{2B} antagonists as anti-cancer agents.

Chapter 3

CHAPTER 3

Notch1-$A_{2A}R$ cross-talk in murine activated CD8+ T cells

3.1 Introduction

CD8+ T cells are activated upon their TCR stimulation in response to cognate peptide MHC II complexes on antigen-presenting cells (APCs) and co-stimulatory molecules, including CD80 and CD86 (Figure 3.1.1). The adenosine receptor mainly expressed on lymphoid cell population is $A_{2A}R$, whose stimulation is able to interfere with the early events upon T cell receptor (TCR) activation determining T cell anergy, in a cAMP-dependent manner (17, 98-100).

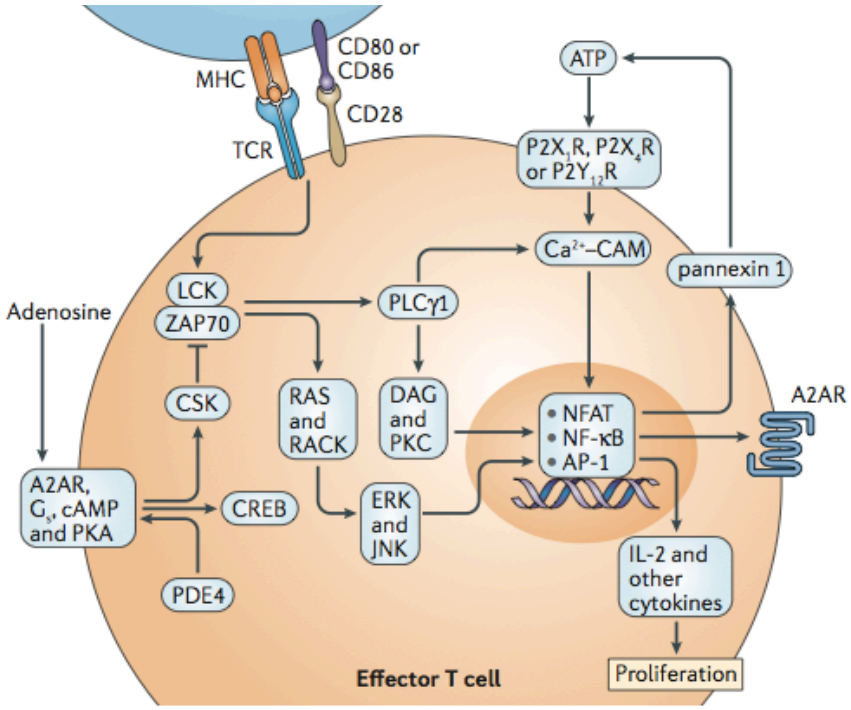

Figure 3.1.1: Purinergic signalling in effector T cells (101).

Adenosinergic modulators of $A_{2A}R$ suppress the activation and effector functions of T cells (17, 98, 102). In naive CD8+ T cells adenosine via $A_{2A}R$ inhibits early TCR signalling events by reducing ZAP 70 tyrosine phosphorylation, which is required for the TCR signal transduction (Figure 3.1.1). This effect is a consequence of reduced activity of the kinase Csk, whose phosphorylation is in

turn inhibited by protein kinase A (PKA) type I (103). In other words, stimulation of $A_{2A}R$ in CD3/CD28 activated T cells, increasing cAMP levels, activates the PKA which inhibits proximal TCR signalling events, including the phosphorylation of ZAP 70, preventing the phorsphorylation of Akt and ERK1/2 and the calcium influx (Figure 3.1.1) (104).

T cells are essential effectors of tumor immunity (18). One of the crucial signalling pathway involved in T-cell development, lineage selection and activation is Notch. Recent studies highlight the pivotal role of Notch signalling in the differentiation and function of several T cell subsets (19). Notch proteins (Notch 1-4) are transmembrane receptors that are activated by engagement of transmembrane-bound ligands (Delta-like 1, 3, 4 and Jagged 1, 2, although Delta-like 3 is likely an inhibitory receptor) (Figure 3.1.2).

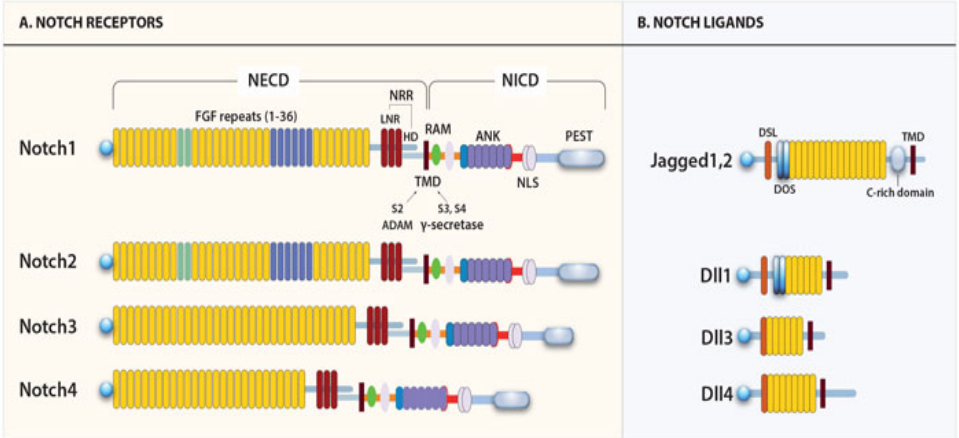

Figure 3.1.2: Schematic diagram of receptors and Notch ligands (105).

The interaction of Notch receptors with their ligands leads to a proteolytic cleavage that can release the active intracellular domain of Notch (NICD) (canonical Notch activation pathway). However Notch can be also activated upon TCR stimulation in a non-canonical fashion in the absence of Notch receptor ligation (20). NICD then translocates into the nucleus where it associates with the transcriptional repressor CSL (CBF1-Suppressor of Hairless-Lag1), recruiting a co-activator complex, resulting in the expression of genes regulated by CSL (103) (Figure 3.1.3).

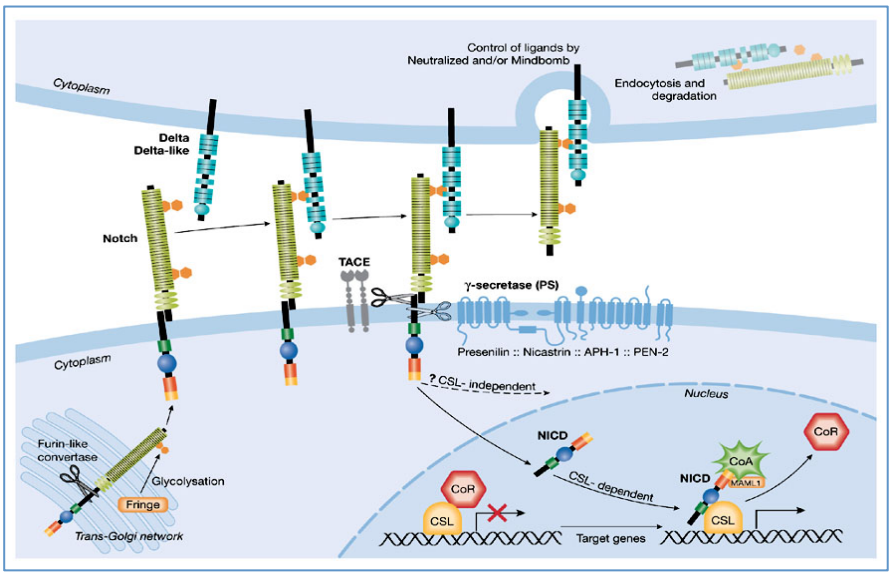

Figure 3.1.3: Schematic diagram of Notch expression and activation (106).

A number of pharmacological strategies have been developed to target Notch signalling pathway at different levels of the cascade, including monoclonal antibodies against receptors and ligands (107-109) and γ-secretase inhibitors (GSIs) that can prevent the last cleavage of Notch, decreasing the levels of NICD (110, 111).

It is well documented that Notch signalling is required for T-cell activation and for the cytotoxic activity of CD8+ T cells (112). Notch1 is also required for the differentiation of CD8+ effector cells (21) and constitutive expression of active Notch1 renders CD8+ T cells resistant to the immune suppressive activity of MDSCs (22).

Here we evaluated the possible Notch1-$A_{2A}R$ signalling pathways cross-talk in activated CD8+ T cells.

3.2 Materials and Methods

3.2.1 Cell isolation

Splenocytes were collected aseptically from the spleen of naïve C57Bl6 mice, NIIC mice and A_{2A}KO (kindly provided by Dr. Sitkovsky) and CD8+ T cells were isolated by immunomagnetic negative selection kit (EasySep Mouse CD8+ T Cell Isolation Kit, Stem Cell Technologies). Briefly, harvested spleens were mechanically digested in sterile PBS (Phosphate-Buffered Saline) and splenocytes suspension was processed with the Isolation Kit, according to manufacturer's instruction, to isolate CD8+ T cell. Isolated cells were seeded on an anti-CD3/CD28 antibodies-coated plate and cells were treated at time 0 or after 24 hours from the activation with the following agents:

- CGS-21680 1 μM, A_{2A}R agonist (Tocris),
- ZM-241385 1 μM, A_{2A}R antagonist (Tocris),
- PF-03084014 1 μM, Notch1 inhibitor (Selleckchem),
- Forskolin 10 μM, adenylate cyclase stimulator (Sigma-Aldrich),
- Cycloheximide 10 μM (Sigma-Aldrich).

CD8+ T cells were grown in RPMI 1640 medium supplemented with 10% FBS, 4 mM L-Glutamine, 50 U/mL penicillin, 50 μg/mL streptomycin and 50 μM 2-mercaptoethanol.

3.2.2 Proliferation assay

To study how the treatments could affect CD8+ T cells proliferation, cells were stained with carboxyfluorescein diacetate succinimidyl ester (CFDA-SE, Life technologies) according to manufacturer's protocol. Stimulated cells were collected after 72 hours of treatments (treated at time 0 or after 24 hours from the activation) and analysed by flow cytometer.

3.2.3 Enzyme-Linked Immunosorbent Assays

Granzyme B and IFN-γ concentration was measured by ELISA kits (Invitrogen by Thermo Fisher Scientific) in the supernatants of CD8+ T cells after 72 hours of treatments (treated at time 0 or after 24 hours from the activation).

3.2.4 Western blotting

Cells were collected and washed in PBS before RIPA buffer lysis (SantaCruz Technology) in which was freshly added 1mM Protease and Phosphatase Inhibitor Cocktail (Thermo Scientific), 1 mM PMSF and 1 mM sodium orthovanadate. After protein concentrations determination, using Bio-Rad protein assay, samples were analysed by 7.5% Criterion TGX Precast Gels (Bio-Rad) and transferred electrophoretically to PVDF membranes (Immobilion-FL Transfer Membrane) or nitrocellulose membranes. Bovine serum albumin (BSA, Sigma) was used to block non-specific binding sites and membranes were incubated then with primary antibodies to evaluate the expression of Cleaved Notch 1 (NICD), Notch1 (C-20-R, sc-6014), pAKT (Ser473), Akt (pan), pGSK-3β (Ser9), GSK-3β (all these antibodies were purchased from Cell Signaling) and GAPDH, β-actin or β-tubulin (Santa Cruz) as protein loading control. After incubation with secondary antibodies, immunoreactive protein bands were detected by enhanced chemiluminescence reagents (Amersham Pharmacia Biotech, Buckinghamshire, UK) and analysed by Las4000 (GE Healthcare Life Sciences).

3.2.5 Real time RT-PCR

mRNA levels from CD8+ T cells were analysed by Real-time PCR. Total RNA was isolated from treated cells using RNeasy Mini kit (Qiagen) following the manufacturer's instructions. Reverse transcription was performed with random hexamer primers or specific primers using the First strand cDNA synthesis Kit (Fermentase Life Science Co., EU) according to the manual. cDNAs were amplified by real time PCR using iTaqTM SYBR Green Supermix with ROX (Bio-RAd, CA). Samples were run in triplicate in a 96well Optical Reaction plate (Applied Biosystems, CA). The PCR reaction conditions were: 50°C for 2 min, 95°C for 5 min, 35 cycles of 95°C for 30 sec, 59°C for 1 min, 72°C for 1 min, followed by dissociation step. Results were analysed by utilizing the 7300 system Software (Applied Biosystems, CA).

The primer sequences used were:

Notch1(Forward):AGCGGGGTATGCAAGGAGTC,(Reverse):CTCGCAGGTTTGACCTTGCC;

Hes1(Forward):CTGGTGCTGATAACAGCGGAATC,(Reverse):AGTGATCGG TAGCACTATTCCAGG;
Myc(Forward):GCAGATCAGCAACAACCGCA,(Reverse):CCAAGACGTTGT GTGTCCGC;
IFNγ(Forward):TGCATCTTGGCTTTGCAGCTC,(Reverse): GGCTTTCAATGAGTGTGCCGT.

3.2.6 cAMP assay

To study the involvement of cAMP pathway in Notch1-modulated signal upon $A_{2A}R$ stimulation, we performed a cAMP assay (abcam_ab65355) according to manufacturer's instruction. cAMP levels were measured in cells after 10 min of treatment with CGS-21680 1μM or Forskolin 10μM. The kit used was made up of recombinant Protein G coated 96-well plate to efficiently anchor cAMP polyclonal antibody on to the plate. cAMP-HRP conjugate directly competed with cAMP present in samples of activated CD8+ T cells and bound to the cAMP antibody on the plate. The amount of cAMP-HRP bound to the plate can easily be determined by reading HRP activity at OD 450 nm. The intensity of OD 450 nm is inversely proportional to the concentration of cAMP in samples.

3.2.7 Statistical analysis

Data are from at least two-three independent experiments and results are expressed as mean ± SEM.

The optical density of the protein bands detected by Western blotting was performed with ImageQuantTL (Ge Healthcare). Data were analysed with GraphPad Prism 6 (GraphPad Software). Two-tailed Student's t test (2-group comparisons) or ANOVA (> 2-group comparisons) were performed as appropriate. P values < 0.05 were considered significant.

3.3 Results

3.3.1 $A_{2A}R$ stimulation leads to reduced expression of NICD and Notch1 in activated CD8+ T cells

Although Notch1 expression and activation is known to be induced in a TCR-dependent manner and its activity is associated with proliferation of T cells and cytokines production (112), the effect of adenosinergic modulators of $A_{2A}R$ on the expression and activity of Notch is not known. To this end we used CD8+ T cells isolated from spleen of C57Bl6 mice. Cells were activated with anti-CD3/CD28 antibodies. Consistent with previous results (112), the expression of Notch1 proteins (the intracellular Notch1 domain, NICD, and the transmembrane Notch 1 portion, Notch1^{TM}) was induced in activated CD8+ T cells compared with unstimulated cells (Figure 3.3.1 A). Interestingly, we found that the expression of Notch 1 proteins was present from 3 hours up to 72 h of TCR stimulation (3-6-24-48 and 72h) (data not shown) (113). Shown are data at 72 h of treatment, but similar results were obtained at all time points. To determine whether activation of $A_{2A}R$ affected the TCR-induced Notch1 expression, CD8+ T cells were treated with the selective agonist of $A_{2A}R$ CGS-21680 (1μM) and activated with anti-CD3/CD28 antibodies. These experiments revealed that stimulation of $A_{2A}R$ leads to reduced expression of TCR-induced expression of Notch1 proteins (Figure 3.3.1 B, C, D, E). The TCR-induced Notch1 expression was inhibited in presence of the γ-secretase inhibitor PF-03084014 (Figure 3.3.1 B, C, D, E). Moreover, the expression of Notch1 proteins was strongly inhibited in presence of both CGS-21680 and the γ-secretase inhibitor PF-03084014 (Figure 3.3.1 B, C, D, E). The effect of CGS-21680 on Notch1 proteins expression was abrogated in presence of the $A_{2A}R$ antagonist ZM-241385 (1μM) (Figure 3.3.1 D, E). Stimulation of A_{2B} receptor with Bay 60-6583 ($A_{2B}R$ selective agonist) and/or its antagonist PSB-1115 ($A_{2B}R$ selective antagonist) did not induce similar effects, ruling out any role of A_{2B} receptor in modulating the activation of Notch1 in CD8+ T cells upon TCR stimulation (Figure 3.3.1 F).

A)

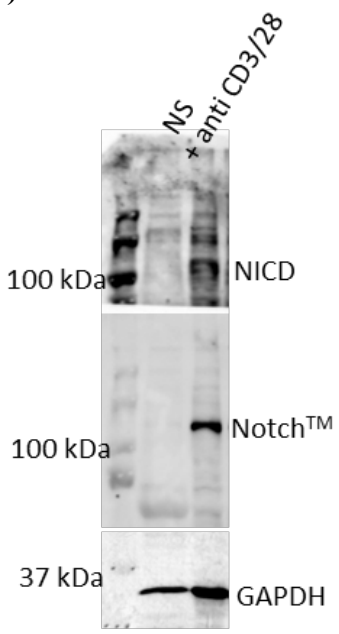
NS
+ anti CD3/28
100 kDa
NICD
100 kDa
Notch™
37 kDa
GAPDH

B)

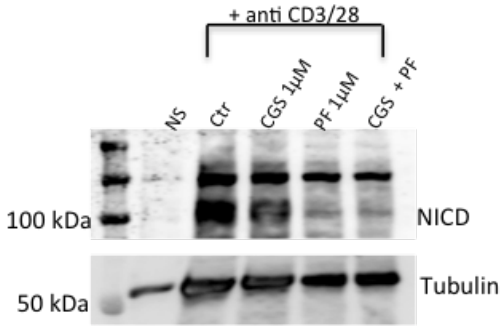
+ anti CD3/28
NS
Ctr
CGS 1µM
PF 1µM
CGS + PF
100 kDa
NICD
50 kDa
Tubulin

C)

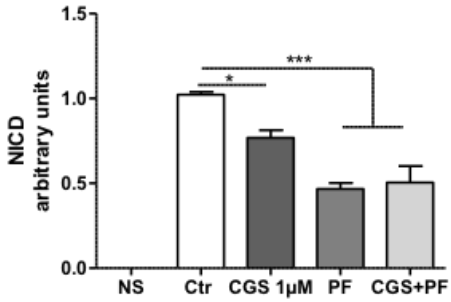
NICD arbitrary units
1.5
1.0
0.5
0.0
*
***
NS
Ctr
CGS 1µM
PF
CGS+PF

D)

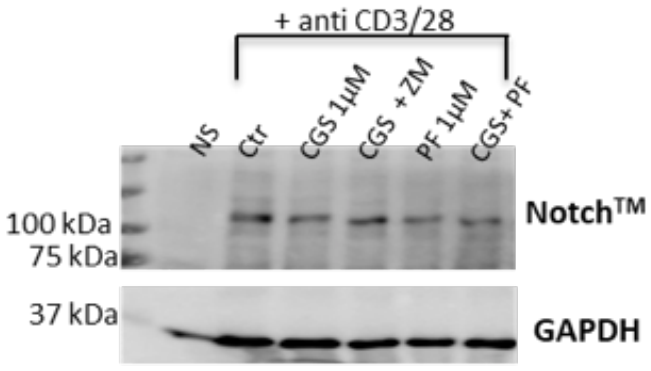
+ anti CD3/28
NS
Ctr
CGS 1µM
CGS + ZM
PF 1µM
CGS+ PF
100 kDa
75 kDa
Notch™
37 kDa
GAPDH

E)

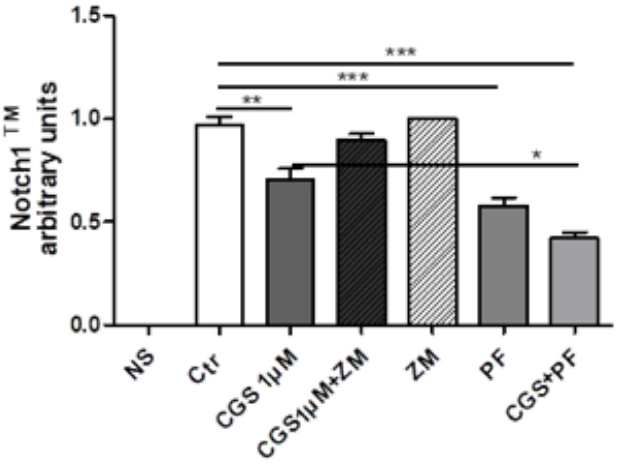

F)

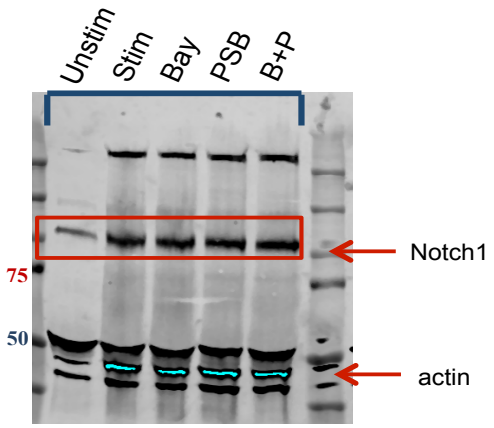

Figure 3.3.1. A) Isolated and activated CD8+ T cells with anti CD3/CD28 antibodies expressed Notch1 proteins upon TCR stimulation (72h). Control cells are indicated as NS. Shown are the Notch1 intracellular domain (NICD) and the transmembrane portion of Nocth1 (Notch^{TM}). **B) and C)** CD8+ T cells treated with an $A_{2A}R$ agonist (CGS-21680, 1 μM for 72 hours) or γ-secretase inhibitor PF (PF-03084014, 1 μM) or in combination (CGS+PF) showed decreased expression of TCR-induced NICD **D) and E)** Expression of Notch1^{TM} in CD8+ T cells treated with an $A_{2A}R$ agonist CGS (CGS-21680, 1 μM), CGS in combination with $A_{2A}R$ antagonist ZM (ZM-241385, 1 μM), γ-secretase inhibitor PF (PF-03084014, 1 μM) or in combination (CGS+PF) for 72 hours, showed decreased expression of NICD. **F)** $A_{2B}R$ agonist treatment (Bay-606583, 1 μM for 72 hours) alone or in combination with its antagonist PSB-1115 (B+P) had no effects on Notch activation in CD8+ T cells. Data represent mean ± S.D. and are from three different experiments. *p<0.5, **p<0.01; ***p<0.001.

These results indicate that stimulation of $A_{2A}R$ resulted in down-regulation of Notch1 proteins in TCR-stimulated CD8+ T cells.

To further investigate the effect of the $A_{2A}R$ agonist on TCR-induced Notch signalling pathway, RT-PCR analyses were performed to analyse the expression of *Notch1* and NICD-targeted genes *Hes1* and *Myc* (109, 110). As shown in Figure 3.3.1 G, the relative transcript levels of *Notch1* remained unchanged upon CGS-21680 administration at 24h, 48h and 72h in activated CD8+ T cells. Conversely, the mRNA levels of Notch1-targeted genes *Hes1* and *Myc* (109, 110) were reduced in cells treated with CGS-21680, PF-03084014 or CGS+PF (Figures 3.3.1 H and I, respectively).

G) *Notch1*

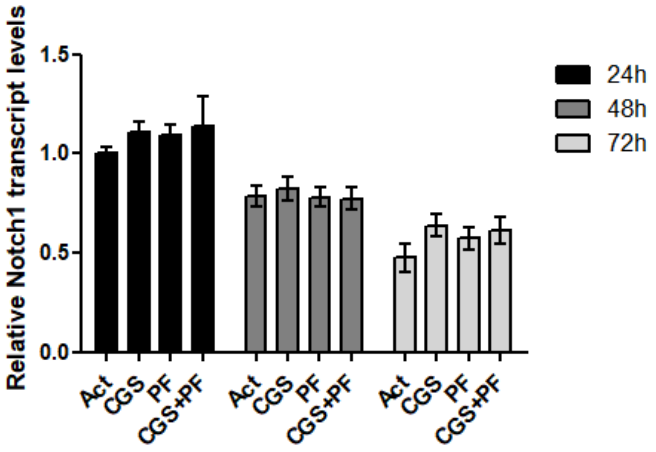

H) *Hes1*

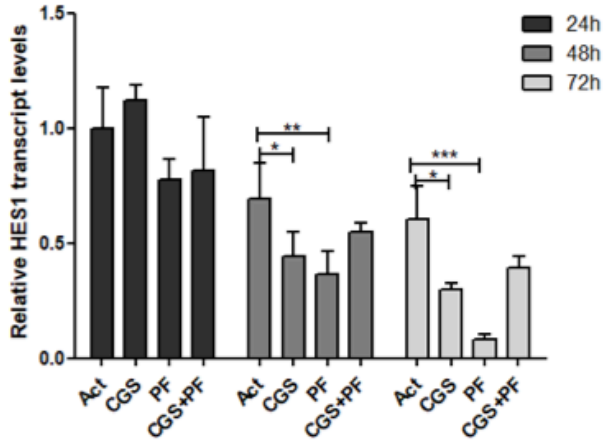

I) *Myc*

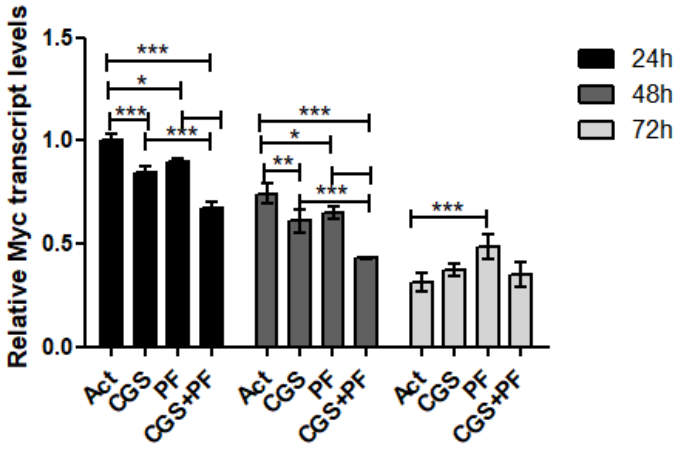

Figure 3.3.1 G) *Notch1* **H)** *Hes1* and **I)** *Myc* relative mRNA levels after 24, 48 and 72 hours of treatment of CD8+ T cells with CGS-21680, PF-03084014 or the combination (CGS+PF) upon activation with anti-CD3/CD28 antibodies. Data represent mean ± S.D. and are from three different experiments. *p<0.5, **p<0.01; ***p<0.001.

Altogether these results indicate that although the stimulation of $A_{2A}R$ in activated CD8+ T cells did not directly control the transcription levels of *Notch1*, it is able to interfere with Notch1-dependent signalling, inhibiting NICD-mediated activity.

3.3.2 $A_{2A}R$ stimulation and Notch1 inhibition strongly reduce the proliferation and effector functions of activated CD8+ T cells

To investigate further the effect of $A_{2A}R$ stimulation on CD8+ T cells we measured the proliferation of T cells and the cytokines production after treatment of cells with CGS-21680 and the γ-secretase inhibitor upon TCR stimulation with anti-CD3/CD28 antibodies. The percentage of proliferating CD8+ T cells was not significantly altered after 72h of activation and treatment with CGS-21680 or PF-03084014 alone, at the concentrations used in this work (Figure 3.3.2 A). However proliferation of activated CD8+ T cells was significantly reduced after treatment with CGS-21680 in combination with PF-03084014 (Figure 3.3.2 A). The levels of Granzyme B (Figure 3.3.2 B) and IFN-γ (Figure 3.3.2 C), measured

in the supernatant of cells, significantly reduced in activated CD8+ T cells treated with CGS-21680 or PF-03084014 alone and even more after CGS+PF administration for 72h. The effect of GCS-21680 on Granzyme B (Figure 3.3.2 B) and IFN-γ (Figure 3.3.2 C) was completely reverted in presence of the antagonist ZM-241385. The levels of IFN-γ were also detected via RT-PCR. The relative transcript levels of *IFN-γ* in activated CD8+ T cells were significantly reduced after CGS-21680 or PF-03084014, alone or in combination, after 24-48 and 72 hours of treatment (Figure 3.3.2 C).

A)

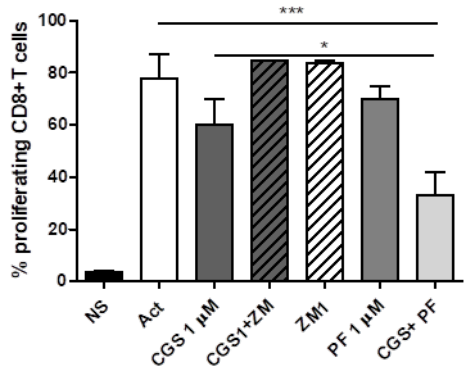

B)

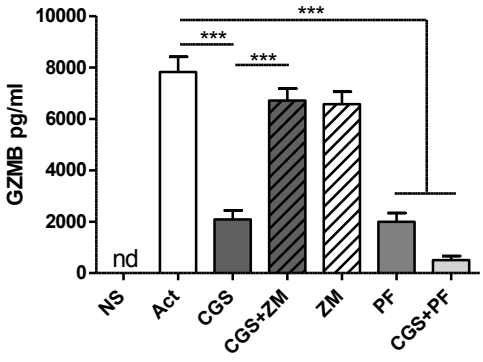

C)

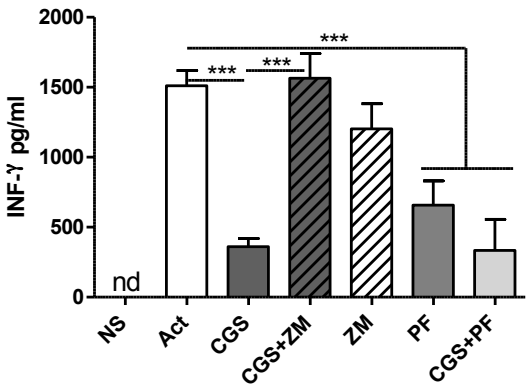

D)

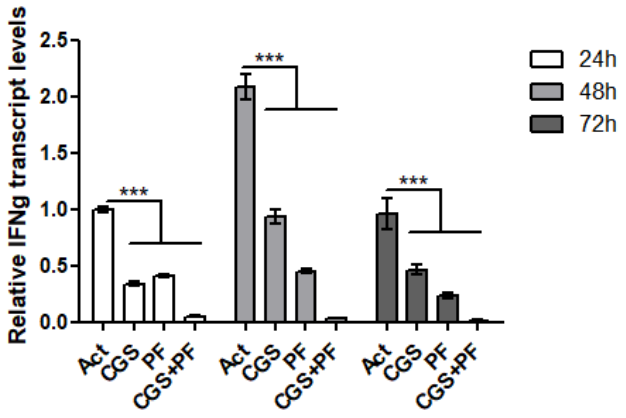

Figure 3.3.2 A) Stimulation of $A_{2A}R$ with CGS-21680 in combination with a GSI (PF-03084014, 1 μM) for 72h significantly decreased proliferation rate. **B)** Granzyme B and **C)** IFN-γ levels and **D)** *IFN-γ* transcript levels in CD8+ T cells treated as described above. Data represent mean ± S.E.M.. and are from three different experiments. *p<0.5; ***p<0.001.

These data confirm that activation of A_{2A} adenosine receptor or inhibition of Notch pathway significantly affect the proliferation and cytokines production of activated CD8+ T cells. Notably, these inhibitory effects were enhanced in cells treated with both agents.

3.3.3 Adenylate cyclase stimulation mimics the effects of $A_{2A}R$ on Notch1 expression in activated CD8+ T cells

Given that stimulation of $A_{2A}R$ inhibits the CD8+ T cells function by impairing the expression and activity of Notch1, we next investigated further the mechanism through which $A_{2A}R$ modulates the Notch signalling pathway. It has previously reported that stimulation of $A_{2A}R$ induce cAMP levels in CD3/CD28-stimulated CD8+ T cells (98, 104). Consistently, we observed that CGS-21680 treatment of CD3/CD28 activated CD8+ T cells increased cAMP levels within few minutes (Figure 3.3.3 A). Using an activator of adenylate cyclase forskolin (10μM), which significantly increased the cAMP levels in activated CD8+ T cells (Figure 3.3.3 B), we found that the expression of Notch1 proteins induced by TCR engagement was significantly inhibited (Figure 3.3.3 C, D and E).

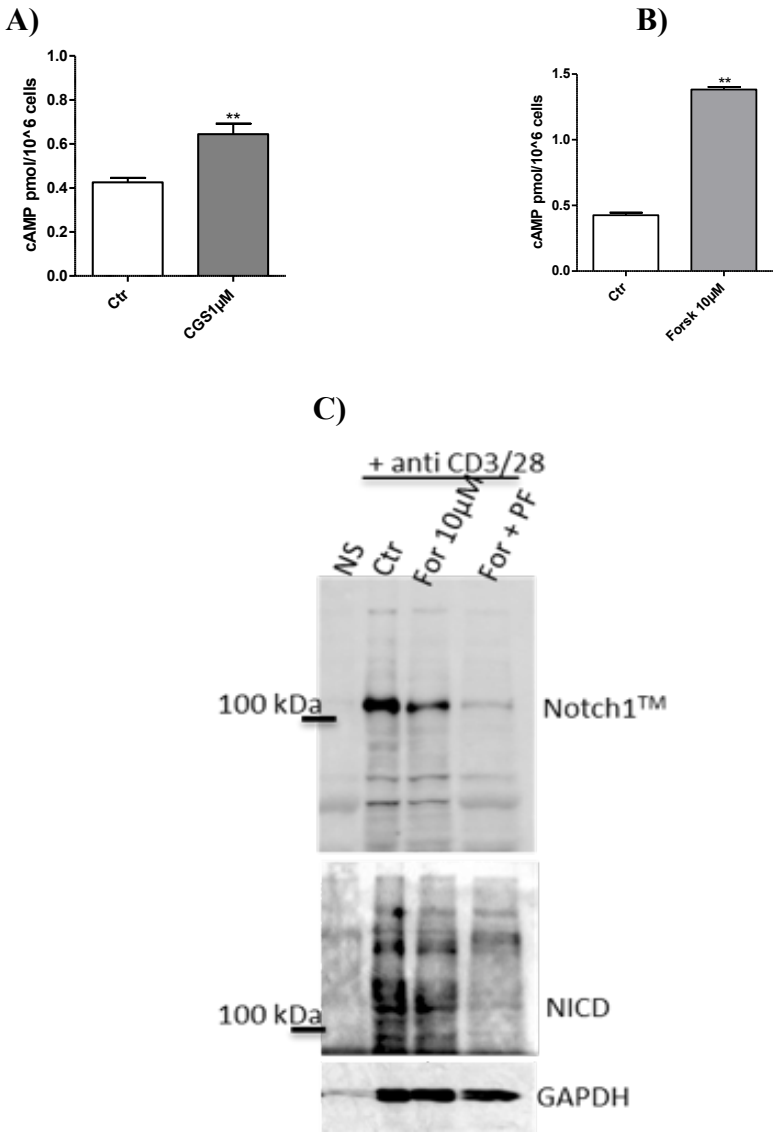
A)
cAMP pmol/10^6 cells
1.0
0.8
0.6
0.4
0.2
0.0
**
Ctr
CGS1µM
B)
cAMP pmol/10^6 cells
1.5
1.0
0.5
0.0
**
Ctr
Forsk 10µM
C)
+ anti CD3/28
NS
Ctr
For 10µM
For + PF
100 kDa
Notch1™
100 kDa
NICD
GAPDH
D)
NICD arbitrary units
1.5
1.0
0.5
0.0
***
*
***
NS
Ctr
PF
Forsk
Forsk+PF
E)
Notch1™ arbitrary units
1.5
1.0
0.5
0.0
***
**
***
NS
Ctr
PF
Forsk
Forsk+PF

Figure 3.3.3 A) and B) cAMP levels in activated CD8+ T cells treated with CGS-21680 (1μM) or not (Ctr) or forskolin 10 μM, respectively. **C)** Representative Western blotting and **D) and E)** densitometric analysis of NICD and Notch 1 expression, respectively, in unstimulated (NS) and activated (Ctr) CD8+ T cells treated with Forskolin alone or in combination with PF-03084014. Data represent mean ± S.E.M. and are from three different experiments. *p<0.5; **p<0.01; ***p<0.001.

These results indicate that the increased levels of cAMP within activated CD8+ T cells after $A_{2A}R$ stimulation can inhibit the TCR-induced Notch expression/activation.

Forskolin was able to affect CD8+ T cells functions as shown in Figures 3.3.3 F, G and H. In particular, Forskolin (10μM) significantly reduced the percentage of proliferating CD8+ T cells after activation and this effect was enhanced in presence of PF-03084014 (Figure 3.3.3 F). Moreover, forskolin significantly reduced IFN-γ (Figure 3.3.3 G) and Granzyme B (Figure 3.3.3 H), released by activated CD8+ T cells.

F) **G)**

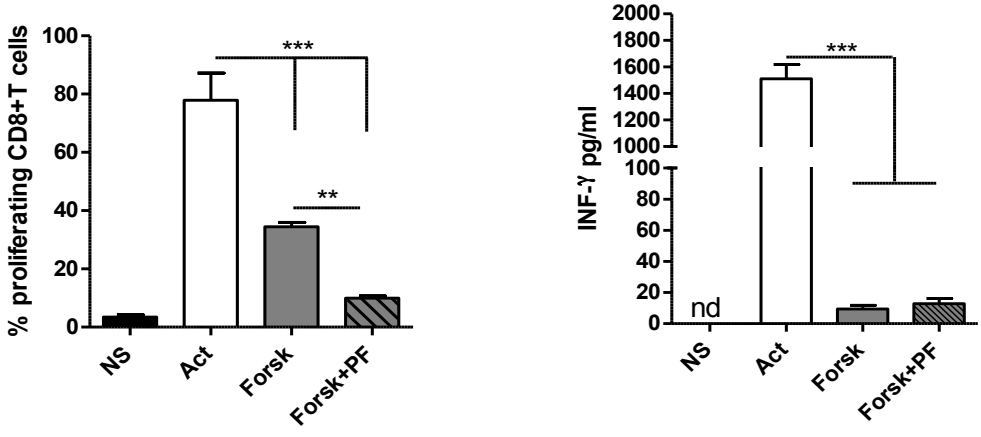

H)

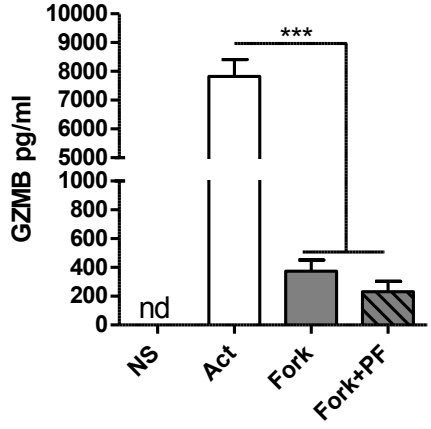

Figure 3.3.3 F) Stimulation of adenylate cyclase with forskolin in combination with PF-03084014 for 72h significantly decreased the proliferation rate of TCR-activated CD8+ T cells. **G)** IFN-γ and **H)** Granzyme B production in CD8+ T cells treated as described above. Data represent mean ± S.E.M.. and are from three different experiments. *p<0.5, **p<0.01; ***p<0.001.

These results suggest that the expression of Notch1 in activated CD8+ T cells can be significantly reduced by cAMP-elevating agents.

3.3.4 $A_{2A}R$ stimulation after TCR activation does not affect CD8+ T cells functions

$A_{2A}R$ stimulation by increasing the levels of cAMP inhibits TCR signalling early events during activation (111), by reducing the Zap70 phosphorylation which is the first event within TCR signal transduction (104). Therefore it is likely that stimulation of $A_{2A}R$ suppresses CD8+ T cells activation by inhibiting the TCR transduction and thus the TCR-dependent Notch induction. To test this, we treated cells with CGS-21680 24h later TCR stimulation with CD3/CD28 antibodies and evaluated the expression of Notch1 proteins. Notably, treatment of cells with CGS-21680 did not affect the expression of Notch1 proteins induced by TCR stimulation (Figure 3.3.4 A, B, C) or treatment of cells with the γ-secretase inhibitor PF (Figure 3.3.4 A, B, C).

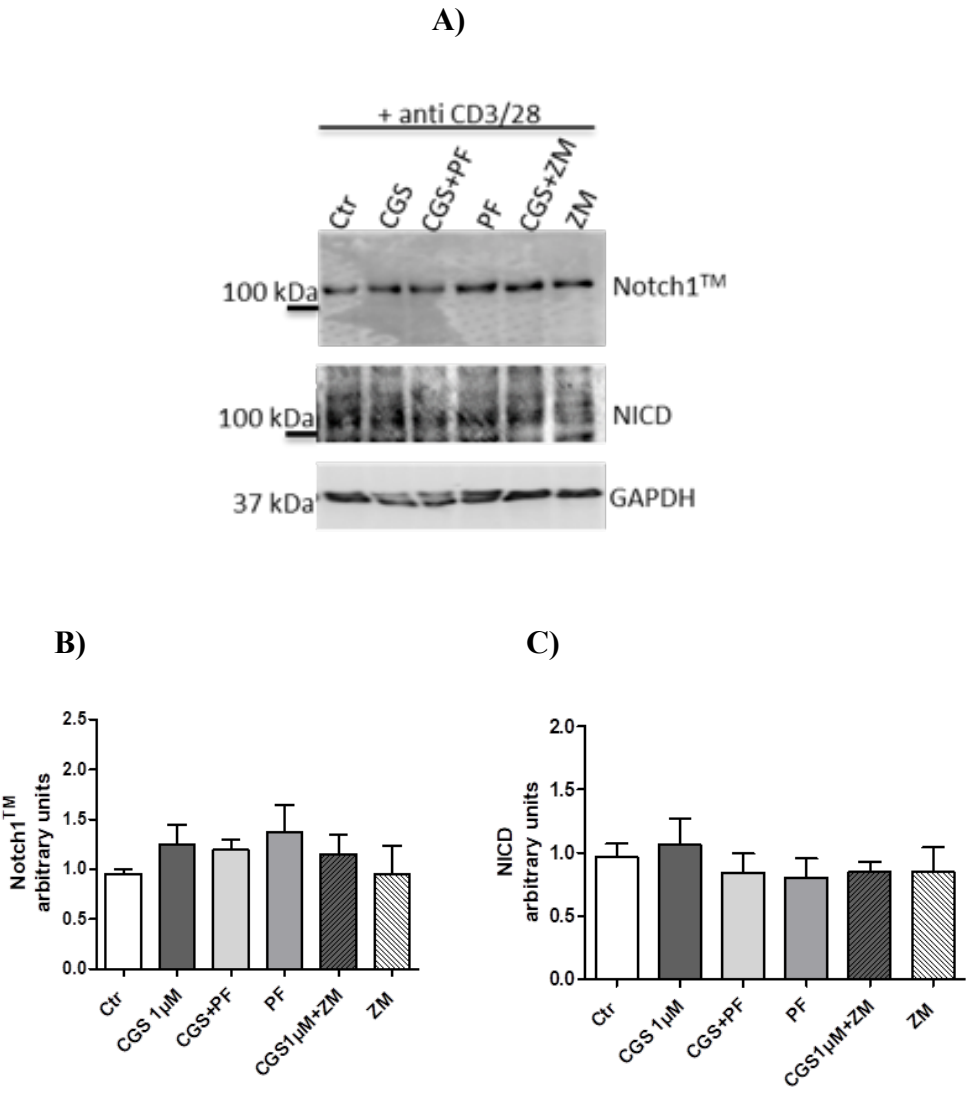

Figure 3.3.4 A) Representative Western blotting of Notch 1^{TM} and NICD in activated CD8+ T cells treated with CGS, PF and ZM 24h later TCR stimulation. **B) and C)** densitometric analysis of Notch 1 and NICD expression, respectively, in CD8+ T cells Treated as described above.

We also observed that CGS-21680 lost its inhibitory effects on proliferation or cytokines release even in combination with PF-03084014 when administered to cells once the TCR stimulation has occurred (Figure 3.3.4 E, F and G). Conversely, the inhibitor of Notch1 significantly reduced the release of IFN-γ and Granzyme B (Figure 3.3.4 F, G).

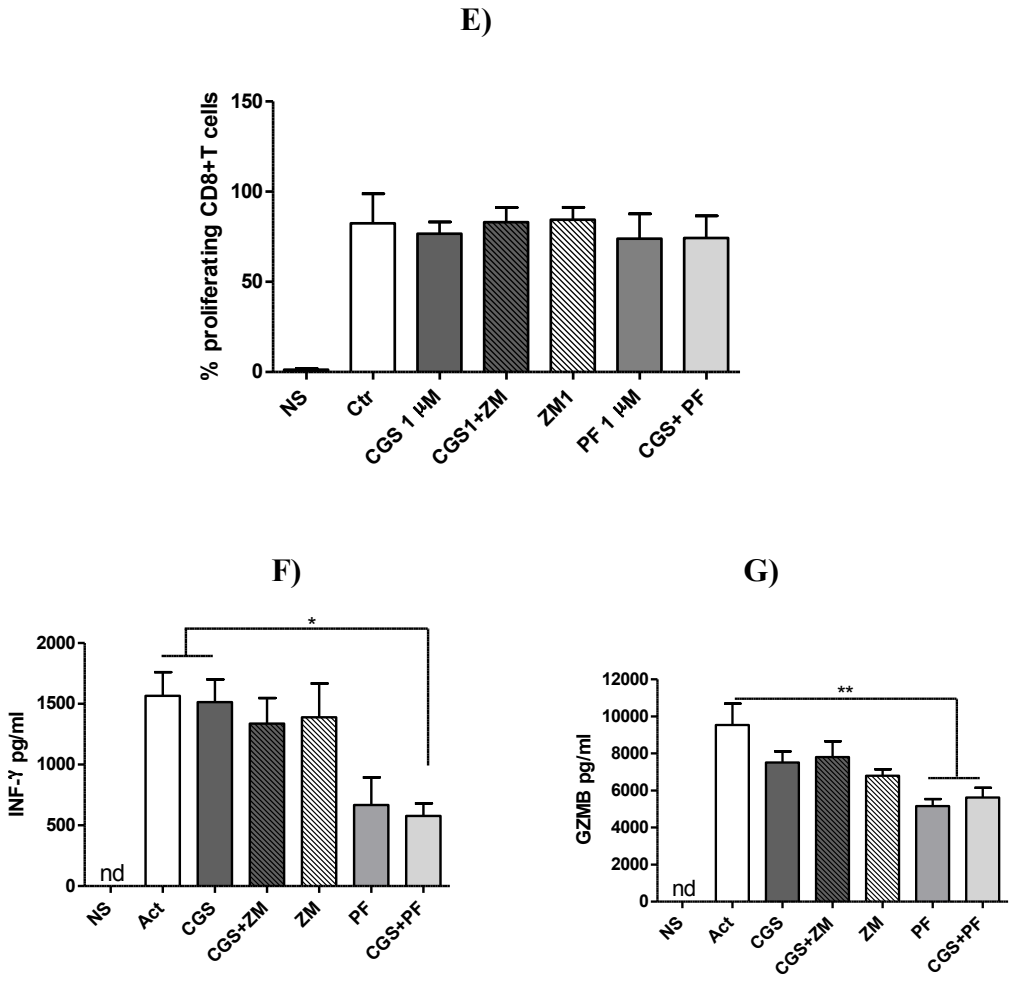

Figure 3.3.4 E) Proliferation rate of isolated and activated CD8+ T cells treated as described above, **F)** IFN-γ production **G)** Granzyme B production. Data represent mean ± S.E.M.. and are from three different experiments. *p<0.5, **p<0.01.

Therefore, the results indicate that the suppressive effects of CGS-21680 through $A_{2A}R$ rely in its capacity to early block the TCR signalling, critical for Notch activation and they are lost once the TCR signalling transduction and thus NICD generation has occurred.

3.2.5 CGS-21680 does not affect NICD stability

It has revealed that adenosine, inhibiting the proximal TCR early events in T cells during activation, could also affect the downstream signalling molecules Akt (104). The protein kinase B (PKB/Akt) controls the activity of the glycogen

synthase kinase 3 (GSK-3) which is inhibited upon phosphorylation (114). Glycogen synthase kinase 3 (GSK-3) is implicated in many processes including regulation of protein stability (115). Both GSK-3α and GSK-3β forms regulate the proteasomal degradation of NICD/Notch 1 (116). In our conditions, we observed that CGS-21680 did not significantly reduced AKT phosphorylation (Figures 3.3.5 A and B), and this effect was associated with unchanged levels of pGSK3β (Ser9) expression (Figures 3.3.5 C and D). It is important to note that independently of Akt status, GSK3 could be directly phosphotylated by PKA, induced by cAMP elevating agents (117). Therefore it is possible that stimulation of $A_{2A}R$, that increases cAMP levels, although slightly reduced pAkt expression, could also on the other hand induce GSK3 phosphorylation/inactivation. Nonetheless, the levels of pGSK3 were unchanged in our experimental conditions.

A)

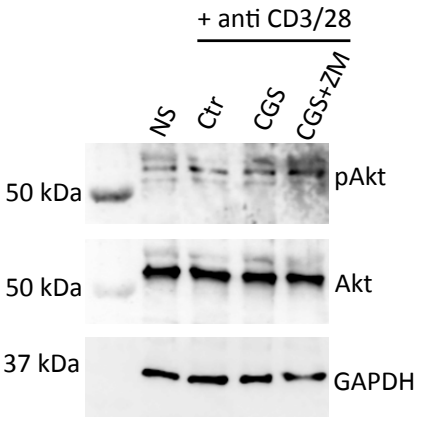

B)

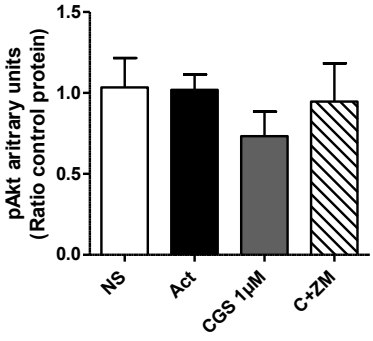

C)

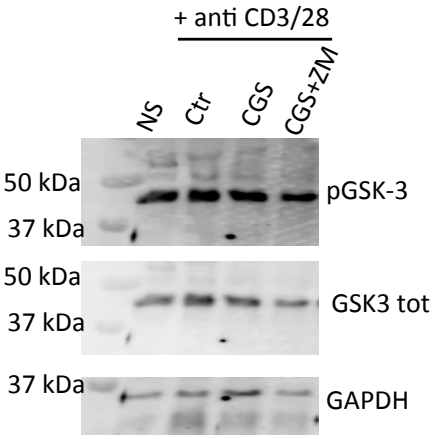

D)

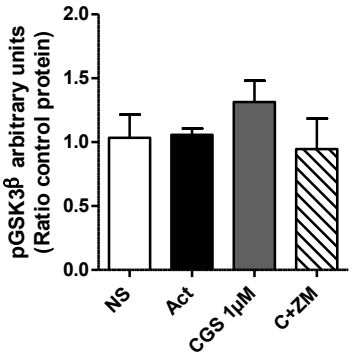

Figure 3.3.5 A) Representative Western blotting and **B)** densitometric analysis on pAKT and total AKT expression in unstimulated (NS) and activated (Act) CD8+ T cells treated with CGS-21680 and ZM-241385. **C)** Representative Western blotting and **D)** densitometric analysis on pGSK3β and total GSK3β expression in CD8+ T cells treated as described above. Data represent mean ± S.E.M. and are from three different experiments.

To confirm that CGS-21680 did not interfere with NICD stability, we treated isolated and activated CD8+ T cells in presence of the inhibitor of protein synthesis cycloheximide 10 μM (CHX) alone and in combination with CGS-21680. We observed that CHX reduced NICD expression after 24 hours and this effect was similar to that observed in cells treated with CGS-21680 in combination (Figure 3.3.5 E) ruling out a possible effect of $A_{2A}R$ agonist on NICD stability.

E)

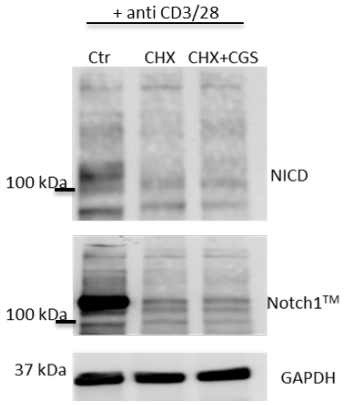

Figure 3.3.5 E) Representative Western blotting of NICD and Notch1^{TM} expression in isolated and activated CD8+ T cells treated for 24 hours with cycloheximide 10 μM (CHX) alone and in combination with CGS-21680.

These results demonstrate that CGS-21680 inhibits the TCR-induced Notch1 signalling pathway rather than protein degradation.

3.3.6 Ectopic expression of N1IC renders CD8+ T cells less susceptible to the suppressive effects of CGS-21680

To determine whether the constitutive activation of Notch1 in CD8+ T cells could affect the suppressive activity of CGS-21680, we used transgenic CD8+ T cells expressing Notch1 (from N1IC mice) under the Granzyme B promoter compared with $N1IC^{f/f}$ cells (22). The expression of Notch1 in these cells occurred 24h later TCR stimulation (data not shown) (22). Therefore, both $N1IC^{f/f}$ and N1IC CD8+ T cells were treated with CGS-21680 or PF-03084014 24h after TCR activation, when the N1IC was over-expressed. Although, treatment of cells with CGS-21680 or with the Notch1 inhibitor PF-03084014 alone after 24h of activation did not influence the proliferation of either $N1IC^{f/f}$ and N1IC CD8+ T cells (Figure 3.3.6 A), co-treatment of cells with both CGS-21680 and PF-03084014 significantly reduced the proliferation of $N1IC^{f/f}$ cells but not those of N1IC CD8+ T cells (Figure 3.3.6 A). Treatment of activated CD8+ T cells over-expressing N1IC with CGS-21680 did not affect the percentage of CD8+IFNγ+T cells (Figure 3.3.6 B) or the expression of Granzyme B (Figure 3.3.6 C). In presence of the Notch1 inhibitor PF-03084014, CGS-21680 was able to reduce the percentage of CD8+IFNγ+T cells (Figure 3.3.6 B) and the expression of Granzyme B (Figure 3.3.6 C) in $N1IC^{f/f}$ cells but not in N1IC CD8+ T cells.

A)

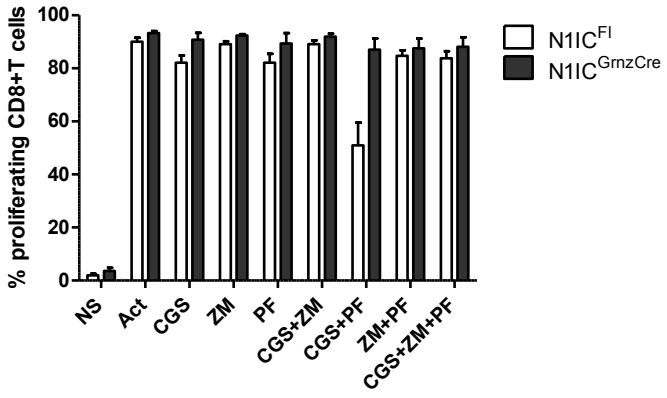

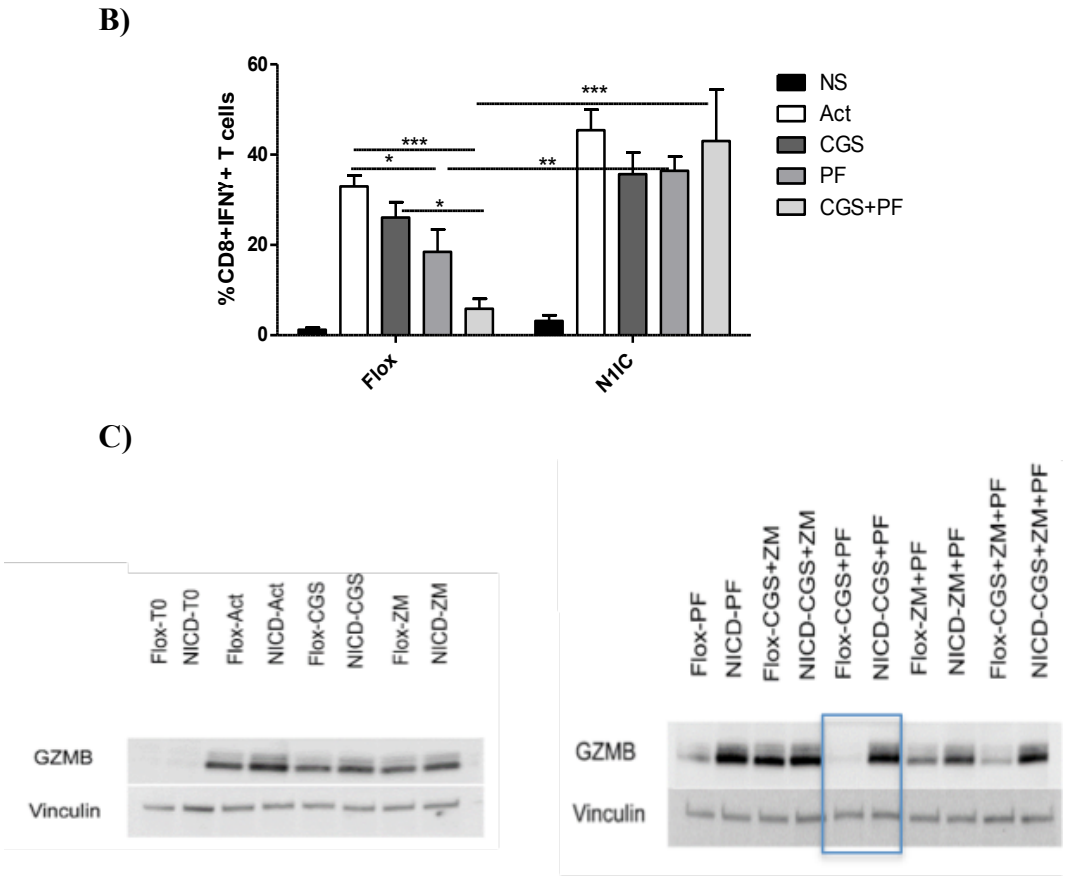

Figure 3.3.6 A) Proliferation rate of isolated and activated CD8+ T cells from spleens of mice overexpressing Notch1 (N1IC CD8+ T cells), treated for 72 hours compared to N1ICf/f cells **B)** percentage of CD8+IFN-γ+ cells **and C)** representative Western blot showing Granzyme B expression in cells treated as described above. Data represent mean ± S.E.M.. and are from three different experiments. *p<0.5, **p<0.01; ***p<0.001.

These results indicate that N1IC CD8+ T cells are less susceptible to the suppressive effects of CGS-21680, confirming that the $A_{2A}R$ suppressive activity through CGS-21680 is, at least in part, dependent on Notch1 inhibition.

3.3.7 A_{2A}KO CD8+ T cells are susceptible to Notch1 inhibition

We finally performed experiments in CD8+ T cells of spleens harvested from mice lacking $A_{2A}R$ (A_{2A}KO mice). As expected, CGS-21680 did not modulate the expression of Notch1 induced by stimulation of the TCR with anti-CD3/CD28

antibodies (Figure 3.3.7 A), or the release of IFN-γ and Granzyme B (Figure 3.3.7 B and C, respectively). Conversely, the experiments revealed that treatment of cells with the γ-secretase inhibitor PF-03084014 (1 μM) inhibits the TCR-induced expression of Notch1 in A_{2A}KO CD8+ T cells (Figure 3.3.7 A). This effect was associated, accordingly, with reduced production of IFN-γ and Granzyme B (Figure 3.3.7 B and C, respectively) suggesting that the inhibition of Notch1 signalling through GSI treatment kept working in a system without A_{2A}Rs. In fact, Notch1 expression was inhibited in GSI treated cells and not in A_{2A}R agonist-treated cells (Figure 3.3.7 A). In the same way, concerning CD8+ T cells functions, IFN-γ and Granzyme B production was reduced in GSI-treated cells but not in A_{2A}R agonist-treated cells (Figure 3.3.7 B and C, respectively), indicating that in cells deficient of A_{2A}R the inhibitory effects of the Nocth1 inhibitor occurs.

A)

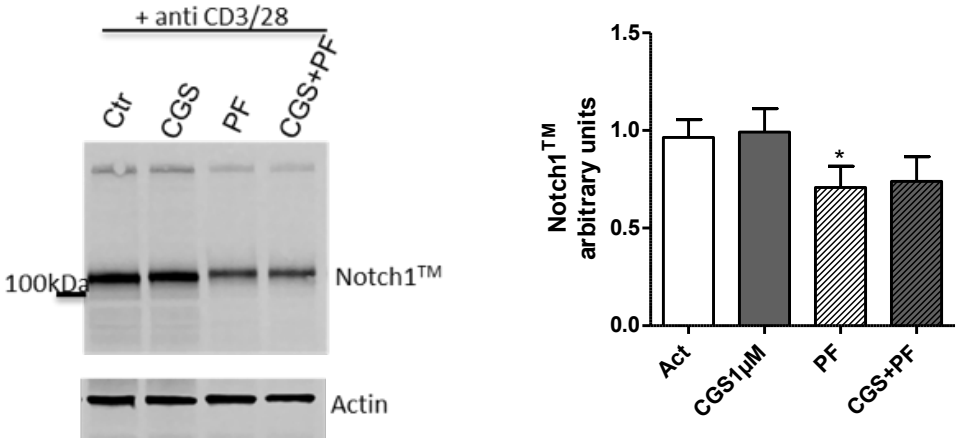

B) IFN- γ

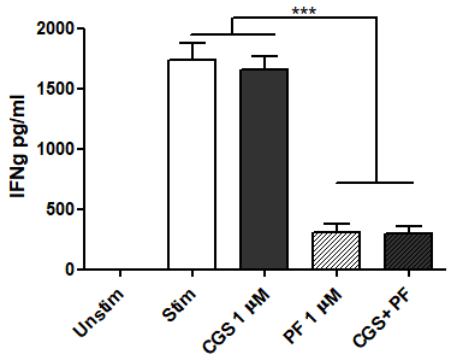

C) Granzyme B

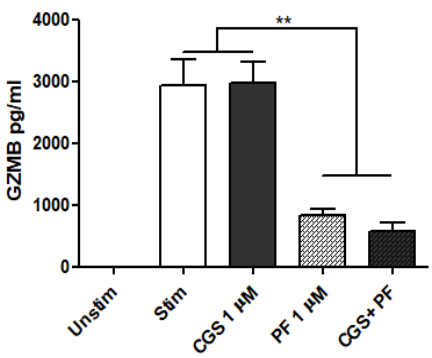

Figure 3.3.7 A) Notch1TM expression in isolated and activated CD8+ T cells from spleens harvested from A_{2A}KO mice, treated for 72 hours with the A_{2A}R agonist (CGS-21680, 1 μM) or with the γ -secretase inhibitor PF-03084014 (1 μM) or both **(A)**, IFN-γ production **(B)** and **(C)** Granzyme B production detected in the supernatant of cells treated for 72 hours as described above . Data represent mean ± S.E.M. and are from three different experiments. **p<0.01; ***p<0.001.

These results demonstrate that the effects of CGS-21680 on TCR-induced Notch1 expression are dependent on A_{2A}R stimulation. Indeed, in CD8+ T cells lacking A_{2A}R the TCR-mediated Notch1 expression was not affected by CGS-21680, nor the cytokines production; whilst inhibition of Notch1 was associated with significant reduction of cytokines levels.

3.4 Discussion

In this study we investigated the possible mechanisms of adenosine-Notch1 crosstalk pathway in regulating CD8+ T cells activation and functions. It is well documented that adenosine is an "immune checkpoint inhibitor" that potently suppresses the activation and cytokines production in T cells in a cAMP/ PKA-dependent manner (the predominant $A_{2A}R$ signalling pathway). A large number of studies demonstrate that blockade of this receptor or inhibition of CD73, which is responsible of the adenosine generation, can potently improve immune responses, especially in the context of cancer (118). Adenosine and adenosinergic modulators of $A_{2A}R$ prevent the activation of CD8+ T cells inhibiting the membrane-proximal signalling of TCR upon anti-CD3/CD28 treatment (104). These effects are dependent on $A_{2A}R$-induced cAMP/PKA pathway, which inhibits the kinases involved in the phosphorylation of Zap70, that is an early event within TCR signalling transduction. Here, we report data on a novel mechanism by which $A_{2A}R$ signals in CD8+ T cells. $A_{2A}R$ agonist controls CD8+ T cells responses, preventing the TCR-mediated induction of Notch1. Notch1 signalling is crucial for T cells development and it is required for optimal proliferation and cytokines production of peripheral T cells (112). Notch signalling deregulation can lead to T cell acute lymphoblastic leukemia (T-ALL) (119, 120).

Notch receptor is activated upon ligation with Notch ligands, undergoing at least three critical proteolytic steps. The intracellular Notch domain (NICD), generated by γ-secretase complex during last proteolytic step, translocates into the nucleus and activates the Notch target genes, including *Hes* and *cMyc* (121). Alternatively, Notch receptor can be activated without Notch ligands interaction, in a non-canonical way through TCR signals (122). The TCR-induced Notch activation is crucial for T cells functions. Indeed, Notch activity mediates the cytotoxic T cells activity through direct regulation of EOMES, perforin and Granzyme B expression (113). The exact mode of Notch1 activation induced by TCR signalling in CD8+ T cells has not been fully characterized. Nonetheless, very recently, it has been demonstrated a mode of TCR-mediated mechanism of Notch

activation and signalling in mature CD4+ T cells (123). As occurred in CD8+ T cells, stimulation of TCR signalling in CD4+ T cells induce Notch processing independently of Notch ligands, generating in turn the intracellular domain of Notch (123). In CD4+ T cells signals from TCR, including Lck, PLC and PI3K that trigger PKC activation, rapidly activate the Notch cleavage and induce endocytosis of the Notch receptor (123).

We observed that in naïve CD8+ T cells stimulation of TCR with anti-CD3/CD28 antibodies induce a rapid expression and activation of Notch1 which persist up to 72h later TCR engagement. Interestingly we found that stimulation of $A_{2A}R$ upon TCR activation significantly reduced the Notch proteins expression and its activity. Indeed, the transcription of *Hes1* and *cMyc*, that are direct targets of Notch-mediated transcription (121), were significantly reduced upon $A_{2A}R$ stimulation. In contrast, the transcription levels of *Notch1* remained unchanged. These results strongly indicate that signals through $A_{2A}R$ prevent the TCR-induced Notch processing and thus its activity rather than direct control of its transcription. In support, the inhibitory effects of $A_{2A}R$ agonist on Notch1 expression were lost once TCR signalling transduction has occurred. These results led us to suggest that stimulation of $A_{2A}R$, which significantly increases cAMP levels, by blocking the early events of TCR signal transduction (98, 104), can led to downregulation of Notch because of impaired TCR-induced processing. We confirmed that the $A_{2A}R$-induced downregulation of Notch was dependent on cAMP/PKA pathway because experiments performed with the adenylate cyclase activator forskolin induced effects in activated CD8+ T cells similar to those obtained with the $A_{2A}R$ agonist. It could be also possible that stimulation of $A_{2A}R$ leads to downregulation of Notch expression/activity by modulating NICD stability. GSK-3 phosphorylation can decrease Notch1 proteins expression and reduce Notch transcriptional activity (116). Our experiments revealed that the phosphorylation levels of GSK-3 remained unchanged upon $A_{2A}R$ stimulation in activated CD8+ T cells, ruling out the possibility that signals via $A_{2A}R$ may regulate NICD protein degradation. Furthermore, GSK-3 phosphorylation/activity is regulated by PKB/Akt. However, although in our experiments $A_{2A}R$ agonist slightly reduced the levels of pAkt, it is not surprising that the levels of pGSK-3

remained unchanged since the activity of GSK-3 can be also controlled by PKA (124).

Other post-translational modifications of NICD upon $A_{2A}R$ stimulation, including membrane trafficking, may also occur. However, this possibility reserves more investigations.

To evaluate the functional consequence of the effects of $A_{2A}R$ agonist on TCR-mediated Notch signalling, we determined the proliferation and cytokines production of activated CD8+ T cells treated with CGS-21680 with or without a γ-secretase inhibitor PF-03084014. γ-secretase complex is required for activation of Notch receptor and inhibitors of this enzyme have been largely used to investigate the downstream targets of the Notch signalling pathway. Despite the γ-secretase inhibitors are not selective for Notch1, because they target all four Notch receptors, we observed that in activated CD8+ T cells the expression and activity of Notch1 induced by TCR engagement were inhibited. These effects were associated with a strongly impairment of cytokines production confirming the important role of Notch for optimal function of mature T cells. The inhibitory effects of GSI on cytokines production occurred in TCR-activated CD8+ T cells even when the TCR signal transduction has already occurred (24 hours later). It is likely that, although Notch activation occurs within few hours following TCR stimulation, we have observed that expression and activity of Notch persist up to 72 hours later TCR stimulation when thus the GSI did not influence anymore the appearance of NICD (that is already happened), but it can still blockade Notch activity in controlling the release of the cytokines IFN-γ and Granzyme B. In support, previous data indicate that the GSI can abrogates the NICD binding as well as the recruitment of NF-kB, which directly regulates IFN-γ, to the perforin and Granzyme B promoters (112, 113).

The inhibitory effects of $A_{2A}R$ agonist were enhanced in presence of the Notch inhibitor. Proliferation of CD8+ T cells, which was strongly inhibited in cells treated with both agents, $A_{2A}R$ agonist and γ-secretase inhibitor, upon TCR stimulation, was not affected in cells 24 hours later TCR activation. These results led us to suppose that since the inhibitory effects of $A_{2A}R$ agonist are lost once TCR transduction has occurred, we observed a significant reduction of T cells

proliferation only when the inhibition of Notch expression and activity, by GSI is combined with the $A_{2A}R$ agonist, which contributes, at least in part, to inhibit the TCR-induced Notch processing.

The inhibitory effects of $A_{2A}R$ agonist are lost in N1IC CD8+ T cells; in contrast the effects of Notch inhibitor occur in $A_{2A}KO$ CD8+ T cells. Indeed, the constitutive activation of Notch1 in CD8+ T cells, isolated from transgenic CD8+ T cells expressing Notch1 under the Granzyme B promoter (after 24h upon TCR activation), affect the suppressive activity of $A_{2A}R$ stimulation compared with $N1IC^{f/f}$ CD8+ T cells. As expected, Notch1 inhibitor blocked the cytokines release in $N1IC^{f/f}$ CD8+ T cells, while N1IC CD8+ T cells were completely resistant. Importantly, combination of Noch1 inhibition and $A_{2A}R$ stimulation induced a significantly inhibitory effect on effector functions of $N1IC^{f/f}$ cells, which was reversed after combination with the $A_{2A}R$ antagonist, but not in N1IC CD8+ T cells. This suggests that expression of N1IC renders CD8+ T cells resistant to the inhibitory effect of the combination of Noch1 inhibition and $A_{2A}R$ stimulation. In other words, CD8+ T cells overexpressing N1IC are less susceptible to the inhibitory effects of $A_{2A}R$ stimulation compared with $N1IC^{f/f}$ cells.

Results in $A_{2A}KO$ cells confirm the critical role of $A_{2A}R$ in reducing activation and function of CD8+ T cells. Its inhibitory effects are at least in part dependent on blocking of Notch1 expression and activity induced by TCR engagement. On the other hands, these results also confirm the crucial role of Notch1 in controlling the functions of CD8+ T cells, including those lacking $A_{2A}R$.

In summary, these data, reveal a novel role for $A_{2A}R$ in regulating T cells effector responses. Stimulation of $A_{2A}R$ leads to downregulation of Notch proteins expression and activity, that is pivotal for optimal functions of mature T cells. Signal through $A_{2A}R$ inhibits the early events of TCR transduction, that trigger Notch receptor proteolytic processing. Understanding the mechanism of cross-talk between these pathways, adenosine and Notch, that are both crucial for proliferation and function of T cells, may help to guide the development of potential strategies to treat disorders in which one or both pathways are deregulated.

Chapter 4

CHAPTER 4

CD73 as a potential marker of response prediction to anti-PD1 therapy in metastatic melanoma patients.

4.1 Introduction

Nowadays, adenosinergic system plays a pivotal role as an anti-tumor therapeutic potential target including $A_{2A}R$ or $A_{2B}R$ antagonists and CD39 or CD73 inhibitors. Inhibition of CD73 or A_{2A}/A_{2B} blockade is able to significantly reduce tumor progression and metastasis in several tumor models, included melanoma (125). New associations and consortia are committed to develop new $A_{2A}R$ antagonists or human monoclonal antibodies against CD73, some of which are already in clinical trials in patients with malignancies (NCT02503774, NCT02655822, NCT02403193, NCT02740985). As widely described in Chapter 1, CD73 (or ecto-5'-nucleotidase) is an ecto-enzyme which hydrolyses the extracellular AMP into adenosine, a potent anti-inflammatory mediator that critically impairs the anti-tumor immune response (1, 125). Importantly, recent evidence suggest that CD73 exists in two different forms. There are both an enzymatic form which is bounded to the membrane of many cell types (including immune cells, endothelial cells and tumor cells) and a soluble one (sCD73) in the serum whose levels are significantly increased in cancer patients compared with healthy individuals (126, 127), as well as in patients with acute inflammatory pancreatitis (128). CD73 is over-expressed and up-regulated in different types of human solid tumors (24) and in general CD73 over-expression is associated to a poor overall survival (OS) or progression-free survival (PFS) (129). Notably, very recently it has been demonstrated that patients who exhibited high tumor CD73 expression developed acquired resistance to immunotherapy (12). In this context, identification and stratification of patients who will benefit from current and new immunotherapies, including anti-CD73 agents, alone or in combination regimen, would be useful. In the last part of this thesis, we proposed to measure soluble CD73 levels in the peripheral blood of patients with advanced melanoma receiving nivolumab as potential biomarker of response to immunotherapy. These

evidence could be very helpful to select patients to an appropriate therapy and then, neutralizing CD73 with clinically validated CD73 monoclonal antibodies could represent a highly potent and innovative therapy to enhance or overcome resistance to immunotherapy.

4.1.1 Metastatic melanoma treatments

Metastatic melanoma (MM) is the most aggressive tumor characterized by a very high rate of relapse and metastasis (130). Over the past years' treatment of metastatic melanoma has been revolutionized with immunotherapy, also including inhibitors of modulatory receptors on T cells (also known as "immune checkpoints"), which can significantly improve T-cell mediated immune response against tumor cells (131). An antibody anti-Cytotoxic T Lymphocyte Antigen-4 (CTLA-4) (ipilimumab, a co-inhibitory receptor expressed on the surface of T-cells) was the first immune checkpoint blocker approved by US Food and Drug Administration (FDA) for metastatic melanoma patients (132). This agent can enhance T-cell proliferation and activation (133) and limit Tregs activity (134) by inducing a long-term regression of melanoma. Unfortunately, the therapeutic benefit of ipilimumab is limited to a small subset of patients (135-137) due to a severe immune-related adverse events and morbidity or even mortality (138-141). Later on other immune checkpoint molecules have been discovered among which we can find antibodies against programmed cell death protein-1 (PD-1, nivolumab, pembrolizumab and atezolizumab). In particular, nivolumab is a monoclonal antibody IgG4, completely human, which acts by blocking PD-1 protein. PD-1 is a receptor expressed on both CD4+ T cells and CD8+ T cells that binds its ligands: PD-L1 expressed on different cell types including tumor cells, or PD-L2 on macrophages and dendritic cells, inhibiting the function of T cells (142). The concurrent blockade of different immune checkpoints might increase the success of immunotherapy in cancer patients (131). In fact, melanoma patients treatment with nivolumab alone or in combination with ipilimumab induce an objective response rate (44%-58%) higher that ipilimumab alone and a longer progression-free survival (143-145). Moreover, combining two different immune-check point blockers results in a lower number of adverse events (146).

Initially, the expression of PD-L1 on melanoma cells was supposed to guide to the success of nivolumab treatment but other studies have showed that patients with PD-L1 negative tumors can also respond to nivolumab treatment (146-148). These reasons highlight the importance to find new biomarkers that better correlate with rates of response to PD-1 blockade (149, 150).

4.2 Materials and Methods

4.2.1 Patients

For this retrospective single-center study was used a total of 37 patients (male, n=21; female n=16) aged >18 years with metastatic stage IV melanoma and samples collected between January 1st 2015 and December 31st 2016 at the Department of Melanoma, Cancer Immunotherapy and Innovative Therapies Unit. N=13 patients of 37 patients (35%) had BRAF V600-mutant melanoma, n=19 patients (51%) were wild-type for BRAF, while n=5 patients included in this study had unknown BRAF status. 27/37 patients (73%) did not have brain metastases, while n=7 patients (19%) had brain metastases. N= 24 patients (65%) had M1c disease and n=19 (51%) had an elevated lactate dehydrogenase level (LDH>480 International Units [IU]/liter).

Patients treatment: patients who had previously received ipilimumab alone or in combination with a BRAF inhibitor (n=7 patients), received nivolumab (3mg/kg) every two weeks until disease progression or unacceptable toxicity appeared. The first patient's tumor response check was after 12 weeks and then every 12 weeks until progression or the discontinuation of treatment according to the Response Evaluation Criteria In Solid Tumors (RECIST).

The overall response rate (ORR) to nivolumab was 24% (9/37: 0 patients with complete response [CR] and 9 patients with partial response [PR]). The disease control rate (DCR) to nivolumab was 46% (17/37: 0 patients CR, 9 PR and 8 with stable disease [SD]). 46% of patients (17/37) showed progressive disease (PD); while 3 patients died before the assessment of response to treatment.

4.2.2 CD73 enzyme activity

To evaluate the CD73 enzyme activity of hydrolysing AMP to adenosine and inorganic phosphate, the concentrations of inorganic phosphate (Pi) was determined in serum with the Malachite Green assay kit (CliniSciences, Italy). CD73 enzyme activity was measured in patients serum obtained from blood sample of each patients withdrawn before starting nivolumab treatment. Briefly,

serum samples (100μg of proteins) were incubated in assay medium containing MgCl2 (10 Mm), NaCl (120 mM), KCl (5 mM), glucose (60 mM), Tris-HCl (50mM), pH 7.4 for 10 min. AMP (2 mM) was added as substrate and samples kept at 37°C for 40 min. To stop the reaction trichloroacetic acid (TCA, final concentration 5% w/v) was added. TCA also contributed to proteins precipitation allowing the measurement of inorganic phosphate (Pi) released during the hydrolysis of AMP using the Malachite Green assay according to the manufacturer's instructions. To have the real value of Pi produced following enzymatic reaction, aspecific Pi released in absence of AMP in each sample was subtracted from the value obtained following incubation with AMP. To determine specificity, experiments were also performed in the presence of the CD73 inhibitor, adenosine 5'-(a, b-methylene) diphosphate (APCP; Tocris Bioscience, Bristol, U.K.) (40-100 μM), which is a non-hydrolysable ADP analogue. For these experiments, samples were incubated with APCP in assay medium for 30 min at 37°C before adding AMP. All samples were run in triplicate; results were expressed as Pi released (pmol/min/mg protein). All reagents, as not indicated otherwise, were from Sigma-Aldrich S.r.l. (Milan, Italy).

4.2.3 Statistical analysis

Differences in sCD73 enzyme activity values across patients' characteristics were evaluated with the Mann-Whitney non parametric test. Chi-square test was used to study associations among categorical variables. Survival curves were estimated with the Kaplan-Meier method and differences evaluated with the log-rank test. Associations between CD73 values and survival times were measured with the Harrel'c. Best cut-off values were located with an R routine implemented on the online software (Cut-off Finder) which maximize differences in survival between the two groups. Hazard Ratios (HR) and their 95% confidence intervals (95% CI) were calculated using the proportional hazard model. Multivariate analysis was performed to identify independent factors associated with survival times.

4.3 Results

4.3.1 sCD73 enzymatic activity in patients with stage IV metastatic melanoma

We started this retrospective study by analysing the basal levels of soluble CD73 (sCD73) enzyme activity in the serum samples of patients with stage IV metastatic melanoma, before starting nivolumab treatment. 70% of the patients presented detectable CD73 enzyme activity. Importantly, in relationship to gender, age, BRAF status (wild-type *versus* mutated), brain metastases, LDH levels and number of previous therapy line, as summarized in Table 1, elevated sCD73 activity was significantly associated with male gender (P=0.007), but not with other variables (Table 1). Indeed, patients with BRAF V600-mutant melanoma had values of sCD73 enzyme activity similar to those measured in BRAF wild-type melanoma (P=0.99) (Table 1). No significant differences in the activity of sCD73 was found between patients with or without brain metastases (P=0.84), in patients with normal LDH versus patients with elevated LDH values (P=0.11), or in relationship to the number of previous line of treatment (P=0.28) (Table 1).

Table 1. sCD73 activity in metastatic melanoma patients

	n	sCD73 activity pmol/min/mg protein [median (range)]	P value*
GENDER			0.007
Male	21	26.7 (0.0-255.3)	
Female	16	0.0 (0.0-75.8)	
AGE			0.16
< 62 years	18	21.9 (0.0-93.7)	
>=62 years	19	6.4 (0.0-255.3)	
BRAF status:			0.99
Wt	19	16.5 (0.0-90.9)	
Mutated	13	13.9 (0.0-255.3)	
BRAIN mets:			0.84
Yes	7	16.0 (0.0-90.9)	
No	27	13.9 (0.0-255.3)	
LDH:			0.11
<480 IU/L	17	7.2 (0.0-90.9)	
>480 IU/L	19	25.2 (0.0-255.3)	
N of previous therapy line			
2	24	10.0 (0.0-93.7)	0.28
>2	12	19.5 (0.0-255.3)	

*Mann-Whitney U test. WT: wild-type; mets: metastasis; LDH=lactate dehydrogenase; IU/L: International Units per Liter; N: Number.

Samples with highest sCD73 enzyme activity were incubated with the non-hydrolysable inhibitor of CD73, APCP (40-100µM) before adding the substrate AMP, to determine the specificity of the reaction. APCP significantly reduced the accumulation of P*i* in a concentration-dependent manner [from 87.337 ± 27.995 pmol/min/mg protein to 55.00 ± 38.658 pmol/min/mg protein (APCP, 40µM) and to 1.375 ± 2.428 pmol/min/mg protein (APCP, 100µM); n=4, $P<0.05$ Mann-Whitney U test] (Figure 1).

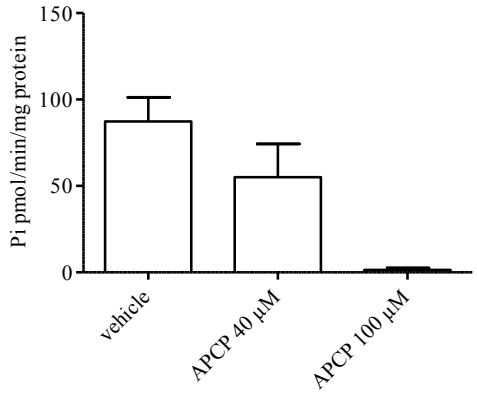

Figure 1: APCP treatment (40-100µM) was able to reduce the activity of CD73. Data are mean ± SEM.

4.3.2 Correlation among sCD73 enzymatic activity and survival

To investigate association between sCD73 enzymatic activity values, overall survival and progression-free survival we calculated the Harrel's C index. We found a good association of c=0.68 (0.45-0.92) for overall survival and c=0.65 (0.44-0.85) for progression-free survival.

Moreover we calculated the optimal cut-off value to establish the sensitivity and specificity of sCD73 enzyme activity thresholds for survival. The optimal cut-off of sCD73 activity for both overall survival and progression-free survival was 27.82 pmol/min/mg protein, as determined by Cut-off Finder online software (Figure 2). Among patients with metastatic melanoma analysed in this study, 27/37 (73%) patients showed a cut-off value of sCD73<27.8 pmol/min/mg protein and 10/37 (27%) patients with sCD73>27.8 pmol/min/mg protein. Median overall survival was not reached in patients with low values of sCD73 enzyme activity (<27.82 pmol/min/mg protein) compared with 6.1 (95%Confidence Interval [CI]: 0-14.8) months for patients with elevated sCD73 enzyme activity (>27.82 pmol/min/mg protein) (Figure 2A; P<0.0001), when patients were follow-up for a median of 24 months. Median progression-free survival was 14.2 months (95% CI: 4.6-23.8) in patients with low sCD73 enzyme activity (<27.82 pmol/min/mg protein) and 2.6 months (95% CI: 1.9-3.3) in patients with sCD73enzyme activity higher than 27.82 pmol/min/mg protein (Figure 2B; P=0.001).

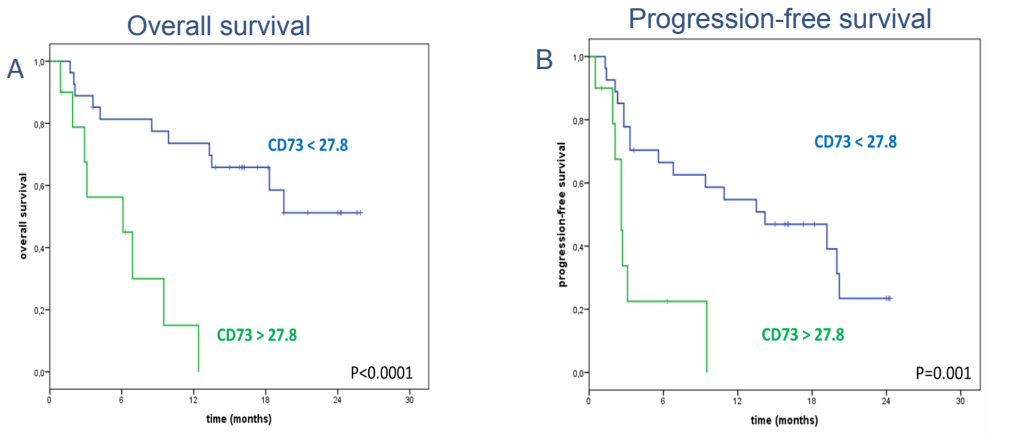

CD73<27.82	CD73>27.82
Not reached	6,1 months (95% CI: 0-14.8)

CD73<27.82	CD73>27.82
14.2 months (95% CI: 4,6-23,8)	2.6 months (95% CI: 1,9-3,3)

Figure 2: Kaplan Meyer curves for **A)** overall survival and **B)** progression-free survival.

4.3.3 sCD73 enzyme activity as possible prognostic factor in metastatic melanoma

To evaluate the impact of gender, age, BRAF status, LDH levels, line of treatment, brain metastasis or basal activity of sCD73 on response to nivolumab, univariate logistic regression was performed. Serum lactate dehydrogenase (LDH) is one of the most important recognized independent prognostic factor in melanoma patients with stage IV disease (113). Elevated LDH levels were found to be significantly associated with worse overall survival and progression-free survival among the patients of this study (Table 3 and Table 4, respectively). The number of previous treatment also impact on progression-free survival (Table 4). Interestingly, we observed that patients with high basal sCD73 enzyme activity (>27.8 pmol/min/mg protein) had 6- and 4-fold increased risk of death and progression, respectively, when compared with patients with sCD73 enzyme activity <27.8 pmol/min/mg protein (Hazard Ratio [HR]=6.27; 95% CI 2.17 – 18.11; P=0.001 and HR=4.24; 95% CI 1.64 - 10.93; P=0.003, respectively) (Table 3 and Table 4, respectively).

Interestingly at multivariate analysis, we found that sCD73 enzyme activity remained the only factor associated with survival, both overall and progression-

free (HR=6.27; 95% CI 2.17 – 18.11; P=0.001) (Table 3 and Table 4, respectively).

Table 3_ Analyses of the associations of sCD73 activity and overall survival

	Univariate	Multivariate
	HR (95% CI) P value	HR (95% CI) P value
GENDER (M vs F)	2.08 (0.80-5.38) P=0.13	n.s.
AGE, years (≥62 vs <62)	1.09 (0.45-2.65) P=0.85	n.s.
BRAF status (mut vs wt)	0.53 (0.19-1.48) P=0.22	n.s.
LDH, IU/L(≥480 vs < 480)	2.72 (1.07-6.88) P=0.03	n.s.
LINE OF TREATMENT (>2 vs 2)	2.38 (0.96-5.94) P=0.06	n.s.
BRAIN METS (yes vs no)	1.04 (0.35-3.12) P=0.94	n.s.
Basal sCD73 activity (≥27.8 vs < 27.8)	6.27 (2.17-18.11) P=0.001	6.27 (2.17-18.11) P=0.001

Table 4_ Analyses of the associations of sCD73 activity and progression-free survival

	Univariate	Multivariate
	HR (95% CI) P value	HR (95% CI) P value
GENDER (M vs F)	1.64 (0.73-3.70) P=0.23	n.s.
AGE, years (≥62 vs <62)	1.30 (0.59-2.89) P=0.52	n.s.
BRAF status (mut vs wt)	0.72 (0.30-1.69) P=0.45	n.s.
LDH, IU/L(≥480 vs < 480)	2.37 (1.04-5.39) P=0.04	n.s.
LINE OF TREATMENT (>2 vs 2)	2.34 (1.02-5.34) P=0.04	n.s.
BRAIN METS (yes vs no)	1.33 (0.53-3.36) P=0.54	n.s.
Basal sCD73 activity (≥27.8 vs < 27.8)	4.24 (1.64-10.93) P=0.003	4.24 (1.64-10.93) P=0.003

Abbreviations: HR=hazard ratio; CI=confidence interval; n.s.: not significant; M=male; F=female; MUT=mutant; WT=wild-type; LDH=lactate dehydrogenase; IU/L: International Units per Liter; METS=metastasis; sCD73=soluble CD73. P values are from Cox proportional hazard Regression models.

4.3.4 Correlation between the sCD73 enzyme activity and clinical response to nivolumab in metastatic melanoma patients

We next found a very novel and interesting association between the response of patients to nivolumab and the value of the enzyme activity of sCD73 measured in the serum before treatment with nivolumab, compared with patients who do not respond to treatment. All patients considered in this study who showed a partial response to nivolumab (PR) or stable disease (SD) had low levels of sCD73 enzyme activity before starting the treatment (Table 5). Accordingly, the disease control rate (DCR) to nivolumab, defined as the proportion of patients with CR, PR and SD, was significantly associated with low pre-treatment sCD73 enzyme activity (<27.8 pmol/min/mg protein) (P= 0.001) (Table 5). Conversely, almost half of the patients who progressed (PD) after nivolumab treatment had elevated basal sCD73 enzyme activity (Table 5).

Table 5_ Response to treatment related to sCD73 enzyme activity levels

	sCD73<27.8pmol /min/mg protein	sCD73>27.8pmol /min/mg protein	pts
CR	-	-	0
PR	9 (100%)	0	9
SD	8 (100%)	0	8
PD	9 (52.9%)	8 (47.1%)	17
DCR (CR+PR+SD)	17 (100%)	0	17

Pts: patients; CR: complete response; PR: partial response; SD: stable disease; PD: progressive disease; DCR: disease control rate.

These results suggest that basal levels of serum sCD73 enzyme activity could help to predict the response to nivolumab in patients with metastatic melanoma.

4.4 Discussion

Nivolumab, as other monoclonal antibodies against PD1/PDL1 pathway, represents the most effective therapeutics in advanced melanoma to date. The identification of biomarkers that predict the clinical response to anti-PD1 drugs still remains a challenge for selecting patients for therapy. Compelling evidence describe that elevated levels of sCD73 activity and expression have been found in the serum of patients with several types of tumor (126, 127) and the expression of CD73 within tumor microenvironment is heterogeneous in primary melanomas and cutaneous melanoma metastases (12), although elevated tumor levels of CD73 have been found in melanoma patients with late-stage disease (128). This raise the question whether the increased levels of sCD73 in the serum might have a prognostic value extending beyond melanoma to other cancers and if it could complement the prognostic value of other biomarkers or histopathologic features to guide also the selection of patients for therapy.

The aim of this study was to identify a potential predictive factor of response to immunotherapy by characterizing CD73 enzymatic activity in melanoma patients receiving nivolumab. This was a single-center retrospective study that initially involved 37 patients. We observed that patients with elevated serum sCD73 enzyme activity had a significantly increased risk of death and disease progression compared to patients with low CD73 enzyme activity. Moreover, we observed that the basal activity of sCD73 in the serum, determined before starting nivolumab treatment, was elevated in patients who do not respond to nivolumab therapy, while patients who benefit from nivolumab treatment had lower levels of sCD73 enzyme activity. Interestingly, the levels of sCD73 enzyme activity were independent from other variables such as the status of BRAF, the presence of brain metastasis and the levels of LDH. Lastly, we did not observe any significant difference in the basal sCD73 enzyme activity levels between patients previously treated with ipilimumab and those treated with BRAF inhibitors if indicated. Certainly, these data need to be validated in a larger and external population to establish the best cut-off reference for sCD73 enzymatic activity and its specificity for metastatic melanoma to support that, prospectively, CD73 could be

used as a biomarker, in addition to known clinical prognostic parameters, in patients with metastatic melanoma.

Conclusions

5. Conclusions

In conclusion, I firstly characterized the role of $A_{2B}R$ within tumor-stroma focusing my attention on two of the most important cell populations involved in tumor growth and angiogenesis: myeloid-derived suppressor cells (MDSCs) and cancer-associated fibroblasts (CAFs). I observed that $A_{2B}R$ stimulation contributes to the adenosine-mediated immunosuppressive effects, by regulating the accumulation of MDSCs within tumor tissue that critically contribute to the pro-angiogenic effects of $A_{2B}R$ within tumor microenvironment. In an attempt to fully characterize the role of $A_{2B}R$ in the surrounding stroma, I then focused my attention also on the activity of stromal fibroblasts within tumor microenvironment upon $A_{2B}R$ stimulation. I observed that $A_{2B}R$ stimulation was able to modulate the activity of stromal fibroblasts that, in turn, produces tumor-promoting soluble factors such as FGF-2 and CXCL12 that are critical players in immunosuppression and angiogenesis. These results provide new insights into the mechanisms through which $A_{2B}R$ regulates intercellular crosstalk in the tumor microenvironment. Importantly, pharmacological blockade of $A_{2B}R$ is able to significantly limit the tumor growth *in vivo*, by reducing the accumulation of MDSCs, tumor angiogenesis and activation of tumor-associated fibroblasts, supporting the therapeutic potential of A_{2B} antagonists as anti-cancer agents.

Secondly, I studied a new immunosuppressive mechanism mediated by $A_{2A}R$ that involves Notch signalling pathway in CD8+ T cells. T cells are essential effectors of tumor immunity (18) and one of the crucial signalling pathways involved in T-cell development, lineage selection and activation is Notch (19). Here, we observed that $A_{2A}R$ stimulation was associated with reduced Notch1 expression and reduced CD8+ T cells functions and these effects were enhanced by inhibiting Notch1 signalling. Moreover $A_{2A}R$ stimulation was not effective once the T cell receptor (TCR) was activated. The inhibitory effects of $A_{2A}R$ stimulation were lost in CD8+ T cells from N1IC mice, in contrast the effects of Notch inhibitor occurred in A_{2A}KO CD8+ T cells. This led me to suppose that the inhibitory effect of $A_{2A}R$ in CD8+ T cells depends, at least in part, on Notch signalling, but

not vice versa.

Finally, I focused my attention on the main ectonucleotidase involved in adenosine synthesis, CD73. Nowadays, adenosinergic system plays a pivotal role as an anti-tumor therapeutic potential target together with adenosine-generating enzymes and possible as predictive factor of response to immunotherapy. We evaluated the associations of sCD73 enzyme activity with clinical outcomes of patients with metastatic melanoma, receiving nivolumab in a retrospective study. I observed that metastatic melanoma patients with high basal serum level of sCD73 enzyme activity, before starting nivolumab treatment, had a lower response rate to nivolumab, shorter survival and higher rates of progression of disease. Patients obtaining partial response to nivolumab or stable disease had low levels of sCD73 activity in the serum. Although these data need to be confirmed and validated, they suggest a predictive role for sCD73. Finding new biomarkers that better correlate with rates of response to PD-1 blockade is a need for oncologists (149, 150) these evidence could be very helpful to select patients to an appropriate therapy and CD73 monoclonal antibodies could potentially represent a highly potent and innovative strategy in combination with currently used immunotherapeutic.

Therefore, the adenosinergic system is one of the most important player in promoting tumor growth. Since adenosinergic-targeted molecules entered in clinical practice for patients with malignancies, understanding the mechanisms by which these molecules modulate immune- and stromal-cells responses in the tumor environment is important for developing new strategies and/or combined therapies for cancer patients.

6. Bibliography

1. Antonioli L, Blandizzi C, Pacher P, Hasko G. Immunity, inflammation and cancer: a leading role for adenosine. Nat Rev Cancer 2013; 13, 842-857.
2. Antonioli L, Pacher P, Vizi ES, Haskó G. CD39 and CD73 in immunity and inflammation. Trends Mol Med 2013; 19:355-67.
3. Yegutkin GG. Enzymes involved in metabolism of extracellular nucleotides and nucleosides: functional implications and measurement of activities. Crit Rev Biochem Mol Biol 2014; 49:473-97.
4. Krysko DV, Garg AD, Kaczmarek A, Krysko O, Agostinis P, Vandenabeele P. Immunogenic cell death and DAMPs in cancer therapy. Nat Rev Cancer. 2012; 12(12):860-75.
5. Fredholm BB, Ijzerman AP, Jacobson KA, Klotz KN, Linden J. International Union of Pharmacology. XXV. Nomenclature and classification of adenosine receptors. Pharmacol Rev 2001; 53:527-52.
6. Borea PA, Gessi S, Merighi S, Varani K. Adenosine as a multi- signalling guardian angel in human diseases: when, where and how does it exert its protective effects? Trends Pharmacol Sci 2016; 37:419-34.
7. Fredholm, B. B. Adenosine, an endogenous distress signal, modulates tissue damage and repair. Cell Death Differ 2007; 14:1315-23.
8. Vijayan D, Young A, Teng MWL, Smyth MJ. Targeting immunosuppressive adenosine in cancer. Nat Rev Cancer 2017; 22,17(12):765.
9. Sitkovsky MV, Hatfield S, Abbott R, Belikoff B, Lukashev D, Ohta A. Hostile, hypoxia-A2-adenosinergic tumor biology as the next barrier to overcome for tumor immunologists. Cancer Immunol Res 2014; 2(7):598-605.
10. St. Hilaire C, Carroll SH, Chen H, Ravid K. Mechanisms of induction of adenosine receptor genes and its functional significance. J Cell Physiol 2009; 218:35-44.
11. Beavis PA, Slaney CY, Kershaw MH, Gyorki D, Neeson PJ, Darcy PK. Reprogramming the tumor microenvironment to enhance adoptive cellular

therapy. Semin Immunol 2016; 28(1):64-72.

12. Reinhardt J, Landsberg J, Schmid-Burgk JL, Ramis BB, Bald T, Glodde N, et al. MAPK Signaling and Inflammation Link Melanoma Phenotype Switching to Induction of CD73 during Immunotherapy. Cancer Res 2017; 77(17):4697-4709.
13. Ryzhov S, Novitskiy SV, Zaynagetdinov R, Goldstein AE, Carbone DP, Biaggioni I, Dikov MM, Feoktistov I. Host A(2B) adenosine receptors promote carcinoma growth. Neoplasia 2008; 10, 987–995.
14. Claudia Sorrentino, Silvana Morello. Role of adenosine in tumor progression: focus on A2B receptor as potential therapeutic target. Cancer Immunol Res 2014; 2:598-605.
15. Sitkovsky MV, Kjaergaard J, Lukashev D, Ohta A. Hypoxia-adenosinergic immunosuppression: tumor protection by T regulatory cells and cancerous tissue hypoxia. Clin Cancer Res 2008; 14:5947–5952.
16. Cekic C, Linden J. Adenosine A2A receptors intrinsically regulate CD8+ T cells in the tumor microenvironment. Cancer Res 2014; 15; 74(24):7239-49.
17. Lappas CM, Rieger JM, Linden J. A2A adenosine receptor induction inhibits IFN-gamma production in murine CD4+ T cells. J Immunol 2005; 174:1073–1080.
18. Tanaka A, Sakaguchi S. Regulatory T cells in cancer immunotherapy. Cell Res 2016; 10.1038/cr.2016.151.
19. Radtke, F., MacDonald, H. R. & Tacchini-Cottier, F. Regulation of innate and adaptive immunity by Notch. Nat Rev Immunol 2013; 13, 427–437.
20. Dongre A, Surampudi L, Lawlor RG, Fauq AH, Miele L, Golde TE, Minter LM, Osborne BA. Non-Canonical Notch Signaling Drives Activation and Differentiation of Peripheral CD4(+) T Cells. Front Immunol 2014; 12;5:54.
21. Duval F, Mathieu M, Labrecque N. Notch controls effector CD8+ T cell differentiation. Oncotarget 2015; 8;6(26):21787-8.
22. Sierra RA, Thevenot P, Raber PL, Cui Y, Parsons C, Ochoa AC, Trillo-Tinoco J, Del Valle L, Rodriguez PC. Rescue of notch-1 signaling in

antigen-specific CD8+ T cells overcomes tumor-induced T-cell suppression and enhances immunotherapy in cancer. Cancer Immunol Res 2014; 2(8):800-11.

23. Sauer AV, Brigida I, Carriglio N, Aiuti A. Autoimmune dysregulation and purine metabolism in adenosine deaminase deficiency. Front Immunol 2012; 27;3:265.
24. Allard D, Allard B, Gaudreau PO, Chrobak P, Stagg J. CD73-adenosine: a next-generation target in immuno-oncology. Immunotherapy 2016; 8(2):145-63.
25. Eltzschig HK, Ibla JC, Furuta GT, Leonard MO, Jacobson KA, Enjyoji K, Robson SC, Colgan SP. Coordinated adenine nucleotide phosphohydrolysis and nucleoside signaling in posthypoxic endothelium: role of ectonucleotidases and adenosine A2B receptors. J Exp Med 2003; 198(5):783-96.
26. Feoktistov I, Biaggioni I. Adenosine A2B receptors. Pharmacol Rev 1997; 49(4):381-402.
27. Yang D, Koupenova M, McCrann DJ, Kopeikina KJ, Kagan HM, Schreiber BM, Ravid K. The A2b adenosine receptor protects against vascular injury. Proc Natl Acad Sci USA 2008; 105:792-6.
28. Sun CX, Zhong H, Mohsenin A, Morschl E, Chunn JL, Molina JG, Belardinelli L, Zeng D, Blackburn MR. Role of A2B adenosine receptor signaling in adenosine-dependent pulmonary inflammation and injury. J Clin Invest 2006; 116:2173-82.
29. Eckle T, Faigle M, Grenz A, Laucher S, Thompson LF, Eltzschig HK. A2B adenosine receptor dampens hypoxia-induced vascular leak. Blood 2008; 111:2024-35.
30. Grenz A, Osswald H, Eckle T, Yang D, Zhang H, Tran ZV, Klingel K, Ravid K, Eltzschig HK. The reno-vascular A2B adenosine receptor protects the kidney from ischemia. PLoS Med 2008; 5:137.
31. Nakatsukasa H, Tsukimoto M, Harada H, Kojima S. Adenosine A2B receptor antagonist suppresses differentiation to regulatory T cells without suppressing activation of T cells. Biochem Biophys Res Commun 2011;

409:114-9.

32. Novitskiy SV, Ryzhov S, Zaynagetdinov R, Goldstein AE, Huang Y, Tikhomirov OY, Blackburn MR, Biaggioni I, Carbone DP, Feoktistov I, Dikov MM. Adenosine receptors in regulation of dendritic cell differentiation and function. Blood 2008; 112:1822-31.
33. Cekic C, Sag D, Li Y, Theodorescu D, Strieter RM, Linden J. Adenosine A2B receptor blockade slows growth of bladder and breast tumors. J Immunol 2012; 188:198-205.
34. Iannone R, Miele L, Maiolino P, Pinto A, Morello S. Blockade of A2b adenosine receptor reduces tumor growth and immune suppression mediated by myeloid-derived suppressor cells in a mouse model of melanoma. Neoplasia 2013; 15:1400-9.
35. Morello S, Miele L. Targeting the adenosine A2b receptor in the tumor microenvironment overcomes local immunosuppression by myeloid-derived suppressor cells. Oncoimmunology 2014; 3: 27989.
36. Hua X, Kovarova M, Chason KD, Nguyen M, Koller BH, Tilley SL. Enhanced mast cell activation in mice deficient in the A2b adenosine receptor. J Exp Med 2007; 204:117-28.
37. Yang D, Zhang Y, Nguyen HG, Koupenova M, Chauhan AK, Makitalo M, Jones MR, St Hilaire C, Seldin DC, Toselli P, Lamperti E, Schreiber BM, Gavras H, Wagner DD, Ravid K. The A2B adenosine receptor protects against inflammation and excessive vascular adhesion. J Clin Invest 2006; 116:1913-23.
38. Mirabet M, Herrera C, Cordero OJ, Mallol J, Lluis C, Franco R. Expression of A2B adenosine receptors in human lymphocytes: their role in T cell activation. J Cell Sci 1999; 112:491-502.
39. Sorrentino C, Miele L, Porta A, Pinto A, Morello S. Myeloid-derived suppressor cells contribute to A2B adenosine receptor-induced VEGF production and angiogenesis in a mouse melanoma model. Oncotarget 2015; 6(29):27478-89.
40. Gabrilovich DI, Nagaraj S. Myeloid-derived suppressor cells as regulators of the immune system. Nat Rev Immunol 2009; 9(3):162-74.

41. Gabrilovich DI, Ostrand-Rosenberg S, Bronte V. Coordinated regulation of myeloid cells by tumours. Nat Rev Immunol 2012; 12(4):253-68.
42. Raber P, Ochoa AC, Rodríguez PC. Metabolism of L-arginine by myeloid-derived suppressor cells in cancer: mechanisms of T cell suppression and therapeutic perspectives. Immunol Invest 2012; 41(6-7):614-34.
43. Nefedova Y, Nagaraj S, Rosenbauer A, Muro-Cacho C, Sebti SM, Gabrilovich DI. Regulation of dendritic cell differentiation and antitumor immune response in cancer by pharmacologic-selective inhibition of the janus-activated kinase 2/signal transducers and activators of transcription 3 pathway. Cancer Res 2005; 65(20):9525-35.
44. Murdoch C, Muthana M, Coffelt SB, Lewis CE. The role of myeloid cells in the promotion of tumour angiogenesis. Nat Rev Cancer 2008; 8(8):618-31.
45. Ryzhov S, Novitskiy SV, Goldstein AE, Biktasova A, Blackburn MR, Biaggioni I, Dikov MM, Feoktistov I. Adenosinergic regulation of the expansion and immunosuppressive activity of CD11b+Gr1+ cells. J Immunol 2011; 187(11):6120-9.
46. Öhlund D, Elyada E, Tuveson D. Fibroblast heterogeneity in the cancer wound. J Exp Med 2014; 211:1503-1523.
47. Pietras K, Ostman A. Hallmarks of cancer: interactions with the tumor stroma. Exp Cell Res 2010; 316:1324-1331.
48. Zhang Y, Qu X. Hypoxia suppresses the production of MMP-9 by human monocyte-derived dendritic cells and requires activation of adenosine receptor A2b via cAMP/PKA signaling pathway. Mol Immunol 2008; 45:2187-95.
49. Feoktistov I, Ryzhov S, Zhong H, Goldstein AE, Matafonov A, Zeng D, Biaggioni I. Hypoxia modulates adenosine receptors in human endothelial and smooth muscle cells toward an A2B angiogenic phenotype. Hypertension 2004; 44:649-54.
50. Zhong H, Belardinelli L, Maa T, Zeng D. Synergy between A2B adenosine receptors and hypoxia in activating human lung fibroblasts. Am J Respir Cell Mol Biol 2005; 32:2-8.

51. Kong T, Westerman KA, Faigle M, Eltzschig HK, Colgan SP. HIF-dependent induction of adenosine A2B receptor in hypoxia. FASEB J 2006; 20:2242-50.
52. Orimo A, Gupta PB, Sgroi DC, Arenzana-Seisdedos F, Delaunay T, Naeem R, Carey VJ, Richardson AL, Weinberg RA. Stromal fibroblasts present in invasive human breast carcinomas promote tumor growth and angiogenesis through elevated SDF-1/CXCL12 secretion. Cell 2005; 121(3):335-48.
53. Brown LF1, Guidi AJ, Schnitt SJ, Van De Water L, Iruela-Arispe ML, Yeo TK, Tognazzi K, Dvorak HF. Vascular stroma formation in carcinoma in situ, invasive carcinoma, and metastatic carcinoma of the breast. Clin Cancer Res 1999; 5(5):1041-56.
54. Eckle T, Grenz A, Laucher S, Eltzschig HK. A2B adenosine receptor signaling attenuates acute lung injury by enhancing alveolar fluid clearance in mice. J Clin Invest 2008; 118:3301–3315.
55. Hart ML, Jacobi B, Schittenhelm J, Henn M, Eltzschig HK. Cutting Edge: A2B Adenosine receptor signaling provides potent protection during intestinal ischemia/reperfusion injury. J Immunol 2009; 182:3965–3968.
56. Abo-Salem OM, Hayallah AM, Bilkei-Gorzo A, Filipek B, Zimmer A, Müller CE. Antinociceptive effects of novel A2B adenosine receptor antagonists. J Pharmacol Exp Ther 2004; 308:358–366.
57. Stagg J, Divisekera U, McLaughlin N, Sharkey J, Pommey S, Denoyer D, Dwyer KM, Smyth MJ. Anti-CD73 antibody therapy inhibits breast tumor growth and metastasis. Proc Natl Acad Sci USA 2010; 107:1547-1552.
58. Suzuki E, Kapoor V, Jassar AS, Kaiser LR, Albelda SM. Gemcitabine selectively eliminates splenic Gr-1+/CD11b+ myeloid suppressor cells in tumor-bearing animals and enhances antitumor immune activity. Clin Cancer Res 2005; 11:6713–6721.
59. Le HK, Graham L, Cha E, Morales JK, Manjili MH, Bear HD. Gemcitabine directly inhibits myeloid derived suppressor cells in BALB/c mice bearing 4T1 mammary carcinoma and augments expansion of T cells from tumor-bearing mice. Int Immunopharmacol 2009; 9:900–909.

60. Saleem SJ, Martin RK, Morales JK, Sturgill JL, Gibb DR, Graham L, Bear HD, Manjili MH, Ryan JJ, Conrad DH. Cutting edge: mast cells critically augment myeloid-derived suppressor cell activity. J Immunol 2012; 189:511–515.
61. Siddiquee K, Zhang S, Guida WC, Blaskovich MA, Greedy B, Lawrence HR, Yip ML, Jove R, McLaughlin MM, Lawrence NJ, Sebti SM, Turkson J. Selective chemical probe inhibitor of Stat3, identified through structure-based virtual screening, induces antitumor activity. Proc Natl Acad Sci USA 2007; 104:7391–7396.
62. Pang M, Ma L, Gong R, Tolbert E, Mao H, Ponnusamy M, Chin YE, Yan H, Dworkin LD, Zhuang S. A novel STAT3 inhibitor, S3I-201, attenuates renal interstitial fibroblast activation and interstitial fibrosis in obstructive nephropathy. Kidney Int 2010; 78:257–268.
63. Sen N, Che X, Rajamani J, Zerboni L, Sung P, Ptacek J, Arvin AM. Signal transducer and activator of transcription 3 (STAT3) and survivin induction by varicella-zoster virus promote replication and skin pathogenesis. Proc Natl Acad Sci USA 2012; 109:600–605.
64. Seluanov A, Vaidya A, Gorbunova V. Establishing primary adult fibroblast cultures from rodents. J Vis Exp 2010; pII: 2033.
65. Feoktistov I, Goldstein AE, Ryzhov S, Zeng D, Belardinelli L, Voyno-Yasenetskaya T, Biaggioni I. Differential expression of adenosine receptors in human endothelial cells: role of A2B receptors in angiogenic factor regulation. Circ Res 2002; 90:531–538.
66. Feoktistov I, Ryzhov S, Zhong H, Goldstein AE, Matafonov A, Zeng D, Biaggioni I. Hypoxia modulates adenosine receptors in human endothelial and smooth muscle cells toward an A2B angiogenic phenotype. Hypertension 2004; 44:649–654.
67. Yang L, DeBusk LM, Fukuda K, Fingleton B, Green-Jarvis B, Shyr Y, Matrisian LM, Carbone DP, Lin PC. Expansion of myeloid immune suppressor Gr+CD11b+ cells in tumor-bearing host directly promotes tumor angiogenesis. Cancer Cell 2004; 6:409–421.
68. Kujawski M, Kortylewski M, Lee H, Herrmann A, Kay H, Yu H. Stat3

mediates myeloid cell-dependent tumor angiogenesis in mice. J Clin Invest 2008; 118:3367–3377.

69. Murdoch C, Muthana M, Coffelt SB, Lewis CE. The role of myeloid cells in the promotion of tumour angiogenesis. Nat. Rev. Cancer 2008; 8:618–631.
70. Chen Z, Han ZC. STAT3: a critical transcription activator in angiogenesis. Med Res Rev 2008; 28:185–200.
71. Niu G, Wright KL, Huang M, Song L, Haura E, Turkson J, Zhang S, Wang T, Sinibaldi D, Coppola D, Heller R, Ellis LM, Karras J, Bromberg J, Pardoll D, Jove R, Yu H. Constitutive Stat3 activity up-regulates VEGF expression and tumor angiogenesis. Oncogene 2002; 21:2000–2008.
72. Siddiquee K, Zhang S, Guida WC, Blaskovich MA, Greedy B, Lawrence HR, Yip ML, Jove R, McLaughlin MM, Lawrence NJ, Sebti SM, Turkson J. Selective chemical probe inhibitor of Stat3, identified through structure-based virtual screening, induces antitumor activity. Proc Natl Acad Sci USA 2007; 104:7391–7396.
73. Pang M, Ma L, Gong R, Tolbert E, Mao H, Ponnusamy M, Chin YE, Yan H, Dworkin LD, Zhuang S. A novel STAT3 inhibitor, S3I-201, attenuates renal interstitial fibroblast activation and interstitial fibrosis in obstructive nephropathy. Kidney Int 2010; 78:257–268.
74. Sen N, Che X, Rajamani J, Zerboni L, Sung P, Ptacek J, Arvin AM. Signal transducer and activator of transcription 3 (STAT3) and survivin induction by varicella-zoster virus promote replication and skin pathogenesis. Proc Natl Acad Sci USA 2012; 109:600–605.
75. Shojaei F, Wu X, Malik AK, Zhong C, Baldwin ME, Schanz S, Fuh G, Gerber H, Ferrara N. Tumor refractoriness to anti-VEGF treatment is mediated by CD11b+Gr1+ myeloid cells. Nat. Biotechnol 2007; 25:911–920.
76. Bergers G, Hanahan D. Modes of resistance to anti-angiogenic therapy. Nat. Rev. Cancer 2008; 8:592–603.
77. Feng W, Song Y, Chen C, Lu ZZ, Zhang Y. Stimulation of adenosine A2B receptors induces interleukin-6 secretion in cardiac fibroblasts via the

PKC-δ–P38 signalling pathway. Br J Pharmacol 2010; 159:1598-1607.

78. Garin-Chesa P, Old LJ, Rettig WJ. Cell surface glycoprotein of reactive stromal fibroblasts as a potential antibody target in human epithelial cancers. Proc Natl Acad Sci USA 1990; 87:7235-7239.
79. Scanlan MJ, Raj BK, Calvo B, Garin-Chesa P, Sanz-Moncasi MP, Healey JH, Old LJ, Rettig WJ. Molecular cloning of fibroblast activation protein alpha, a member of the serine protease family selectively expressed in stromal fibroblasts of epithelial cancers. Proc Natl Acad Sci USA 1994; 91:5657-5661.
80. Feig C, Jones JO, Kraman M, Wells RJ, Deonarine A, Chan DS, Connell CM, Roberts EW, Zhao Q, Caballero OL, Teichmann SA, Janowitz T, Jodrell DI, Tuveson DA, et al. Targeting CXCL12 from FAP-expressing carcinoma-associated fibroblasts synergizes with anti-PD-L1 immunotherapy in pancreatic cancer. Proc Natl Acad Sci USA 2013; 110:20212-20217.
81. Piret JP, Mottet D, Raes M, Michiels C. CoCl2, a chemical inducer of hypoxia-inducible factor-1, and hypoxia reduce apoptotic cell death in hepatoma cell line HepG2. Ann N Y Acad Sci 2002; 973:443-447.
82. Turner N, Grose R. Fibroblast growth factor signalling: from development to cancer Nat Rev Cancer 2010; 10:116-129.Kong T, Westerman KA, Faigle M, Eltzschig HK, Colgan SP. HIF-dependent induction of adenosine A2B receptor in hypoxia. FASEB J 2006; 20:2242-2250.
83. Yu Y, Gao S, Li Q, Wang C, Lai X, Chen X, Wang R, Di J, Li T, Wang W, Wu X. The FGF2-binding peptide P7 inhibits melanoma growth in vitro and in vivo. J Cancer Res Clin Oncol 2012; 138:1321-1328.
84. Aguzzi MS, Faraone D, D'Arcangelo D, De Marchis F, Toietta G, Ribatti D, Parazzoli A, Colombo P, Capogrossi MC, Facchiano A. The FGF-2-Derived Peptide FREG Inhibits Melanoma Growth In Vitro and In Vivo. Mol Ther 2011; 19:266-273.
85. Reiland J, Kempf D, Roy M, Denkins Y, Marchetti D. FGF2 binding, signaling, and angiogenesis are modulated by heparanase in metastatic melanoma cells. Neoplasia 2006; 8:596-606.

86. Guo F, Wang Y, Liu J, Mok SC, Xue F, Zhang W. CXCL12/CXCR4: a symbiotic bridge linking cancer cells and their stromal neighbors in oncogenic communication networks. Oncogene 2016; 35:816-826.
87. Righi E, Kashiwagi S, Yuan J, Santosuosso M, Leblanc P, Ingraham R, Forbes B, Edelblute B, Collette B, Xing D, Kowalski M, Mingari MC, Vianello F, et al. CXCL12/CXCR4 blockade induces multimodal antitumor effects that prolong survival in an immunocompetent mouse model of ovarian cancer. Cancer Res 2011; 71:5522-5534.
88. Yang JC, Haworth L, Sherry RM, Hwu P, Schwartzentruber DJ, Topalian SL, Steinberg SM, Chen HX, Rosenberg SA. A randomized trial of bevacizumab, an anti-vascular endothelial growth factor antibody, for metastatic renal cancer. N Engl J Med 2003; 349:427–434.
89. Hurwitz H, Fehrenbacher L, Novotny W, Cartwright T, Hainsworth J, Heim W, Berlin J, Baron A, Griffing S, Holmgren E, Ferrara N, Fyfe G, et al. Bevacizumab plus Irinotecan, Fluorouracil, and Leucovorin for Metastatic Colorectal Cancer. N Engl J Med 2004; 350:2335–2342.
90. Sandler A, Gray R, Perry MC, Brahmer J, Schiller JH, Dowlati A, Lilenbaum R, Johnson DH. Paclitaxel-carboplatin alone or with bevacizumab for non-small-cell lung cancer. N Engl J Med. 2006; 355:2542–2550.
91. Mansfield AS, Nevala WK, Lieser EA, Leontovich AA, Markovic SN. The immunomodulatory effects of bevacizumab on systemic immunity in patients with metastatic melanoma. Oncoimmunology 2013; 2:e24436.
92. Shojaei F, Wu X, Malik AK, Zhong C, Baldwin ME, Schanz S, Fuh G, Gerber H, Ferrara N. Tumor refractoriness to anti-VEGF treatment is mediated by CD11b+Gr1+ myeloid cells. Nat. Biotechnol 2007; 25:911–920.
93. Chen Z, Han ZC. STAT3: a critical transcription activator in angiogenesis. Med Res Rev 2008; 28:185–200.
94. Yang C, He L, He P, Liu Y, Wang W, He Y, Du Y, Gao F. Increased drug resistance in breast cancer by tumor-associated macrophages through IL-10/STAT3/bcl-2 signaling pathway. Med Oncol 2015; 32(2):352.

95. Monteagudo C, Ramos D, Pellín-Carcelén A, Gil R, Callaghan RC, Martín JM, Alonso V, Murgui A, Navarro L, Calabuig S, López-Guerrero JA, Jordá E, Pellín A. CCL27-CCR10 and CXCL12-CXCR4 chemokine ligand-receptor mRNA expression ratio: new predictive factors of tumor progression in cutaneous malignant melanoma. Clin Exp Metastasis 2012; 29:625-637.
96. Toyozawa S, Kaminaka C, Furukawa F, Nakamura Y, Matsunaka H, Yamamoto Y. Chemokine receptor CXCR4 is a novel marker for the progression of cutaneous malignant melanomas. Acta Histochem Cytochem 2012; 45:293-299.
97. Sarchio SN, Scolyer RA, Beaugie C, McDonald D, Marsh-Wakefield F, Halliday GM, Byrne SN. Pharmacologically antagonizing the CXCR4-CXCL12 chemokine pathway with AMD3100 inhibits sunlight-induced skin cancer. J Invest Dermatol 2014; 134:1091-1100.
98. Huang S, Apasov S, Koshiba M, Sitkovsky M. Role of A2a extracellular adenosine receptor-mediated signaling in adenosine-mediated inhibition of T-cell activation and expansion. Blood 1997; 90(4):1600-10.
99. Raskovalova T, Lokshin A, Huang X, Su Y, Mandic M, Zarour HM, Jackson EK, Gorelik E. Inhibition of cytokine production and cytotoxic activity of human antimelanoma specific CD8+ and CD4+ T lymphocytes by adenosine-protein kinase A type I signaling. Cancer Res 2007; 67(12):5949-56.
100. Zarek PE, Huang CT, Lutz ER, Kowalski J, Horton MR, Linden J, Drake CG, Powell JD. A2A receptor signaling promotes peripheral tolerance by inducing T-cell anergy and the generation of adaptive regulatory T cells. Blood 2008; 111(1):251-9.
101. Cekic C and Linden J. Purinergic regulation of the immune system. Nat Rev Immunol 2016 Mar; 16(3):177-92.
102. Koshiba M, Kojima H, Huang S, Apasov S, Sitkovsky. Memory of extracellular adenosine A2A purinergic receptor-mediated signaling in murine T cells. MV J Biol Chem 1997; 272(41):25881-9.
103. Mustelin T, Tasken K. Positive and negative regulation of T-cell activation

through kinases and phosphatases. Biochem J 2003; 371 (Pt1): 15-27.

104. Linnemann C, Schildberg FA, Schurich A, Diehl L, Hegenbarth SI, Endl E, Lacher S, Muller CE, Frey J, Simeoni L, Schraven B, Stabenow D, Knolle PA. Adenosine regulates cd8 t-cell priming by inhibition of membrane-proximal t-cell receptor signalling. Immunology 2009; 128:e728–737.
105. Maria P. Yavropoulou, Anna Maladaki, John G. Yovos. The role of Notch and Hedgehog signaling pathways in pituitary development and pathogenesis of pituitary adenomas. HORMONES 2015, 14(1):5-18.
106. Radtke F, Schweisguth F, Pear W. The Notch 'gospel'. EMBO reports 2005; 6, 1120-1125.
107. Panin VM, Papayannopoulos V, Wilson R, Irvine KD. Fringe modulates Notch ligand interactions. Nature 1997; 387: 908–912.
108. Bruckner K, Perez L, Clausen H, Cohen S. Glycosyltransferase activity of Fringe modulates Notch Delta interactions. Nature 2000; 406: 411–415.
109. Moloney DJ, Panin VM, Johnston SH, Chen J, Shao L, Wilson R, Wang Y, Stanley P, Irvine KD, Haltiwanger RS. Fringe is a glycosyltransferase that modifies Notch. Nature 2000; 406: 369–375.
110. Olsauskas-Kuprys R, Zlobin A, Osipo C. Gamma secretase inhibitors of Notch signaling. Onco Targets Ther 2013; 23;6:943-55.
111. Espinoza I, Pochampally R, Xing F, Watabe K, Miele L. Notch signaling: targeting cancer stem cells and epithelial to mesenchymal transition. OncoTargets Ther 2013; 6: 1249–1259.
112. Palaga T, Miele L, Golde TE, Osborne BA. TCR-mediated Notch signaling regulates proliferation and IFN-gamma production in peripheral T cells. J Immunol 2003; 15;171(6):3019-24.
113. Cho OH, Shin HM, Miele L, Golde TE, Fauq A, Minter LM, Osborne BA. Notch regulates cytolytic effector function in CD8+ T cells. J Immunol 2009; 182(6):3380-9.
114. Cao Q, Karthikeyan A, Dheen ST, Kaur C, Ling EA. Production of proinflammatory mediators in activated microglia is synergistically regulated by Notch-1, glycogen synthase kinase (GSK-3β) and NF-κB/p65

signalling. PLoS One 2017; 12(10):e0186764.

115. Xu P1, Qiu M, Zhang Z, Kang C, Jiang R, Jia Z, Wang G, Jiang H, Pu P. The oncogenic roles of Notch1 in astrocytic gliomas in vitro and in vivo. J Neurooncol 2010; 97(1):41-51.
116. Jin YH1, Kim H, Oh M, Ki H, Kim K. Regulation of Notch1/NICD and Hes1 expressions by GSK-3alpha/beta. Mol Cells 2009; 27(1):15-9.
117. Kuo YH, Chen CC, Lin P, You YJ, Chiang HM1. AKT/Glycogen Synthase Kinase 3 Beta/Microphthalmia-associated Transcription Factor and Tyrosinase-related Protein 1/Tyrosinase. Curr Pharm Biotechnol 2015; 16(12):1111-9.
118. Burnstock G. Purinergic Signalling: Therapeutic Developments. Front Pharmacol 2017; 8:661.
119. Ellisen LW1, Bird J, West DC, Soreng AL, Reynolds TC, Smith SD, Sklar J. TAN-1, the human homolog of the Drosophila notch gene, is broken by chromosomal translocations in T lymphoblastic neoplasms. Cell 1991; 66(4):649-61.
120. Pear WS, Aster JC, Scott ML, Hasserjian RP, Soffer B, Sklar J, Baltimore D. Exclusive development of T cell neoplasms in mice transplanted with bone marrow expressing activated Notch alleles. J Exp Med 1996; 183(5):2283-91.
121. Barbara A. Osborne and Lisa M. Minter. Notch signalling during peripheral T-cell activation and differentiation. Nature Reviews Immunology 2007; 7, 64-75.
122. Tsukumo SI, Yasutomo K. Regulation of CD8+ T Cells and Antitumor Immunity by Notch Signaling. Front Immunol 2018; 9:101.
123. Steinbuck MP, Arakcheeva K, Winandy S. Novel TCR-Mediated Mechanisms of Notch Activation and Signaling. J Immunol 2018; 200(3):997-1007.
124. Fang X, Yu SX, Lu Y, Bast RC Jr, Woodgett JR, Mills GB. Phosphorylation and inactivation of glycogen synthase kinase 3 by protein kinase A. Proc Natl Acad Sci U S A 2000; 97(22):11960-5.
125. Ohta A A Metabolic Immune Checkpoint: Adenosine in Tumor

Microenvironment. Front Immunol 2016; 29;7:109.

126. Huang Q, Durham NM, Sult E, Wu Y, Liu J, Holoweckyj N, et al. Levels and enzyme activity of CD73 in primary samples from cancer patients. [abstract]. In: Proceedings of the 106th Annual Meeting of the American Association for Cancer Research 2015; Philadelphia, PA. Philadelphia (PA): AACR; Cancer Res 2015;75(15 Suppl):Abstract nr 1538. doi:10.1158/1538-7445.AM2015-1538.
127. Hay C, Sult E, Huang Q, Hammond S, Mulgrew K, McGlinchey K, et al. MEDI9447: enhancing anti-tumor immunity by targeting CD73 In the tumor microenvironment. Cancer Res 2015; 75Abstract nr 285.
128. Maksimow M, Kyhälä L, Nieminen A, Kylänpää L, Aalto K, Elima K, et al. Early prediction of persistent organ failure by soluble CD73 in patients with acute pancreatitis. Crit Care Med 2014; 42(12):2556-64.
129. Wang R, Zhang Y, Lin X, Gao Y, Zhu Y. Prognostic value of CD73-a denosinergic pathway in solid tumor: A meta-analysis and systematic review. Oncotarget 2017; 8(34):57327-36.
130. Cummins DL, et al. Cutaneous malignant melanoma Mayo Clin. Proc 2006; 81: 500-7.
131. Pardoll DM. The blockade of immune checkpoints in cancer immunotherapy. Nat Rev Cancer 2012; 12(4):252-64.
132. Hodi FS, O'Day SJ, McDermott DF, Weber RW, Sosman JA, Haanen JB, Gonzalez R, Robert C, Schadendorf D, Hassel JC, Akerley W, van den Eertwegh AJ, Lutzky J, Lorigan P, Vaubel JM, Linette GP, Hogg D, Ottensmeier CH, Lebbé C, Peschel C, Quirt I, Clark JI, Wolchok JD, Weber JS, Tian J, Yellin MJ, Nichol GM, Hoos A, Urba WJ. Improved survival with ipilimumab in patients with metastatic melanoma. N Engl J Med 2010; 363:711-23.
133. Leach DR, Krummel MF, Allison JP. Enhancement of antitumor immunity by CTLA-4 blockade. Science 1996; 271(5256):1734-6.
134. Selby MJ, Engelhardt JJ, Quigley M, Henning KA, Chen T, Srinivasan M, Korman AJ. Anti-CTLA-4 antibodies of IgG2a isotype enhance antitumor activity through reduction of intratumoral regulatory T cells. Cancer

Immunol Res 2013; 1(1):32-42.

135. Ribas A, Chmielowski B, Glaspy JA. Do we need a different set of response assessment criteria for tumor immunotherapy? Clin Cancer Res 2009; 15(23):7116-8.
136. Wolchok JD, Hoos A, O'Day S, Weber JS, Hamid O, Lebbé C, et al. Guidelines for the evaluation of immune therapy activity in solid tumors: immune-related response criteria. Clin Cancer Res 2009; 15(23):7412-20.
137. Hodi FS, O'Day SJ, McDermott DF, Weber RW, Sosman JA, Haanen JB, et al. Improved survival with ipilimumab in patients with metastatic melanoma. N Engl J Med 2010; 363(8):711-23.
138. Weber JS, Kähler KC, Hauschild A. Management of immune-related adverse events and kinetics of response with ipilimumab. J Clin Oncol 2012; 30(21):2691-7.
139. Bertrand A, Kostine M, Barnetche T, Truchetet ME, Schaeverbeke T. Immune related adverse events associated with anti-CTLA-4 antibodies: systematic review and meta-analysis. BMC Med 2015; 13:211.
140. Eggermont AM, Chiarion-Sileni V, Grob JJ, Dummer R, Wolchok JD, Schmidt H, et al. Prolonged Survival in Stage III Melanoma with Ipilimumab Adjuvant Therapy. N Engl J Med 2016; 375(19):1845-1855.
141. Coens C, Suciu S, Chiarion-Sileni V, Grob JJ, Dummer R, Wolchok JD, et al. Health-related quality of life with adjuvant ipilimumab versus placebo after complete resection of high-risk stage III melanoma (EORTC 18071): secondary outcomes of a multinational, randomised, double-blind, phase 3 trial. Lancet Oncol 2017; 18(3):393-403.
142. Disis ML. Immune regulation of cancer. J Clin Oncol 2010; 28(29):4531-8.
143. Larkin J, Chiarion-Sileni V, Gonzalez R, Grob JJ, Cowey CL, Lao CD,et al. Combined Nivolumab and Ipilimumab or Monotherapy in Untreated Melanoma. N Engl J Med 2015; 373(1):23-34.
144. Wolchok JD, Chiarion-Sileni V, Gonzalez R, Rutkowski P, Grob JJ, Cowey CL, et al. Overall Survival with Combined Nivolumab and Ipilimumab in Advanced Melanoma. N Engl J Med 2017;

10.1056/NEJMoa1709684.

145. Hodi FS, Chesney J, Pavlick AC, Robert C, Grossmann KF, McDermott DF, et al. Combined nivolumab and ipilimumab versus ipilimumab alone in patients with advanced melanoma: 2-year overall survival outcomes in a multicentre, randomised, controlled, phase 2 trial. Lancet Oncol 2016; 17(11):1558-68.
146. Weber J, Mandala M, Del Vecchio M, Gogas HJ, Arance AM, Cowey CL, et al. Adjuvant Nivolumab versus Ipilimumab in Resected Stage III or IV Melanoma. N Engl J Med 2017; 10.1056/NEJMoa1709030.
147. Madore J, Vilain RE, Menzies AM, Kakavand H, Wilmott JS, Hyman J, et al. PD-L1 expression in melanoma shows marked heterogeneity within and between patients: implications for anti-PD-1/PD-L1 clinical trials. Pigment Cell Melanoma Res 2015; 28(3):245-53.
148. Festino L, Botti G, Lorigan P, Masucci GV, Hipp JD, Horak CE, et al. Cancer Treatment with Anti-PD-1/PD-L1 Agents: Is PD-L1 Expression a Biomarker for Patient Selection? Drugs 2016; 76(9):925-45.
149. Friedman CF, Postow MA. Emerging Tissue and Blood-Based Biomarkers that may Predict Response to Immune Checkpoint Inhibition. Curr Oncol Rep 2016; 18(4):21.
150. Mahoney KM, Atkins MB. Prognostic and predictive markers for the new immunotherapies. Oncology (Williston Park) 2014; 28 Suppl 3:39-48.